Utrecht University

Synthesis of activity-based carbocyclic probes for the specific inhibition and detection of glucuronidases

Minor Internship Research Report

Gino Prestifilippo
MSc. Drug Innovation
Student number 9675477

I. Acknowledgements

I would like to thank Dr. Ing. Tom Wennekes for the opportunity to do my minor internship under his guidance, as well as for providing a space where I could perform my syntheses within the scope of the thesis, and for taking the role of the first assessor.

I would like to thank Prof. Dr. Roland Pieters for taking the role of the second assessor.

I would like to thank Helena Ehren for sharing her expertise and her guidance throughout the creation of this thesis. Her input has been invaluable.

I generally would like to express my gratitude for the opportunity to learn from everyone involved, as well as for providing me with my first practical experience in sugar chemistry. The project has proven to be a truly valuable learning experience and has shaped my aspirations for my future chemistry career.

Finally, I would like to thank Diana Ungureanu and Milo for their support and encouragement while composing this thesis.

II. Assessors

First Assessor: Dr. Ing. Tom Wennekes

Second Assessor: Prof. Dr. Roland Pieters

III. Table of Contents

IV. List of Abbreviations

2,2,2-trifluoroethanol	TFE
Benzyloxycarbonyl	Cbz
Cytidine diphosphate	CDP
Cytidine monophosphate	CMP
Ethyl acetate	EtOAc
Galactose	Gal
Glucose	Glc
Glucuronic Acid	GlcA
Glycan-binding protein	GBP
Guanosine diphosphate	GDP
L-Fucose	Fuc
Mannose	Man
N-Acetylgalactosamine	GalNAc
N-Acetylglucosamine	GlcNAc
Nucleotide diphosphate	NDP
Nucleotide triphosphate	NTP
Petroleum ether	PE
Sialic Acid	Sia/Neu5Ac
Single-electron transfer	SET
Thin Layer Chromatography	TLC
Triphenylphosphine oxide	TPPO
Uridine diphosphate	UDP
Xylose	Xyl

V. Abstract

Glucuronidases are part of the glycosidase enzyme family that cleaves polysaccharide chains in organisms. In humans, *exo*-acting β-glucuronidase and *endo*-acting heparanase were identified as the main glucuronidases, though, despite their important function in the body, their disfunction plays a significant role in various diseases, including Sly syndrome, Crohn's disease and cancer. To design novel drugs to treat these diseases, understanding the role of these enzymes in pathology is crucial. Though structures have been identified that can act as irreversible inhibitors and activity-based probes, the current generation lacks the enzyme specificity required to be utilized as diagnostic tools.

A cyclophellitol derivative with an aziridine warhead, which was previously synthesized and evaluated by *Wu et al.,* showed a higher specificity as a glucuronidase inactivator than its predecessors. A crucial step in its synthesis, the installation of the aziridine ring, is, however, met with poor yields and side-product formation, and requires four individual reaction steps. The goal of this project was to explore an alternative one-step method to install the aziridine warhead utilizing Du Bois' catalyst and O-(2,4-dinitrophenyl)hydroxylamine (DPH).

Although the final structure could not be synthesized due to time constraints, the work in this thesis shows that the ester located at the C6 position may not need to be reduced whilst generating the cyclophellitol aziridine scaffold. This could potentially allow for a milder, more convenient implementation of the COO^- functionality at a later stage. Furthermore, it was shown that BCl_3 could be used for an effective debenzylation of the carbocycle intermediate with good yields under mild conditions.

VI. Layman Abstract

When you get sick with a disease like cancer, there can be many reasons why. One of these reasons is when certain enzymes, which are proteins that regulate all sorts of processes in your body, are not functioning correctly.

To better treat diseases, it is important that we better understand the role that these enzymes play while you are sick. Researchers may use molecules that act as probes and will attach themselves to specific enzymes, which then allows their activity to be measured in different situations.

Sometimes, these probes are inspired by molecules found in nature. In Japan, a molecule called cyclophellitol was found in a mushroom species, which was found to attach itself to enzymes that play an important role in cancer development, but because it also attaches itself to other enzymes, it is difficult to use cyclophellitol as a research tool. Because of this, many researchers have been looking for ways to improve its specificity.

In 2017, Liang Wu and his colleagues found that be modifying the original cyclophellitol structure by replacing the three-membered oxygen ring by a three-membered nitrogen ring (an aziridine), and by adding a functional group (a carboxylate) in a specific position, the selectivity of this probe could be improved a lot. However, adding the aziridine is a difficult process. In this project, the goal is to see whether it can be done in an easier, faster way.

Although there was not enough time to create the final molecule and install the aziridine, some important data could be gathered that could potentially help with the adding of the carboxylate at a later stage in the synthesis. This could be helpful for future researchers that may want to investigate optimizing the synthesis of this molecule.

1. Introduction

This work focuses on an irreversible inhibitor, examined for its inhibitory properties towards a specific class of enzymes, namely glucuronidases. To allow for a deeper level of understanding by readers of any background, subchapters 1.1. and 1.2. aim to introduce the cellular compounds modified by these enzymes, glycans, and their biological roles. Subchapter 1.3. then outlines an overview of the different types of enzymes that catalyse glycosidic bond modifications, as well as their mechanisms, which is relevant for understanding the inhibition mechanism of the probe that is discussed in this work. Finally, subchapters 1.4. and 1.5. focus on human glucuronidase enzymes in particular, as well as the irreversible inhibitor that is the subject of this project.

1.1. Glycans and glycosylations.

Glycans are sugar-based polymers that, amongst others, cover the exterior of a cell.[1] They are also referred to as polysaccharides and are made up of monosaccharides that are linked through glycosidic bonds.[2] However, when glycans are connected to other biomolecules such as lipids (glycolipids) or proteins (glycoproteins), other bonds are also possible, such as N-, S- and C-linked glycans.[3] Some examples of these bonds are presented in figure 1.

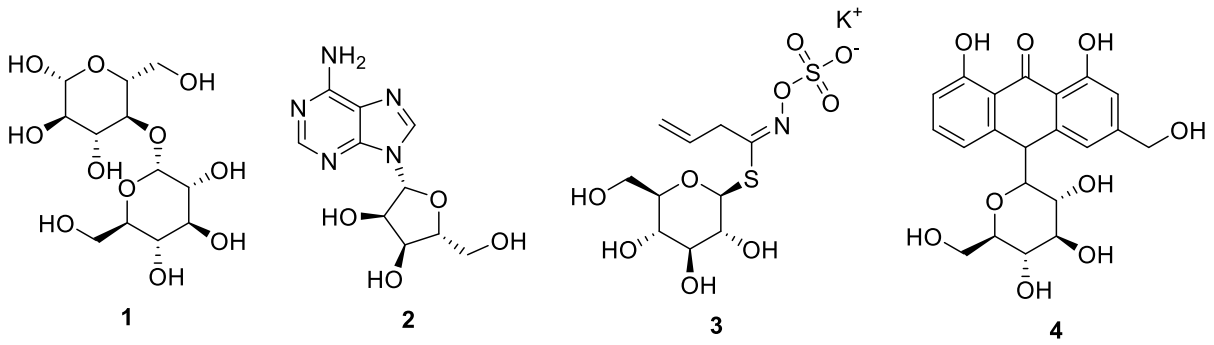

Figure 1. Examples of different glycosidic bonds. Maltose (**1**) contains an O-glycosidic bond; Adenosine (**2**) contains an N-glycosidic bond; Sinigrin (**3**) contains an S-glycosidic bond; Aloin (**4**) contains a C-glycosidic bond.

The formation of these bonds plays a large role in the formation of connections between glycans and other biomolecules, as well as in structural and functional regulation of, for example, proteins, which is why these bonds are often formed within the context of a post-translational modification.[4–6] Several examples shall be presented in the following chapter.

In table 1, several examples are described for the natural occurrence of the formation of said bonds, as well as several examples of their clinical relevance.

Glycosylations play a larger role in biological organisms than merely synthesising polysaccharides and glycoconjugates. Research has shown that various natural compounds undergo glycosylations for various reasons, such as increasing the hydrophilicity of a molecule, thus potentially improving the bioavailability of said compound.[7] Another is the regulation of the activity of certain biomolecules. The attachment of glycosyl residues can “activate” compounds, affecting both the reactivity and selectivity.[8]

Table 1. Several examples of different glycosylations. The table includes an example of its common occurrence, as well as its clinical relevance.

Bond formation	**Common occurrence**	**Examples of clinical relevance**
O-linked glycosylation	• The most common form of glycosylation in natural, biological systems. • Sugar attachment to proteins via serine or threonine residues (proteoglycans).[9] • Sugar attachment to certain lipids (glycosphingolipids).[10]	• Determination of blood groups via Lewis epitopes.[9] • Involved in tumour metastasis.[11]
N-linked glycosylation	• Sugar attachment to proteins via asparagine residues (proteoglycans).[12]	• Modifications in natural N-linked glycosylation processes are linked to many diseases, including rheumatoid arthritis and cancer.[13,14] • Plays an important role in proper protein folding.[15]
S-linked glycosylation	• Uncommon in nature, but is produced by certain modified	• More resistant than traditional O-glycans to

	bioorganisms.[16,17] Occurs via cysteine residues.[18]	hydrolysis and enzymatic degradation.[19] • Unnatural glycans are investigated for their use as O-glycan mimics within the context of pharmaceutical applications.[19,20]
C-linked glycosylation	• C-glycosylation occurs between a tryptophan residue and a mannose sugar.[21]	• Significant increase in stability towards hydrolysis and enzymatic degradation compared to O-glycan analogues.[22] • Like S-linked glycans, C-linked glycans are researched as O-glycan mimics with a higher resistance against degradation.[23]

1.2. The biological role of glycans.

Throughout the years, it has been well-established that glycans play a significant role in the growth and survival of all biological organisms. One example is that almost all proteins produced by ribosomes require glycosylation to initiate and regulate protein folding, so post-translational glycosylation of proteins is essential in this process.[24,25] Another example is the added stability that adding glycans to certain amino acid residues of proteins provides. *N*-linked glycans play a significant role in this; the connection of a glycan to an asparagine residue appears to exert its stabilising effect in the form of conformational changes, which leads to a preference of the structure to adhere to a more compact conformational structure.[26] Finally, the recognition of glycans is essential when it comes to intercellular communication, which occurs via glycan-binding proteins (GBPs).[27–29]

Concurrently, a plethora of glycans have been identified, of which the function is yet to be discovered. *Strasser (2014)* describes how the function of many *N*-glycans in plants is still unknown[30], while *Stone et al. (2016)* describe the obscurity of the function of many *O*-glycans in viral pathogenesis.[31]

This, then, leads to the next topic: the role of glycans in pathogenesis. Researchers have found that glycans play a significant role in the interaction between a host and a pathogen, regardless of whether the nature of said pathogen is bacterial or viral.[32] In a review, *Zhao et al. (2021)* describe that glycans on the spike protein of SARS-CoV-2 are vital for virus-host interactions.[33] The virus utilises the spike protein to protrude into the host cell.[34,35] Then, it appears that the spike protein is glycosylated by the host, which not only allows for improved interaction with the cell surface, but also obscures the underlying polypeptide of the spike protein, hindering the formation of antibodies by the host (referred to in literature as a "glycan shield").[36–38]

In bacteria, glycans play many roles, from colonisation to host-cell invasion. For instance, *Vollmer et al. (2019)* describe the role O-acetylation and deacetylation of glycans play in the cell wall of *Streptococcus pneumoniae*. It gives the bacteria a resistance against lysozyme-mediated extermination, thus providing a survival advantage.[39] Interestingly, host glycans can also benefit invading bacterial pathogens. It is well established that anatomical barriers of the immune system, such as the gastrointestinal- and respiratory tract, are heavily glycosylated on their surface.[40,41] Several bacterium species, however, utilise these glycans to thrive in these environments. An example is the species *Bacillus subtilis*, which utilises the YesU protein to adhere to and colonise on the host cell via fucosylated glycans.[42]

Finally, it was also found that certain toxins utilise glycans to target specific parts of an organism. As the structure of glycoconjugates can widely differ between different cell types, species and types of tissue, toxins made up of lectin complexes can be utilised to achieve a high specificity rate.[43,44] An example is the toxin produced by *Clostridium botulinum* known as Botulinum neurotoxin A, or simply Botox. A study by *Yao et al. (2016)* found that the toxin requires the recognition of two elements for binding: a specific peptide moiety, as well as a specific N-glycan, which is present on the synaptic vesicle glycoprotein 2 family of every vertebrate.[45,46] This allows the toxin to target motoneurons with a remarkable specificity, and researchers seek to understand this

mechanism better to potentially exploit this specificity within the context of novel pharmaceuticals.[47]

1.3. Enzymatic catalysis of glycosidic bond modifications.

Glycosylations can occur both enzymatically and non-enzymatically (also called glycations).[48] This paper, however, shall focus on enzyme-mediated reactions involving glycans.

1.3.1. Glycosyl transferases.

As described in chapter 1.1, there are several different types of glycosylations, and while their mechanisms may vary, several aspects remain the same across all variants.

1.3.1.1. Similarities between glycosylation reactions.

In general, three similarities can be observed across all glycosylation reactions.

First, glycosylations are an enzymatic process. Glycosylation is known to be a tremendously complex process, in which many enzymatic steps are involved.[49] Describing these enzymes in a generalised sense far exceeds the scope of this thesis, but they are generally referred to as glycosyl transferases. Most of these enzymes are present in the rough endoplasmic reticulum and Golgi apparatus, though some can also be found in the cytoplasm.[50]

Second, glycosylation reactions often involve activated nucleotide sugars. Activated nucleotide sugars function as glycosyl donors. In order for saccharides to achieve this activated form, they react with nucleotide triphosphates. While a large variety of these nucleotide sugars are found in nature, a total of nine have been identified in humans, as well as a natural pentose, which is incorporated in glycans as though it were a sugar, which can be divided into four categories.[51–53] These are presented in table 2.

Table 2. An overview of the nine nucleotide sugars found in the human body, as well as one pentose (CDP-D-Ribitol), which was found to be incorporated in glycans as though it were a monosaccharide.

Uridine Diphosphates	UDP-α-D-Glc, UDP-α-D-Gal, UDP-α-D-GalNAc, UDP-α-D-GlcNAc, UDP-α-D-GlcA, UDP-α-D-Xyl
Guanosine Diphosphates	GDP-α-D-Man, GDP-β-L-Fuc

Cytidine Monophosphate	CMP-β-D-Neu5Ac
Cytidine Diphosphates	CDP-D-Ribitol

Finally, glycosylation reactions are site-specific. This means that enzymes related to glycosylations are located in the endoplasmic reticulum, as well as several different compartments of the Golgi apparatus.[54] *Brockhausen (2006)* created an overview of several membrane-bound glycosyl transferases in the cis-, medial- and trans compartment of the Golgi apparatus, which is shown in figure 2.[55] It should be noted that these different compartments function under different pH (ER: pH 7.2; cis Golgi: pH 6.7; medial Golgi: pH 6.5; trans Golgi: pH 6.3), suggesting that certain glycosyl transferases may have different pH optima.[56]

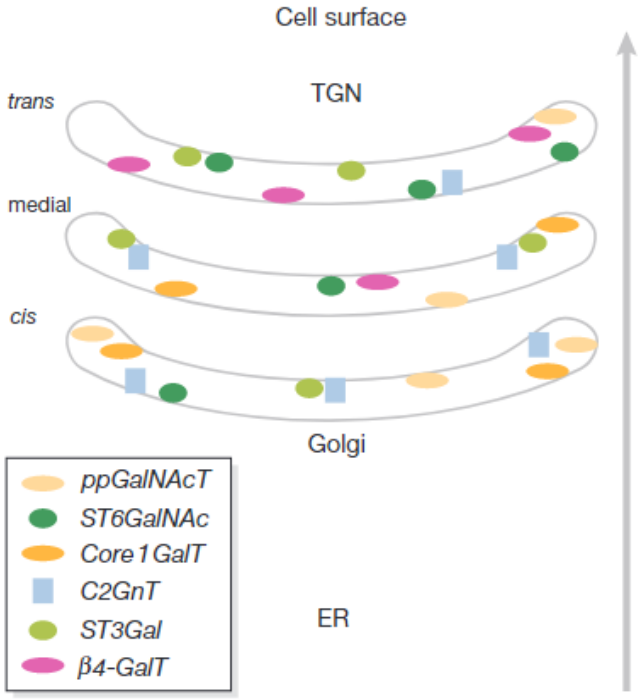

Figure 2. Distribution of several glycosyl transferases in the Golgi Apparatus. The pH decreases from the ER to the trans compartment of the Golgi apparatus. Taken from *Brockhausen (2006)*.

1.3.1.2. Proposed mechanisms of glycosylation reactions.

While the overall mechanism of glycosyl transferases is generally the same, one can differentiate between the effect the reaction has on the stereochemistry of the anomeric centre. To this end, glycosyl transferases are divided into retaining and inverting enzymes.[57]

When inverting glycosyl transferases are involved, an S_N2 reaction causes an inversion of the stereochemistry at the anomeric site. The glycosyl acceptor hydroxy group (usually at the C4) "attacks" the hydroxy group at the C1 of the activated glycosyl donor. The nucleotide diphosphate acts as a leaving group to complete the stereochemical inversion at the anomeric site.[58]

This mechanism is shown in figure 3.

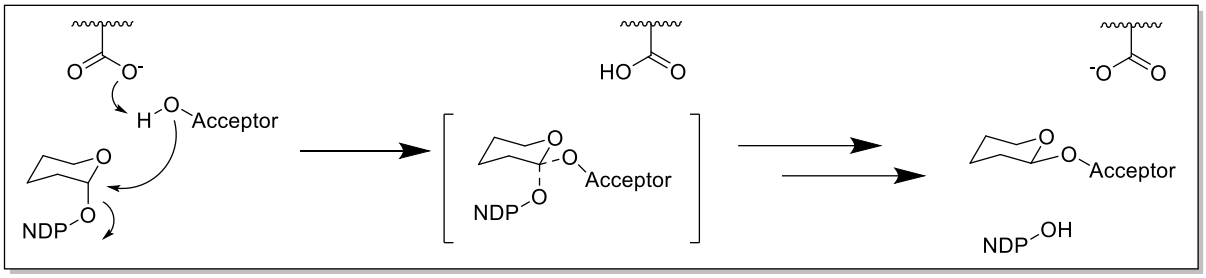

Figure 3. Proposed mechanism of inverting glycosyl transferases. A base deprotonates the glycosyl acceptor, which then proceeds to attack the nucleotide sugar (S_N2). This displaces the nucleotide diphosphate group, leading to an inversion of the stereochemistry at the anomeric centre.

The mechanism of retaining glycosyl transferases is less straightforward, as it has been a topic of debate in the scientific community. Research suggests that the exact mechanism may depend on the family of the glycosyltransferase enzyme, providing evidence that, while so-called "family 6" glycosyl transferases may follow a double-displacement mechanism due to the placement of a specific nucleophilic residue in the active site, other retaining enzymes appear to lack this nucleophilic site, prompting the theory that a single-displacement mechanism may be more likely for other glycosyltransferase families.[59]

An example is alpha-1,3-galactosetransferase. Here, the Glu317 residue functions as the nucleophile, initiating the reaction by attacking the activated hydroxy and binding to the sugar molecule. Then, the glycosyl acceptor displaces Glu317 at the anomeric centre, leading to the retention of the original stereochemistry.[60] In this case, the reaction would occur in a "double-inverting" manner.

This mechanism can be seen in figure 4.

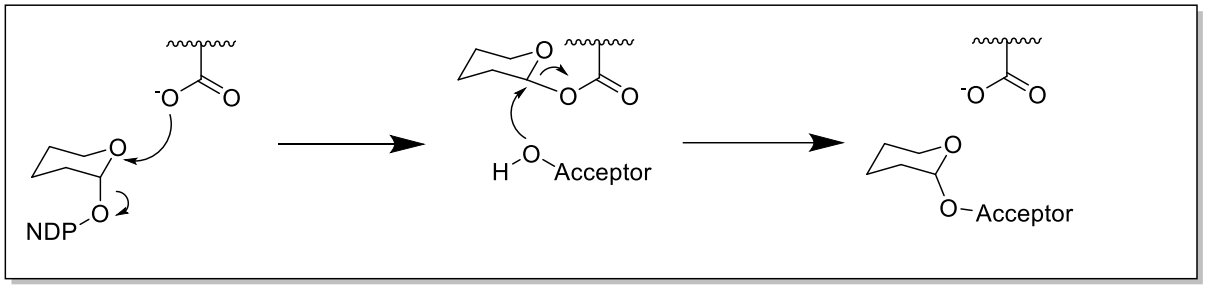

Figure 4. Proposed double-displacement mechanism of glycosyl transferases. In an initial step, a nucleophile in the active site of the enzyme displaces the nucleotide diphosphate group. This is followed by a nucleophilic attack of the glycosyl acceptor, leading to a double inversion, thus retaining the original stereochemistry.

In the case of the single-displacement reaction scheme, several mechanisms have been proposed, all of which involve an oxocarbenium intermediate. In this mechanism, it is hypothesised that the glycosyl donor dissociates, leading to the aforementioned oxocarbenium ion, which would then be stabilised by dipole effects exerted by polar protein residues. However, *Schuman et al. (2013)* argue that, in the case of a unimolecular dissociation, a loss of stereo configuration would be inevitable, and propose that this retention of stereo configuration may be achieved through steric hindrance, which is achieved with bulky residues in the active site.[59,61]

Another proposed mechanism by various researchers suggests a partial dissociation of the nucleotide diphosphate leaving group, during the nucleophilic attack of the glycosyl acceptor, following an S_Ni scheme.[62–65] However, this mechanism, too, is met with criticism within the scientific community. For example, *Soya et al. (2010)* suggest that this transition state would both sterically and entropically be unfavourable.[66]

Finally, an "S_Ni-like" mechanism suggests that the reaction may involve a short-lived ion pair, which then changes its position in the active site of the enzyme to allow for the nucleophilic attack of the glycosyl acceptor that leads to an overall retention of the stereochemistry at the anomeric centre. This reaction, unlike the previously described mechanism, could be described as a step-wise S_Ni mechanism.[67,68]

An overview of all three proposed mechanisms is shown in figure 5.

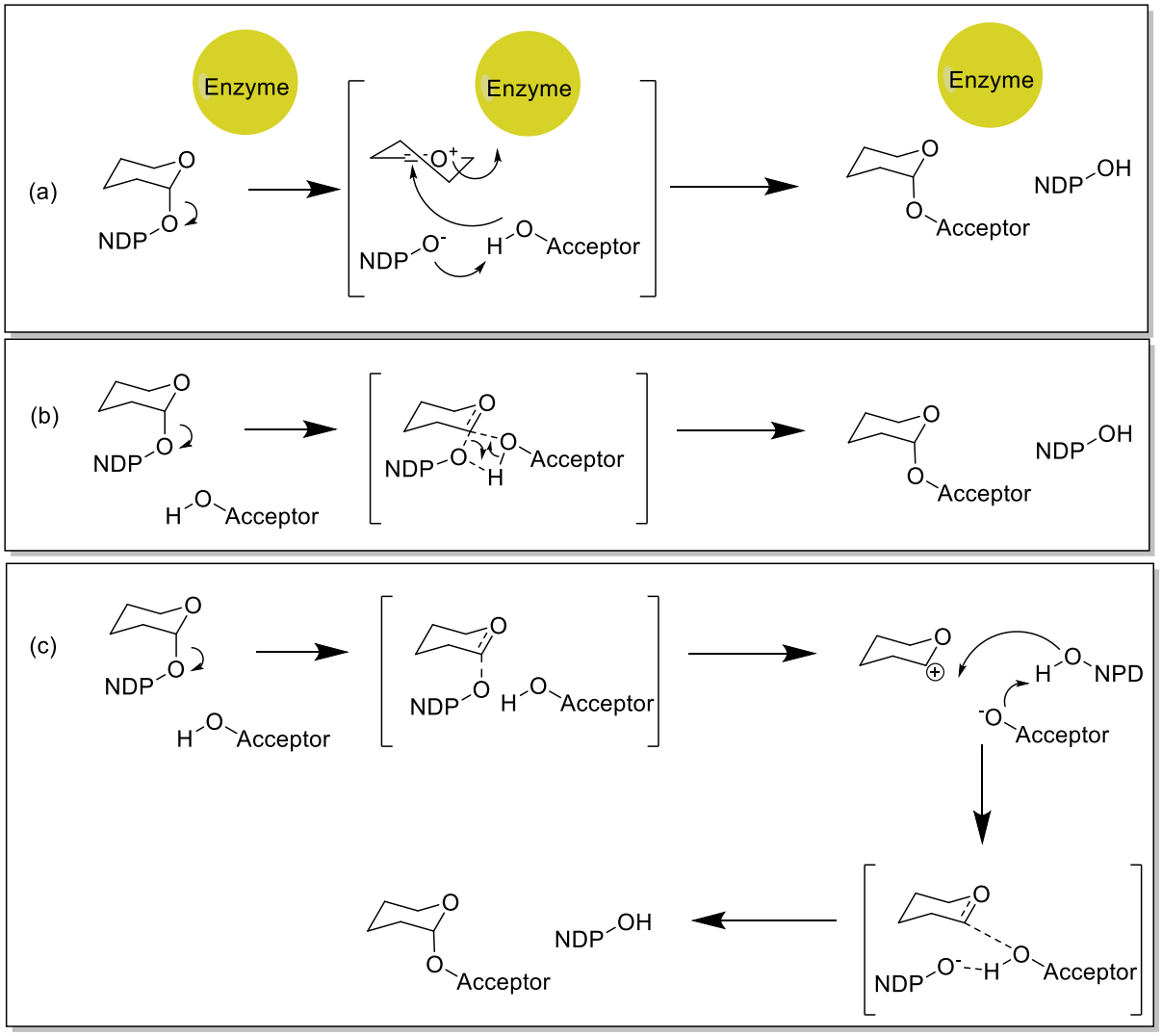

Figure 5. Three proposed single-displacement mechanisms for retaining glycosyl transferases. (a) shows a unimolecular dissociation, followed by a stereoselective nucleophilic attack by the glycosyl acceptor, facilitated by the steric hindrance of the enzyme; (b) shows a partial dissociative mechanism, coordinated by the nucleotide diphosphate group; (c) shows a step-wise S_Ni mechanism via an ion pair intermediate.

1.3.2. Glycoside hydrolases.

Contrary to glycosyl transferases, glycoside hydrolases (or glycosidases) break down complex carbohydrate chains such as glycans. These enzymes are highly important for most living organisms due to their role in nutrition obtainment. Similar to glycosyl transferases, they can be found in the endoplasmic reticulum and Golgi apparatus, the lysosome, the gut, and even in saliva.[69–73]

1.3.2.1. Various classifications of glycosidic hydrolases.

Glycosidic hydrolases can be classified by several different factors. Two important classifications shall briefly be discussed here.

Endo- and exo-acting glycosidases.

Endo refers to the fact that these enzymes will cleave a substrate somewhere in the middle of a polysaccharide, while *exo* refers to selective cleaving of the (often) non-reducing end of a sugar chain.[74]

α- and β-glycosidases.

A glycoside hydrolase enzyme is either an α- or β-glycosidase depending on whether it cleaves α- or β-glycosidic bonds. An example of this is the comparison between alpha-glucosidase and beta-glucosidase; whilst they both release glucose after the hydrolysis reaction, the enzyme that is utilised depends on whether this is alpha- or beta-glucose.[75,76]

1.3.2.2. Proposed mechanisms of glycosidic hydrolases.

Similar to glycosyl transferases, glycosidases can be categorised as either inverting or retaining, and, as the name suggests, these reactions require a water molecule. Contrary to glycosyl transferases, it appears that the double displacement mechanism is widely accepted to be correct.

In inverting glycosidases, two protein residues actively participate in the hydrolysis reaction as catalysts: an acid and a base (often protonated and deprotonated glutamic- or aspartic acid). The base deprotonates a water molecule, which then attacks the saccharide unit at the anomeric centre. This creates an oxocarbenium transition state, ultimately leading to the breakage of the glycosidic bond.[77]

The mechanism, first proposed by *Koshland (1953),* of an inverting glycosidase is shown in figure 6.[78] This figure shows the hydrolysis of an alpha-glycosidase.

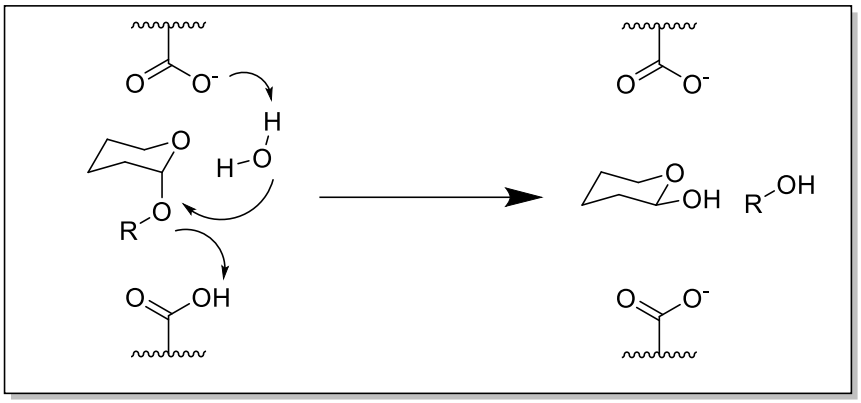

Figure 6. Mechanism of an (alpha) inverting glycosidase-catalysed hydrolysis of a polysaccharide as proposed by *Koshland (1953)*.

In the case of retaining glycosidases, the glycosidic bond is initially protonated by the acid catalyst in the active site. In a following step, the base catalyst performs a nucleophilic attack on the anomeric centre to assist in the departure of the leaving group, leading to the covalent binding of the saccharide to the enzyme. Finally, the deprotonated acid catalyst deprotonates a water molecule, of which the hydroxide ion hydrolysis the bond between the enzyme and the saccharide, leading to a product with the same stereochemistry as the starting material at the anomeric center.[78]

This mechanism, also proposed by *Koshland (1953)*, is presented in figure 7.

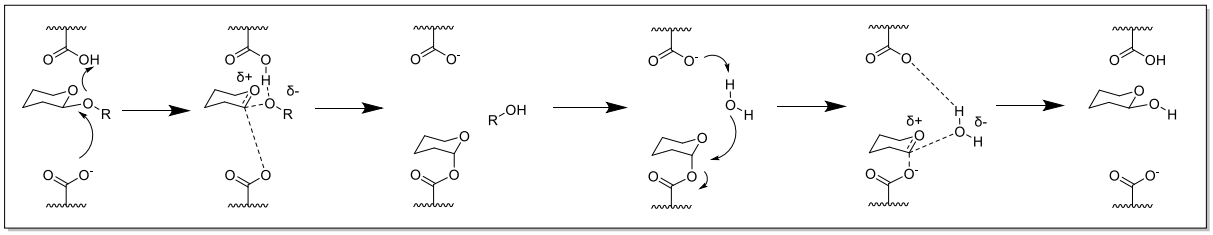

Figure 7. Mechanism of an (alpha) retaining glycosidase-catalysed hydrolysis of a polysaccharide as proposed by *Koshland (1953)*.

Discovering the mechanisms of various enzymes is still an ongoing process that occupies many researchers, leading to various interesting discoveries. One such example is the T4 phage lysozyme, also known as T4L, which was found to hydrolyse peptidoglycans in the bacterial cell wall. In a review by *Davies & Henrissat (1995)*, a table with glycosidases from a variety of species was published with their respective mechanism, and at the time of publishing, the mechanism of T4L was still unknown.[79] A short while afterwards, *Matthews et al. (1995)* found that this enzyme has an inverting mechanism.[80] Interestingly, *Brockerman et al. (2019)* showed that, by

substituting a threonine residue in the active site with a histidine residue, the mechanism changed to a retaining one.[81] This suggests that, like glycosyl transferases, it is likely that there are multiple different mechanisms via which glycosidases could function.

1.4. The role of β-glucuronidases.

Throughout the years, a large number of glycosidases have been identified and characterised, both natural, found in living organisms and engineered, and have been classified in an intricate family system.[82,83]

β-Glucuronidases are part of the glycosidase family 2, which specifically aid in the hydrolysis of β-glucuronic acid residues.[84,85] In nature, a plethora of different β-glucuronidases have been identified, with over 270 found in microbes found in the human gut.[86] In humans, however, two were found to be most prevalent: *Exo*-acting β-glucuronidase and *Endo*-acting heparanase.

1.4.1. <u>*Exo*-acting β-glucuronidase.</u>

Exo-acting β-glucuronidase was found to hydrolyse a variety of non-reducing ends of glycans and is predominantly present in the lysosomes.[87] The crystal structure was determined by *Sly et al. (2013)* and a representation is presented in figure 8.[73]

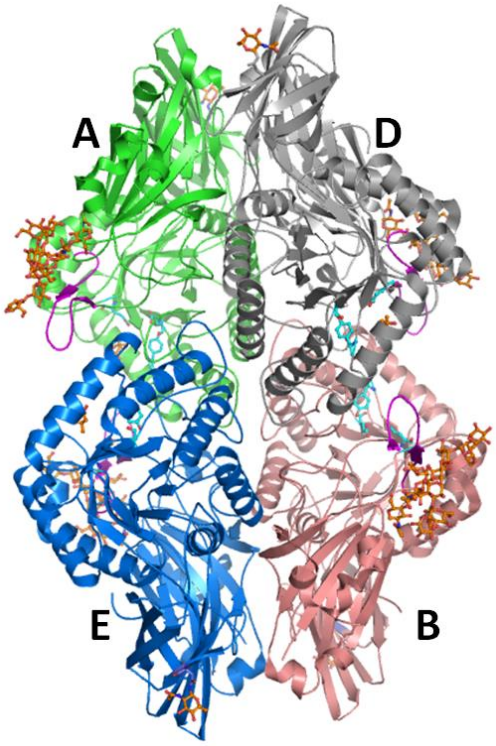

Figure 8. A cartoon model of the overall structure of *exo*-acting β-glucuronidase. The figure shows the four subunits of the enzyme, each presented in a different colour. Taken from *Sly et al. (2013)*.

Exo-acting β-glucuronidase is classified as a retaining glycoside hydrolase, with two glutamic acid residues (Glu540 and Glu451) acting as catalysts in the active site of the enzyme during hydrolysis.[85]

As these enzymes are vital for the complete metabolism of macromolecules in the body, a deficiency often leads to disease. A deficiency of *exo*-acting β-glucuronidase is called mucopolysaccharidosis type VII, also known as Sly Syndrome. The inability to adequately break down glycans leads to a build-up, which may lead to fetal death in the womb, while survivors often have to live with enlarged organs or limbs and suffer from various other complications, including sleep apnea and other musculoskeletal abnormalities.[88–90] Treatments at the time of writing this thesis include injecting phosphorylated murine *exo*-acting β-glucuronidase to prevent mucopolysaccharide accumulation in tissue other than the brain, and gene therapy was suggested by *Wolfe et al. (1992)*, utilising a retroviral vector to transport an *exo*-acting β-glucuronidase gene to stem cells to allow for long-term expression of the healthy enzyme.[91,92] This was, indeed, found to partially cure Sly Syndrome by reducing lysosomal storage in both the spleen and the liver.[91]

1.4.2. *Endo*-acting heparanase.

Like the *exo*-acting β-glucuronidase, *endo*-acting heparanase is a retaining glycosidic hydrolase, with the Glu225 and Glu343 participating in the hydrolysis. However, as an *endo*-acting enzyme, this heparanase specifically hydrolyses heparan sulfate side chains at a site that is not the end of a polysaccharide. Like *exo*-acting β-glucuronidase, it is also present in the lysosomes, but in addition, it can be found in the extracellular matrix.[93] Its structure was first determined by *Wu et al. (2015)*, and a 3D model is presented in figure 9.[93,94]

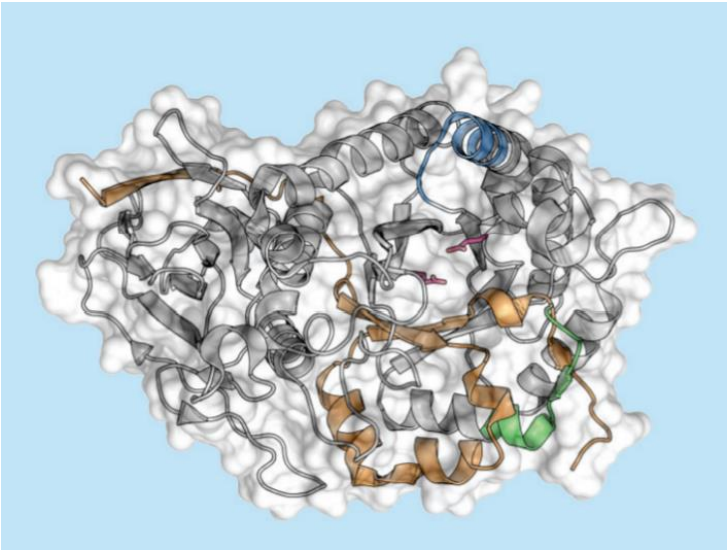

Figure 9. A 3D model of human *endo*-acting heparanase, based on its crystal structure as determined by *Wu et al. (2015).* Taken from *Rivara et al. (2016)*.

This enzyme is notorious among researchers, being a very negative marker in various pathological scenarios.[95] This is because heparan sulfate side chains play a major role in various extracellular processes, such as maintaining the structural integrity of a cell, as well as cellular organisation via interactions with various compounds in the body.[96–101] It thus comes as no surprise that heparanase plays a significant role in tumour progression, but was also found to play a role in other disorders such as Crohn's disease[102] and rheumatoid arthritis[103], but also in rare diseases such as vulvodynia[104] and AA amyloidosis[105].

As the role of heparanase in disease is due to overexpression, treatments commonly involve the inhibition of the enzyme. This includes inhibitions with sulfated polysaccharides[106], pseudosugars[107], heparanase-specific antibodies[108] and nucleic acid-based inhibitors[109], among others.

Inhibitors cannot only be utilised for the treatment of enzymatic disorders, but also to further study their role in disease. In the following chapter, the use of irreversible inhibitors for investigating these β-glucuronidases shall be further discussed.

1.5. The use of irreversible inhibitors for investigating the role and function of β-glucuronidases in diseases.

Using an irreversible inhibitor is an excellent way to assess the role an enzyme plays, both in diseased and healthy tissue. These include catalytic and metabolic pathways, as well as the roles enzymes play in pathology.[110]

Whilst a reversible inhibitor may simply compete with the regular substrate of an enzyme, thus slowing down its conversion kinetics, an irreversible inhibitor will bind covalently to the enzyme at its active site. This bond cannot readily be broken under regular circumstances, thus preventing further conversion.[111]

In many cases, the inhibitor contains an electrophilic group that then reacts with a nucleophilic residue in the active site of the enzyme. These groups may be aldehydes, alkenes, Michael acceptors or nitrogen mustards, among many others.[112]

Whilst inhibitors are readily found in nature as part of metabolic processes, many are also produced artificially in the laboratory.[113,114] These inhibitors can then be utilised in many different ways, including as novel drugs (with approximately 29% of drugs approved in 2019 being enzyme inhibitors)[115] and antibiotics (by inhibiting enzymes vital for the survival of bacterial pathogens)[116,117]. In addition to this, many pesticides and herbicides used in agriculture are enzymatic inhibitors.[118,119]

When it comes to designing novel inhibitors, researchers will often get inspired by natural compounds such as the regular substrate of an enzyme and adjust it to give it inhibiting properties. In other cases, natural inhibitors are adjusted to increase stability, reactivity and/or selectivity.

1.5.1. The discovery of cyclophellitol & its derivatives as an irreversible inhibitor.

Whilst screening for a β-glucosidase inhibitor, *Atsumi et al. (1990)* found that a compound isolated from the mushroom *Phellinus* sp. showed a high inhibition efficacy. Upon further investigation, this compound was identified as cyclophellitol (**5**), as shown

in figure 10.[120] Whilst having a similar structure to β-glucose (**6**), it contains an epoxide instead of an acetal, to which it owes its inhibitory properties.

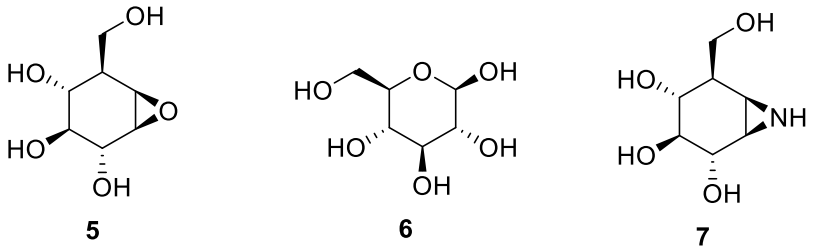

Figure 10. Cyclophellitol (**5**), β-glucose (**6**) and cyclophellitol aziridine (**7**).

Once cyclophellitol is recognised by the enzyme, it undergoes an acid-catalysed ring-opening reaction with the nucleophilic site of the enzyme, leading to an ester bond which cannot be hydrolysed, thus irreversibly inhibiting the enzyme.[121] The mechanism is presented in figure 11.

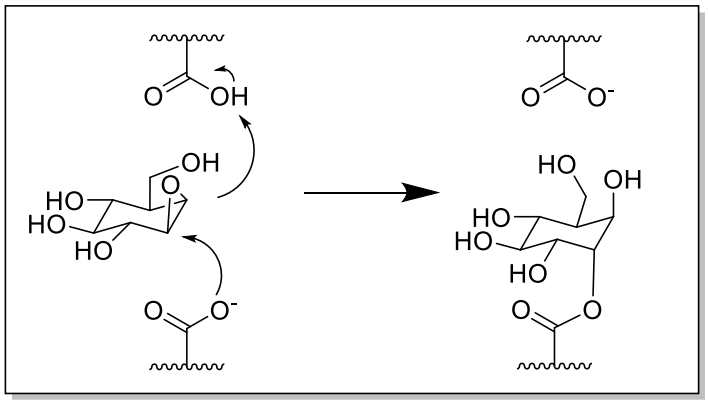

Figure 11. Irreversible inhibition of a β-glucosidase by cyclophellitol.

In 1991, the total synthesis of cyclophellitol, as well as some of its derivatives, was published by *Tatsuta et al. (1991)*, who also found that the aziridine analogue may have a higher inhibitory activity in the case of certain β-glucosidases.[122]

Throughout the years, researchers have synthesised further derivatives of these structures in an attempt to not only boost selectivity and activity, but also to improve these compounds as analytical tools.

Several activity-based probes (ABPs) could be generated using cyclophellitol as a starting point. These ABPs generally consist of a warhead (the reactive moiety, here the aziridine), a linker and a tag to label and visualize the target. Some examples were synthesised by *Kallemeijn et al. (2012)*. The introduction of a fluorescent tag on a

cyclophellitol- or cyclophellitol-aziridine scaffold, as seen in (**8**) and (**9**) (figure 12), allowed for the visualisation of these enzymes in living tissue.[123]

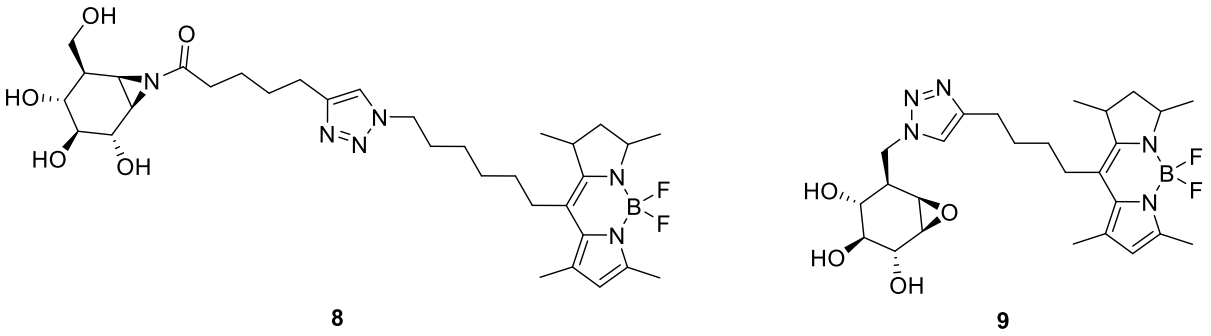

Figure 12. Fluorescent Cyclophellitol-aziridine ABP (**8**) and Cyclophellitol ABP (**9**).

Another study by *Ben Bdira et al. (2016)* used cyclophellitol-aziridine ABPs to investigate whether the stability of a specific β-glucosidase could be influenced by introducing a hydrophobic moiety. Indeed, the connection of an adamantane moiety to the probe (**10**) could significantly increase the melting temperature of the enzyme, thus presenting another example in which these cyclophellitol-based inhibitors can be utilised in research.[124] The probe is presented in figure 13.

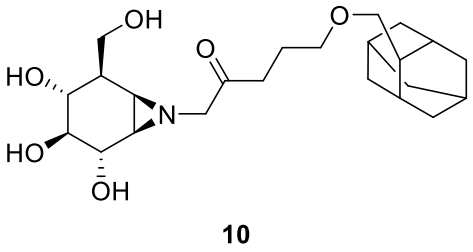

Figure 13. Structure of a cyclophellitol-aziridine ABP with a hydrophobic adamantane moiety.

1.5.2. Improving probe selectivity to target β-glucuronidases.

Whilst a plethora of cyclophellitol-based probes were synthesised to investigate β-glucosidases, it is important to note that the main scaffold that interacts with the enzyme largely remains the same, leaving much to be desired when it comes to the selectivity of the probes.

As the name suggests, β-glucuronidases specifically cleave the bonds between a compound and glucuronic acid. To visualise this, an example reaction is presented in figure 14, where 2-naphthol glucuronide (**11**) is hydrolyzed.[125]

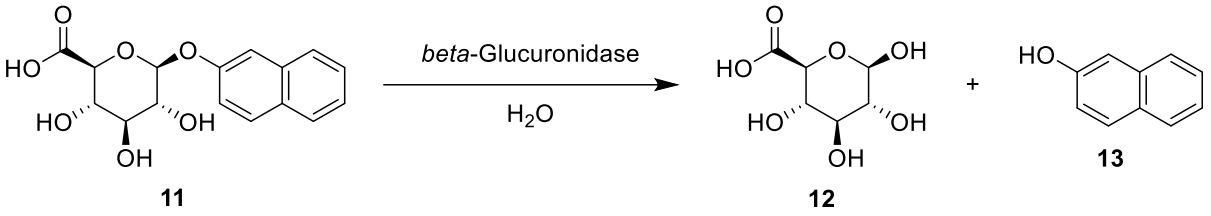

Figure 14. Hydrolysis of 2-naphthol glucuronide (**11**) to glucuronic acid (**12**) and naphtalen-2-ol (**13**).

A clear difference can be noted when comparing glucuronic acid (**12**) to cyclophellitol (**5**) and β-glucose (**6**). The carboxylic acid at the C6 position does not change the hydrolysis, so it likely plays a key role in substrate recognition. Indeed, a study done by *Wu et al. (2015)* reveals that the carboxylate interacts with multiple amino acid moieties in the active site of *endo*-acting heparanase (figure 15).[94]

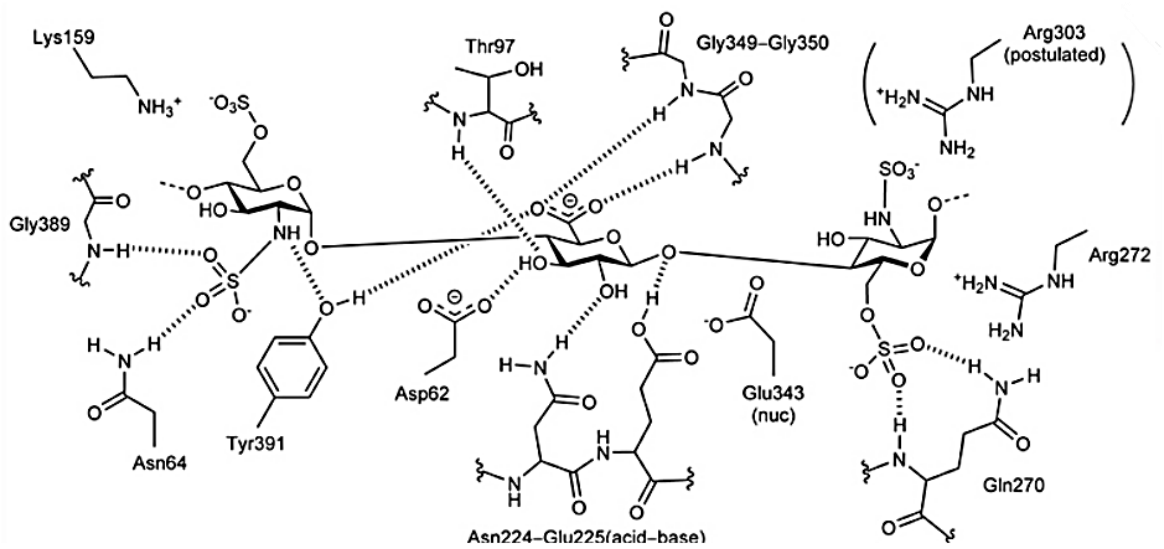

Figure 15. Substrate interactions in *endo*-acting heparanase. The image shows an interaction between the carboxylate group and the amino acid residues Gly349-Gly350 and Tyr391. Taken from Wu et al. (2015).

Wu et al. (2017) proposed a new probe. Its structure was similar to the one published by *Kallemeijn et al. (2012)*, with a key difference being the oxidised alcohol at the C6 in an attempt to more closely mimic glucuronic acid. Indeed, this key difference showed superior specificity compared to its predecessors, labelling both the aforementioned *exo*-acting β-glucuronidase, as well as *endo*-acting heparanase. Nevertheless, off-target effects were still not completely excluded, with the probe also binding to

glucocerebrosidase and β-galactosidase, as well as ProHSPE, a proenzyme of *endo*-acting heparanase, which still limits its usage in clinical applications.[123,126]

The structure of this novel β-glucuronidase probe is presented in figure 16.

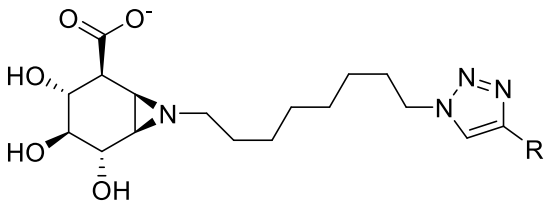

14

Figure 16. Structure of the novel β-glucuronidase ABP (**14**) by *Wu et al. (2017)*. Various groups have been attached to the spacer, such as biotin and Cy5.

1.5.3. Novel synthesis pathway of the β-glucuronidase ABP (**14**).

The synthesis of this novel ABP can be divided into three parts: the generation of the carbocycle, the consequent aziridination, and finally, the introduction of the tag. In the following subchapters, the first two parts of the synthesis shall be examined more closely.

1.5.3.1. Creating the carbocycle.

The synthesis pathway starts from D-xylose (**15**), which undergoes the strategic instalment and removal of several protecting groups. Initially, the hydroxy-group at the anomeric centre is methylated via a Fischer-methylation to yield **16**. This is followed by a tritylation reaction of the primary hydroxy group attached to the C5 of the xylofuranose ring, yielding **17**. Consequently, the hydroxy groups at the C2 and C3 positions are benzylated (**18**), followed by the removal of the previously installed trityl group (**19**).[126,127]

These initial steps are shown in figure 17.

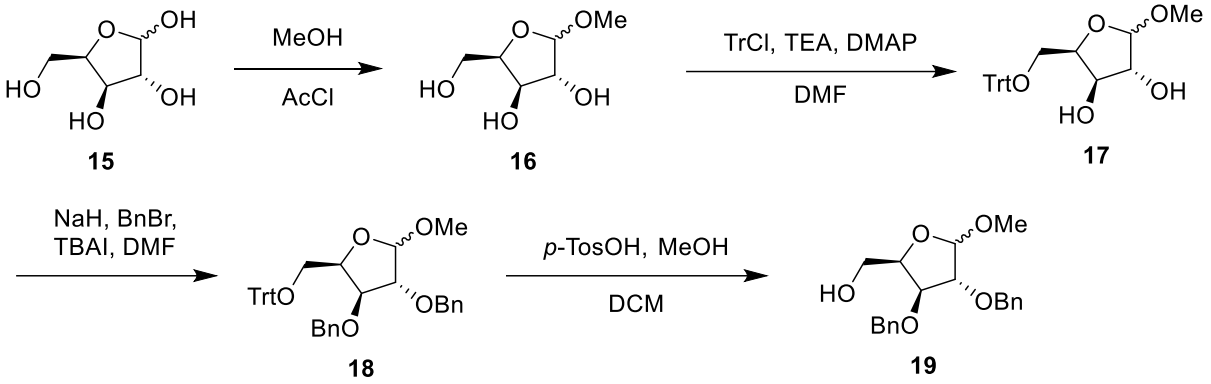

Figure 17. D-xylose undergoes several strategic protecting group instalments and removals, leading to a fully protected xylofuranose ring, with only the hydroxy group at the C5 position exposed.

The synthesis pathway proceeds via the iodination of the hydroxy group at the C5 position (**20**), which then enables a Bernet-Vasella fragmentation reaction. The resulting aldehyde (**21**) undergoes an indium-induced coupling reaction with ethyl 4-bromocrotonate (**22**) to yield a diene structure **23**. Finally, **23** undergoes a Grubbs Olefin Metathesis to yield carbocycle **24**.[126,127]

The abovementioned steps are visualised in figure 18.

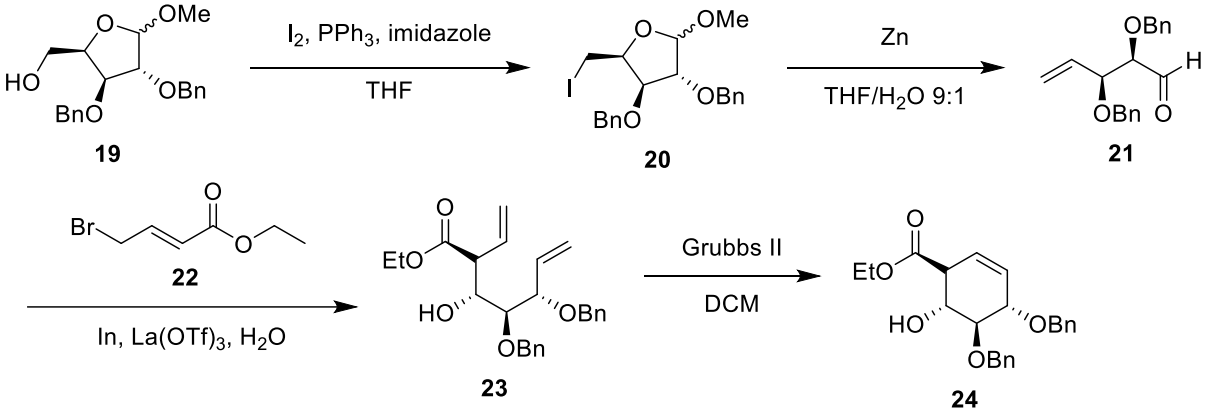

Figure 18. The previously partially protected D-xylose ring is iodinated, followed by a fragmentation reaction. The resulting aldehyde then undergoes a coupling reaction to yield a diene, which ultimately forms the desired carbocycle.

1.5.3.2. Implementation of the aziridine ring and generation of the carboxylic acid.

In an initial step, the ester positioned at the C6 is reduced to an alcohol (**25**) using DiBAl-H. The resulting structure undergoes four steps to introduce the aziridine ring with the correct stereochemistry (**26**). Finally, the aziridine ring is protected with a benzyloxycarbonyl (Cbz) group (**27**), which allows for the oxidation of the hydroxy group position at the C6 (**28**) without opening the ring. Finally, the ring is deprotected

using lithium and ammonia to yield the aziridine cyclophellitol scaffold with a carboxylic acid position at the C6 (**29**).[126,127]

The previously described synthesis pathway is presented in figure 19.

All in all, the synthesis pathway described in the previous two chapters contains 17 individual steps, which would then need to be followed by the introduction of a spacer and tag, as well as the removal of the benzyl groups at the C2 and C3 positions. Based on the reported yields, the total yield for these 17 steps is approximately 12.5%.

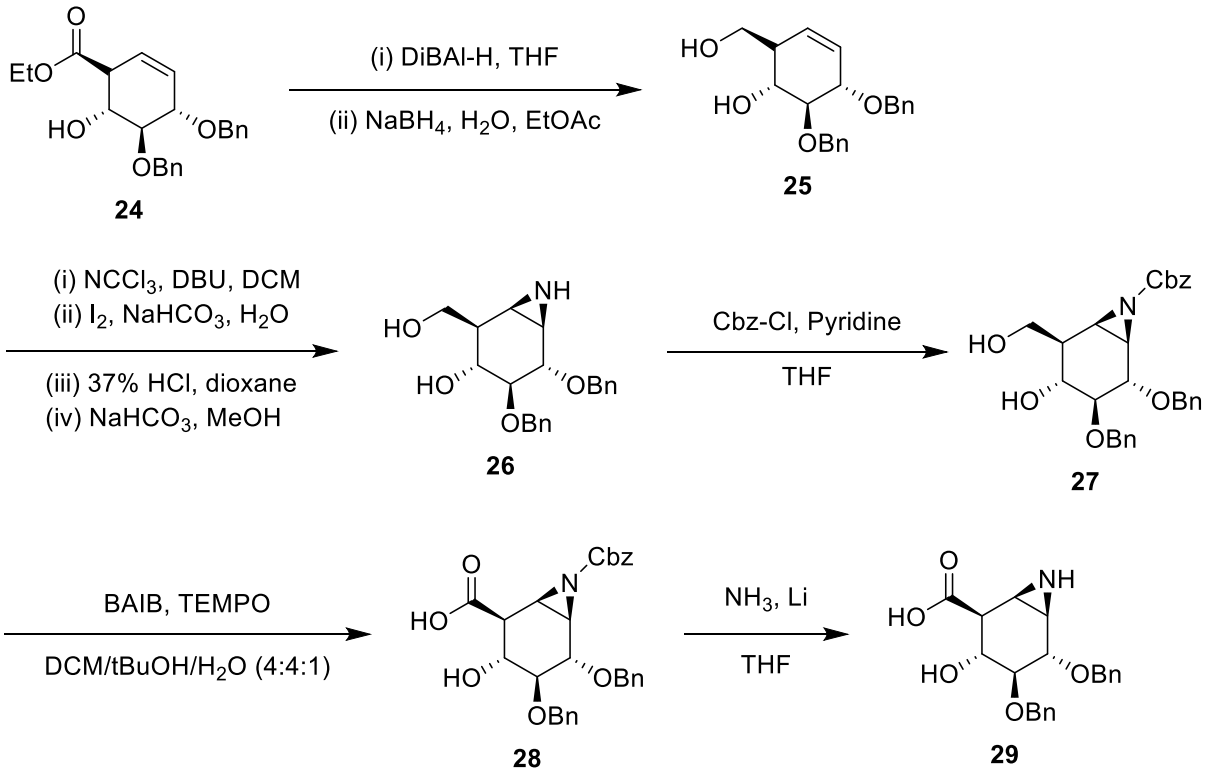

Figure 19. Introducing the aziridine ring to the carbocycle, followed by the oxidation of the C6 hydroxy group without opening the aziridine ring.

2. Aims of this study

2.1. Motivation

Clearly, a lot of progress has been made in the last years regarding the development of a β-glucuronidase-specific activity-based probe. However, due to off-target effects remaining a persistent problem, more research will have to be done on the design of a probe with a higher selectivity.

To generate the main aziridine cyclophellitol scaffold, the generation of the aziridine ring onto the carbocycle is a key step. However, utilising current methods, the four required steps take more than two days in reaction time, which does not include the time required to purify the component after each step. Additionally, the formation of many by-products and only moderate yields leave much to be desired. A more efficient aziridination would be highly beneficial for not only further investigating possible adjustments to the current structure, but may also enable a more convenient synthesis of an optimised probe in the future for clinical application.

2.2. Objective

This study aims to explore whether the aziridine ring can be installed via an alternative, one-step reaction, with the option to potentially influence the stereospecificity via protecting group strategies.

The focus of this project shall lie on synthesising the aforementioned carbocycle via a similar synthesis pathway, after which the aziridine ring is implemented via the usage of 2,4-dinitrophenylhydroxylamine (DPH, **30**) and Du Bois' catalyst ($Rh_2(esp)_2$, **31**), both shown in figure 20.

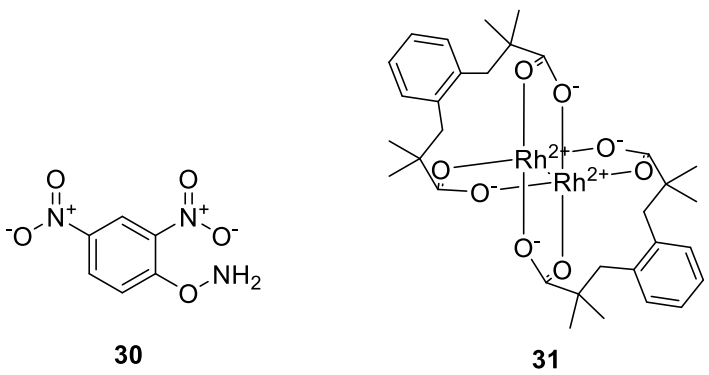

30 **31**

Figure 20. The structures of DPH (**30**) and Du Bois' catalyst (**31**), to be used in the aziridination of the carbocycle.

The synthesis pathway commences via the formation of the carbocycle, utilising D-xylose as a starting point due to the favourable stereochemistry of the hydroxy groups. These steps mimic those previously described in literature, with several minor adjustments in the reaction conditions in an attempt to optimise yield and purity. An overview is presented in figure 21.

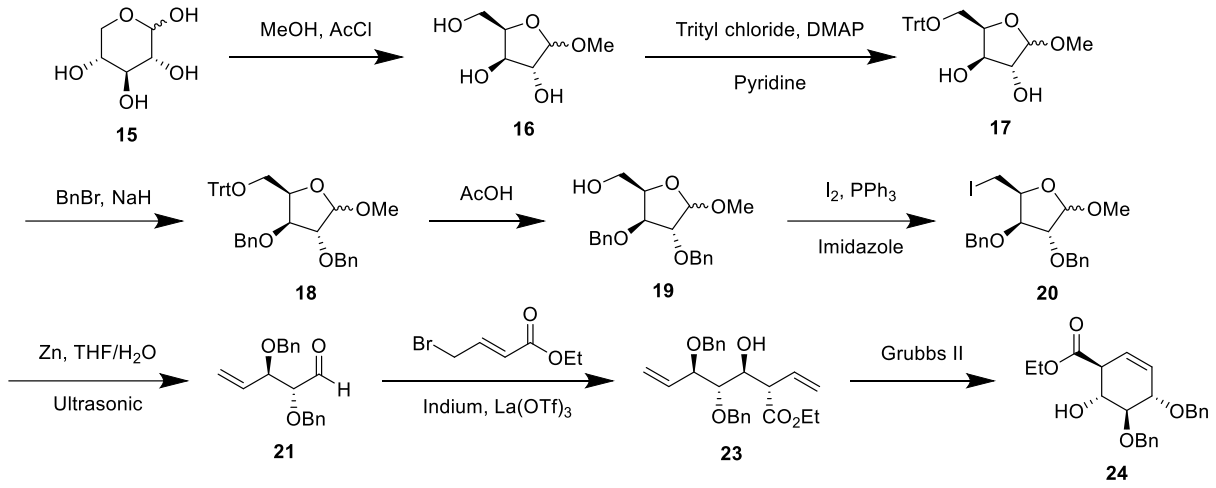

Figure 21. Synthesis pathway of **24**, starting from D-xylose (**15**).

Following the synthesis of carbocycle **24**, the benzyl protection groups are initially removed to prevent any interaction between the benzylic aromatic rings and the aromatic rings of Du Bois' catalyst. This way, the influence of intermolecular interactions on the success or failure of the implementation of the aziridine ring can be limited.

In order to keep the ester and double bond intact, **24** will undergo a mild debenzylation reaction via BCl_3. This reaction scheme is shown in figure 22.

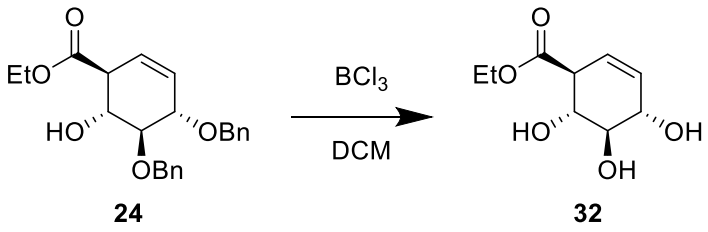

Figure 22. Synthesis pathway of debenzylated carbocycle **32**.

In a subsequent step, the free hydroxy groups are acetylated. This way, the reactivity and specificity of the aziridination reaction can be observed with minimal influence of

the carbocycle, as *Jat et al. (2014)* found that hydroxy groups in the vicinity of the double bond may have a directing effect.[128] The acetylation is presented in figure 23.

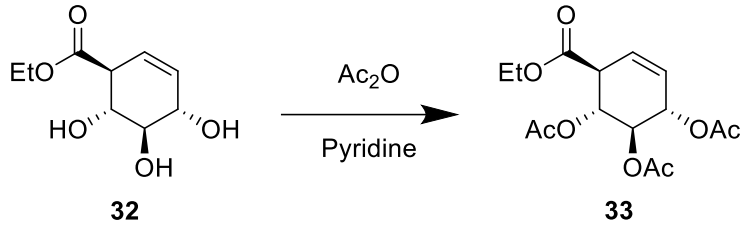

32 **33**

Figure 23. Synthesis pathway of **33**, illustrating the acetylation of the deprotected carbocycle **32**.

Finally, the double bond of the carbocycle shall be aziridinated via the DPH/$Rh_2(esp)_2$ strategy, which shall be further discussed in a later chapter. Important aspects that shall be considered when analysing the success of the reaction are its stereospecificity, with the D-(+)-form being preferred, and overall conversion. This final step is depicted in figure 24.

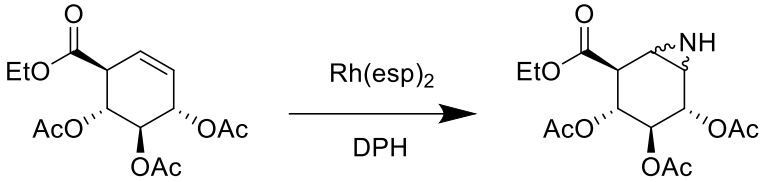

33 **34**

Figure 24. Synthesis pathway to **34**, illustrating the aziridination of fully protected carbocycle **33**.

One final key difference between the presented synthesis pathway and the previously described synthesis is the conservation of the ester functionality at the C6. Within the scope of this project, this has several benefits. First, as previously described, a hydroxy group in the vicinity of the double bond may have a directing effect on the aziridination, which is not desired in preliminary experiments. Second, the ester may be a convenient precursor to the desired carboxylate function. This could either occur immediately within a laboratory setting[1], or the ester moiety could be exploited for its ability to improve cellular uptake, upon which the ester would be hydrolysed via metabolic enzymes (esterases).[129]

[1] Such a method shall be further discussed in the outlook of this thesis.

3. Results and Discussion

In the following chapter, the conducted reactions shall be described in a logical order while discussing the future potential and/or problems when relevant. Unless specifically relevant for the discussion, spectra will be included in the appendix and referred to.

3.1. The synthesis of the carbocycle.

3.1.1. Fischer glycosylation of D-xylose (**15**) to generate methyl xylofuranoside (**16**).

The synthesis of the carbocycle commences with the methylation of the hydroxyl group at the anomeric centre of D-xylose to generate an acetal. Whilst this reaction is frequently described in literature utilising methanolic hydrogen chloride, it is also described using acetyl chloride and dry methanol to generate the required dry acid *in situ*, and this is the method that was chosen within the scope of this project for its convenience. The protocol of *Alcaide et al. (2014)* was followed to synthesise methyl xylofuranoside (**16**) (figure 25).[130,131] No precise conversion rate was determined, as the crude product was used for the following reaction.

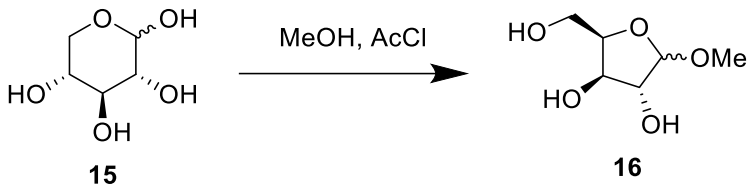

15 **16**

Figure 25. The synthesis of **16**.

In literature, it is described that the resulting product is a 1:1 mixture of the α/β anomers.[132] It should be noted that the anomers do not need to be separated within the proposed synthesis pathway, as the fragmentation reaction will ultimately lead to a singular product.

3.1.2. Tritylation of the C5 primary alcohol (**17**).

To ensure that the C5 hydroxy group can be selectively deprotected prior to its iodination, it was tritylated based on a protocol previously described by *Jeffrey et al. (2014)* to synthesize **17** with an isolated yield of 85% (figure 26).[133]

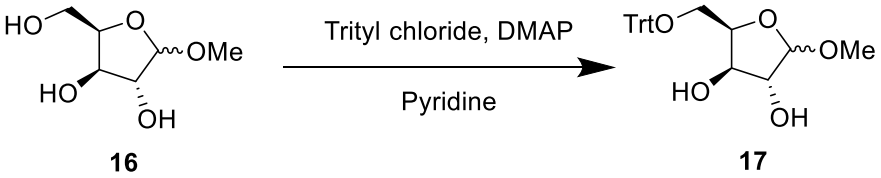

16 **17**

Figure 26. The synthesis of **17**.

3.1.3. The benzylation of **17** to yield the fully protected xylofuranose ring (**18**).

To ensure that the C5 hydroxy group was selectively iodinated, all other hydroxy groups needed to be protected. To this end, the C2 and C3 hydroxy groups were benzylated as done previously by *Jeffrey et al. (2014)* and *Alcaide et al. (2015)*.[131,133]

Ultimately, **18** could be isolated with a yield of 89% (figure 27).

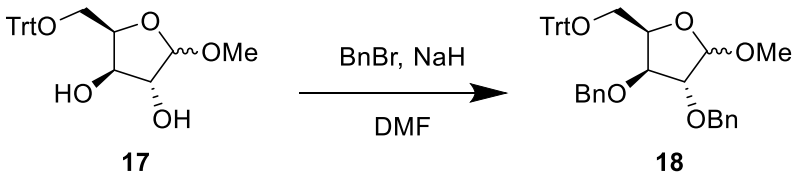

17 **18**

Figure 27. The synthesis of **18**.

Several safety aspects needed to be considered during this benzylation reaction. *Yang et al. (2019)* published an excellent review on the underappreciated danger that NaH/DMF mixtures pose, describing a self-heating process that would commence at temperatures as low as 26 °C, capable of heating a reaction mixture well above 100 °C.[134] In addition to this, they found that a mixture of DMF, NaH and silicone oil will start to decompose exothermically at temperatures as low as 76 °C.[135] It was thus important that the temperature of the reaction was controlled, the reaction mixture was adequately diluted, and a sufficiently large flask was utilised.

3.1.4. Deprotection of the C5 primary alcohol (**19**).

To enable the iodination to facilitate the fragmentation reaction, the primary alcohol at the C5 position had to selectively be deprotected. This could be done selectively without affecting the other protecting groups based on a protocol previously described by *France et al. (2004)*.[136]

19 could be isolated with a yield of 97% (figure 28).

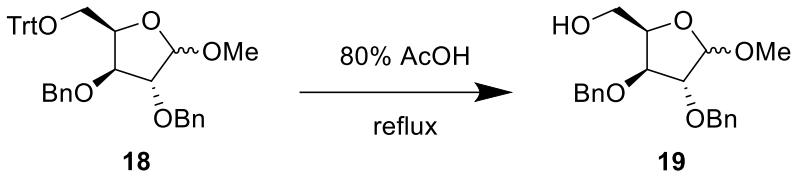

18 **19**

Figure 28. The synthesis of **19**.

3.1.5. The iodination of the C5 primary alcohol (**20**).

The iodination of the C5 primary alcohol is the last step required for the Bernet-Vasella fragmentation, required for the construction of the carbocycle. The selective iodination of this position was optimised by *Skaanderup et al. (2002)*, who investigated this reaction for similar fragmentation reactions.[132]

To facilitate the iodination, **19** was dissolved in dry THF. While iodination reactions were more commonly done in toluene, *Skaanderup et al. (2002)* found that the poor solubility of certain sugars presented an issue for the universal application of the reaction, describing THF as a superior solvent which allowed the reaction to take place at lower temperatures.[137]

Triphenylphosphine and imidazole were then added to the reaction mixture. While triphenylphosphine has always been a common reagent in bromination and chlorination reactions, its utilisation in iodination reactions has historically been somewhat limited due to its ability to form an insoluble salt with iodine.[138,139] Imidazole is added to the reaction mixture to prevent this salt formation.[140]

20 could be obtained with a conversion rate of 67%, though a significant amount of starting material could also be isolated from the reaction mixture (figure 29).

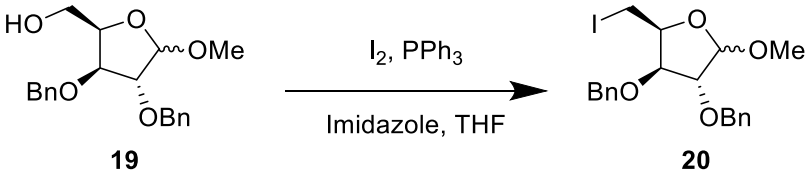

19 **20**

Figure 29. The synthesis of **20**.

3.1.6. Bernet-Vasella Fragmentation (**21**).

As previously described in chapter 2 of this thesis, the xylofuranose ring is opened in order to extend the chain and finally synthesise the desired carbocycle. The Bernet-Vasella Fragmentation reaction is a zinc-mediated stereo-controlled fragmentation reaction that leads to an olefinic aldehyde structure.[141]

The hypothesised mechanism of the reaction is described as undergoing a zinc-mediated single electron transfer (SET) step, leading to the insertion of the zinc. This can be compared to the formation of a Grignard reagent. A second SET step causes the fragmentation of the heterocyclic sugar cycle, after which $Zn^{II}(OMe)I$ is eliminated to form the aldehyde moiety.[142] An overview of this proposed mechanism is presented in figure 30.

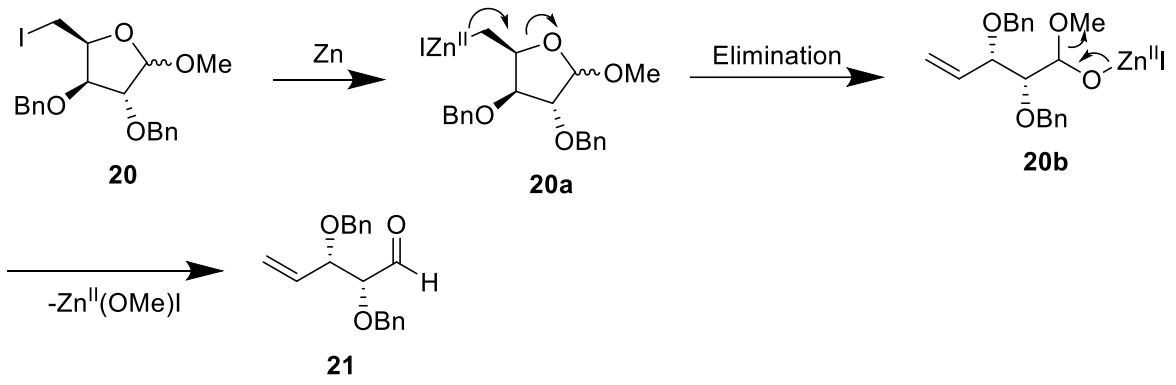

Figure 30. Illustration of the proposed mechanism of the Bernet-Vasella Ring-Opening reaction.

For this reaction, powdered zinc was utilised, which initially had to be activated with hydrochloric acid to remove the oxide layer to allow the reaction to occur. After stirring zinc powder in 1M HCl for one hour, the zinc was washed with water and diethyl ether, followed by drying under vacuum.

20 was then dissolved in a 9:1 degassed mixture of THF and water, and after adding the activated zinc, the reaction mixture was sonicated at 40 °C until the completion of the reaction. The reaction progress was followed closely by TLC. Alas, this reaction was not without its complications. Several attempts to generate the desired aldehyde failed following the protocol described above, and so alternative methods were attempted. One deviation from the original protocol was the usage of stronger acid to activate the zinc (3M and 6M HCl), though this did not appear to benefit the conversion. Another protocol by *Win-Mason et al. (2011)* describes utilising a different solvent

system (EtOH/H_2O/AcOH 40:2:1) and heating the reaction mixture to reflux instead of using a sonicator, but this, too, did not seem to positively benefit the conversion of the reaction.[143]

As the *Win-Mason* protocol did not work, it could be excluded that the sonicator is the root of the problem, and the use of variously concentrated hydrochloric acid solutions would suggest that the initial activation may not be the problem. Upon confirming that **20** was, indeed, the correct structure, it was determined that the most likely cause for this hurdle was the reformation of the zinc oxide layer during the isolation, washing and drying of the activated zinc, indicating that I had not mastered this part of the procedure yet sufficiently. Finally, **20** was successfully converted into the desired olefinic aldehyde with a conversion rate of 49% (figure 30).

3.1.7. Indium-induced coupling reaction (**23**).

To generate the desired six-membered carbocycle, the initially synthesised olefinic aldehyde needed to be extended. This was done via a Barbier coupling – an indium-induced coupling reaction, commonly utilised to connect an alkyl halide to a ketone or aldehyde.[144]

This reaction required Lanthanum(III) trifluoromethanesulfonate ($La(OTf)_3$) as a water-compatible Lewis acid catalyst, which has been described in several pieces of literature as vital for a satisfactory conversion rate.[145–147] $La(OTf)_3$ could conveniently be synthesised in the laboratory via the addition of lanthanum oxide to an excess of triflic acid.

For the Barbier coupling, **21**, ethyl 4-bromocrotonate, indium (in the form of a fine powder) and $La(OTf)_3$ were utilized to facilitate the formation of **23**, which could be isolated with a yield of 53% (figure 31).

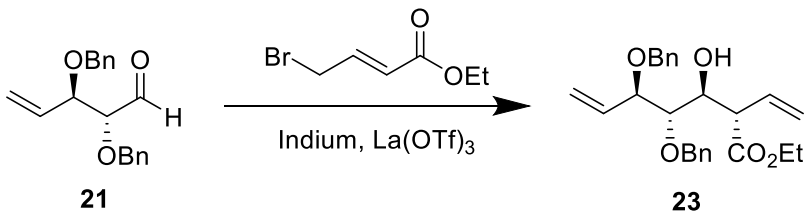

21 **23**

Figure 31. The synthesis of **23**.

3.1.8. Grubbs Ring-Closing Metathesis for the formation of the carbocycle (**24**).

With the diene **23** now available, it was possible to generate the desired carbocycle **24**. This could conveniently be achieved via a Grubbs Ring-Closing Metathesis, requiring the second generation Grubbs catalyst, a ruthenium catalyst commonly utilised for the formation of novel olefinic bonds.[148–150]

Ultimately**, 24** could be synthesized with a conversion rate of 83% (figure 32).

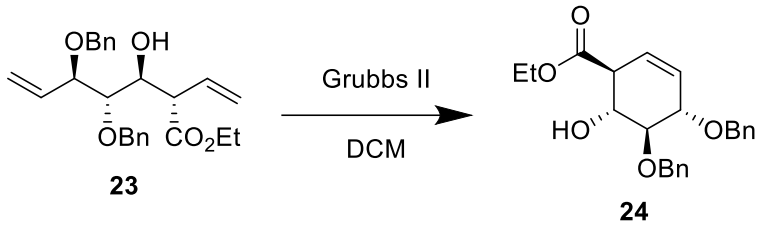

Figure 32. The synthesis of **24**.

3.2. Functionalisation of the carbocycle.

As previously described, the goal of this project is to find a more convenient method for the aziridination of the carbocycle to establish the desired cyclophellitol aziridine scaffold. The experiments toward this objective are described in the following chapters.

3.2.1. Debenzylation of the carbocycle (**32**).

As mentioned in chapter two of this thesis, the removal of the benzyl groups is done in an initial step to prevent potential interactions between Du Bois' catalyst at the final step and the aromatic rings of the benzyl groups. To this end, a mild debenzylation protocol was chosen, which utilises BCl_3 and is based on a protocol previously described by *Xie et al. (2005).* In the publication, the compound that was studied has a double bond, suggesting that this method would not affect the double bond of **24**.[151] However, prior to this reaction, it was unknown whether the ethyl ester moiety would not be affected.

Indeed, **32** could be isolated with a conversion rate of 74% (figure 33).

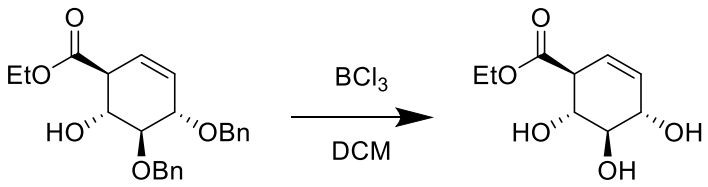

24 **32**

Figure 33. The synthesis of **32**.

It should be noted that this reaction was attempted at -40 °C as well, though this led to the formation of a side product, which could not be separated from **32** via column chromatography and was not further identified.

3.2.2. Acetylation of the hydroxy groups (**33**).

In a final step before the aziridination of the carbocycle, the goal was the acetylation of all free hydroxy groups to prevent any possible directing effects that may affect the stereoselectivity of the reaction. The protocol utilised for this, too, was described in the publication by *Xie et al. (2005)*.[151]

In this experiment, **32** was added to a 2:1 mixture of dry pyridine:Ac_2O, and was stirred for 15 hours. However, this method did not yield the desired product. Instead, the main product appears to be a pyridinium derivative. The recorded NMR spectra suggest a structure that is similar to pyridinium acetate, one of the by-products of the reaction, but the presence of ethyl ester peaks in both the ^{1}H- and ^{13}C NMR spectra suggests that it underwent an additional transformation.[152] Regardless, this would suggest that **32** may be sensitive under these conditions. Despite the analysis of all fractions collected from the column chromatography purification, as well as the water phase from the initial wash, the product could not be isolated.

Another attempt was made, during which the reaction progress was closely followed with TLC and immediately terminated after the starting product was completely consumed. Then, in order to prevent potential complications during the washing step, the crude product was immediately purified via column chromatography. Alas, this led to the same result (appendix, figures 59 and 60).

Despite several optimisation attempts, I did not succeed in acetylating the debenzylated carbocycle with the above-described reaction conditions (figure 34). Due to time constraints, the precise reason was not further investigated.

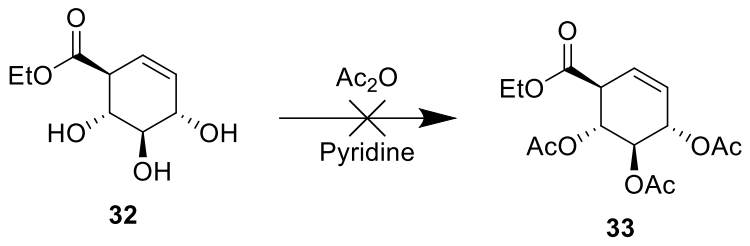

32 **33**

Figure 34. The synthesis of **33**.

4. Conclusions

Within the scope of this thesis, various valuable pieces of information could be gathered on the potential synthesis of a β-glucuronidase irreversible inhibitor. While time constraints prevented the synthesis of target compound **34**, the establishment that the deprotected carbocycle with ester moiety (**32**) could effectively be synthesized may prove to be an efficient asset for synthesizing the ultimate cyclophellitol aziridine probe, as this may suggest that the reduction of the ester to the primary alcohol and later oxidation to the desired carboxylate functionality, as described in literature, may not be required, saving several steps in the final synthesis pathway. The outlook of this thesis aims to explore several possibilities in this regard.

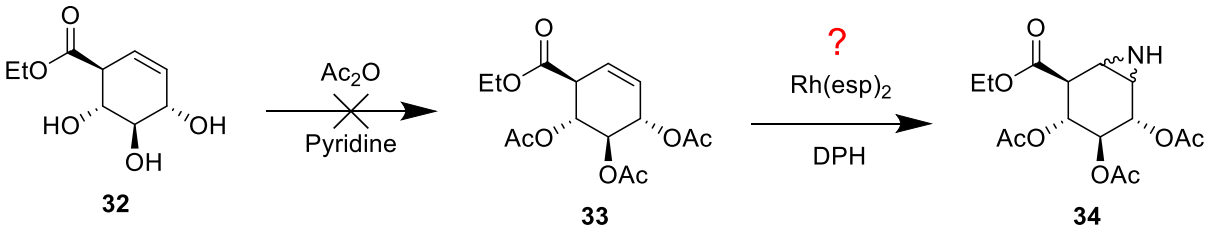

Figure 35. The result of the experiments within the scope of this thesis.

As previously mentioned, and shown in figure 35, the results of the experiments within the project have shown that the chosen acetylation conditions are not suitable for **32**, as the variation of various factors, including reaction time and purification, led to the same result. Nevertheless, this knowledge can be utilized to explore not only alternate reaction conditions, but also to potentially investigate the usage of different protection groups altogether. This, too, is further explored in the outlook of this thesis, especially regarding the proposed reaction conditions for the one-step aziridination.

5. Outlook

Building on the results of this project, several possible routes could be explored in the future towards the development of a more efficient synthesis pathway towards the desired cyclophellitol aziridine-based probe. Several of these shall be discussed in the following chapter, as well as some hypotheses on the potential further improvement of the selectivity of the final probe to specifically target the desired β-glucuronidases.

5.1. Acetylation of the carbocycle.

As described in this thesis, the classic approach of acetylating the free hydroxy groups of a carbocycle with a mixture of dry pyridine and acetic anhydride did not lead to the desired structure **33**, despite being widely reported as being utilized for the acetylation of similar structures.[153–155] This leads to the hypothesis that the ester functionality in the C6 position of the carbocycle may be incompatible with these reaction conditions. The NMR data of the isolated product of the attempted acetylation reaction appears to support this. While the precise structure of the product was not identified, the appearance of characteristic peaks of an ethyl ester, along with characteristic pyridine peaks, suggest an interaction between the ester functionality and either pyridine or pyridinium acetate, a side product that is formed during the reaction.

Though it cannot be excluded entirely that the unsuccessful conversion may have been due to other factors, such as how dryness of the reagents, it may nevertheless be beneficial to explore alternative means of acetylation. In literature, acetylation reactions are described under a variety of reaction conditions with excellent yields for their respective structures, providing several alternative routes to explore. While the usage of acetic anhydride appears to be nigh universal in these reactions, the base, in particular, appears to be variable. *Dou & Jiang (2016)* conducted an acetylation reaction on 6-keto-lithocholic acid methyl ester using sodium carbonate in dry DCM at room temperature, reporting a 96% yield.[156] As this structure contains an ester moiety that in unaffected by these conditions, as well as the mild reaction conditions overall, it may prove to be a lucrative alternative to the classic pyridine protocol.

Alternatively, the same structure described above was synthesized using a combination of triethylamine and DMAP as a catalyst in anhydrous ethyl acetate by *Liang et al. (2020)*, resulting in shorter reaction times and a yield of 98%.[157] Additionally, *Zhou et al. (2018)* utilized the same conditions to acetylate a structure

with both a double bond and an ethyl ester, suggesting that these conditions are, indeed, compatible with the functional groups present in the carbocycle synthesized in this project.[158] An overview of the methods described above is presented in figure 36.

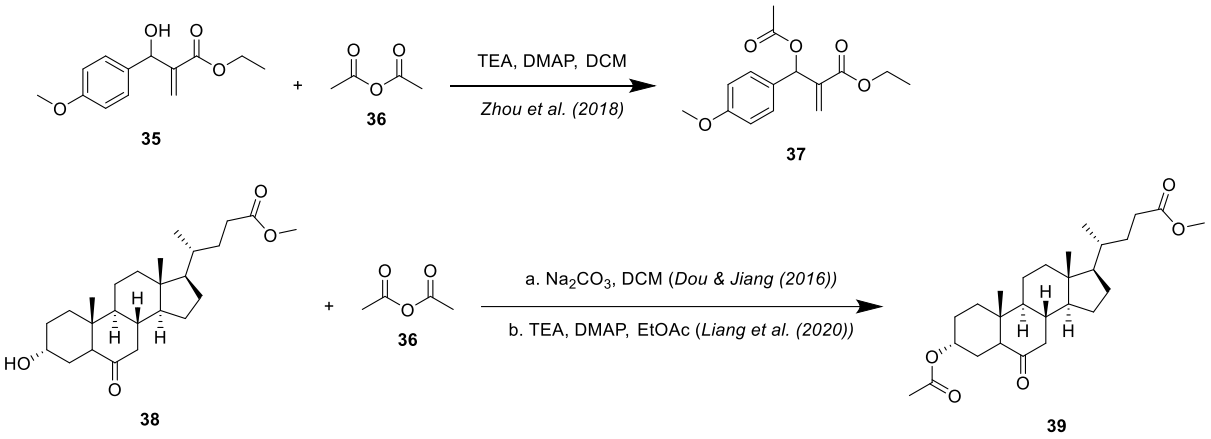

Figure 36. An overview of potential alternative acetylation reaction conditions.

Alternatively, an alternate acetylation reagent may be considered. *Hribernik et al. (2021)* describe the acetylation of sugar hydroxy groups by adding the starting material to dry acetyl chloride at room temperature with a methyl ester present in the structure. This may provide yet another possible acetylation method that is compatible with the functional moieties of carbocycle **32**.[159,160]

5.2. The aziridination of the carbocycle.

As time constraints prevented an attempt at the intended aziridination reaction under the chosen conditions, it is currently unclear whether these conditions are compatible with the carbocycle. However, while verification via experiments would certainly be necessary, various data from literature may provide an indication for the potential success of the reaction.

Previously, *Jat et al. (2014)* conducted various experiments using DPH and Du Bois' catalyst for the aziridination of various compounds. In particular, the synthesis of Methyl (Z)-8-[3-(2R-hydroxyoctyl)aziridine-2-yl]octanoate (**40**) may provide evidence of the stability of esters, as well as hydroxy groups under these reaction conditions. Further, the group successfully synthesized 5-(3,3-Dimethylaziridin-2-yl)-3-methylpent-2(E)-en-1-yl acetate (**41**), showing that the acetoxy group also is not impacted by the reaction. Finally, various cyclic alkenes were aziridinated within the scope of the publication with good yield, providing evidence that the usage of DPH and

Du Bois' catalyst for the aziridination reaction is not limited by the cyclic or acyclic nature of the compound.[128,159,161]

An overview of the previously discussed reactions is presented in figure 37.

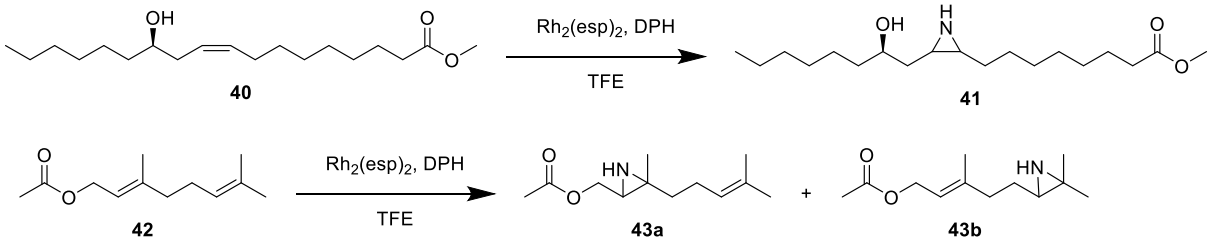

Figure 37. An overview of previously conducted aziridination reactions of compounds with similar functional groups as carbocycle **33** using Du Bois' catalyst and DPH.

5.3. Optimising the stereoselectivity of the aziridination reaction.

While the reactions described in the previous subchapter may provide some indication of the success of the targeted aziridination reaction, the stereoselectivity of the reaction remains an important factor that is yet to be explored. *Jat et al. (2014)* describe that, in most cases, a racemic mixture is formed with no specific preference for either diastereomer.[128]

However, one of the synthesized compounds by the aforementioned group stands out. When attempting the aziridination of cholesterol, the β-aziridine was solely formed, which is attributed to a potential directing effect of the C3 hydroxy group in the case of cyclic alkenes. This same directing effect could be exploited when synthesizing the desired cyclophellitol aziridine derivative, though an alternate protection group strategy may need to be used to enable this.

Figure 38 shows one potential strategy that may enable the exclusive formation of the correct diastereomer. To selectively protect the C2 and C4 hydroxy groups, a protocol based on the work of *Gersbach et al. (2011*) may be used. In this protocol, $tBu_2Si(OTf)_2$ and pyridine are utilized to selectively protect a 1,3-diol. [162]

With the C3 hydroxy group unprotected, the utilization of the aforementioned aziridination conditions could potentially lead to the stereoselective formation of the β-diastereomer, though this would need to be experimentally verified. Additionally, the ultimate removal of the di-tert-butylsilyl group may prove complicated. The protocol by

Gersbach et al. (2011) uses a hydrogen fluoride pyridine complex, but unfortunately, hydrogen fluoride is well-known to open the aziridine ring.[163–165] However, *Vedejs et al. (2000)* have shown that a methylated aziridine is compatible with the aforementioned deprotection conditions.[166] While the protection and deprotection will add additional steps to the complete synthesis pathway, it may be beneficial in terms of final yield. The final demethylation of the aziridine ring without affecting the other functional moieties of the molecule may be achieved via a protocol proposed by *Kok et al. (2010)*. Here, a combination of *m*-CPBA and iron powder is used to remove the methyl group without causing a subsequent ring opening via a two-step Polonovski-type reaction. The paper has shown that the reaction can be conducted without affecting hydroxy groups, and as *m*-CPBA can be utilized to form esters from ketones, it is unlikely that the ethyl ester shall be affected.[167] An overview of the proposed, hypothetical synthesis pathway is shown in figure 38.

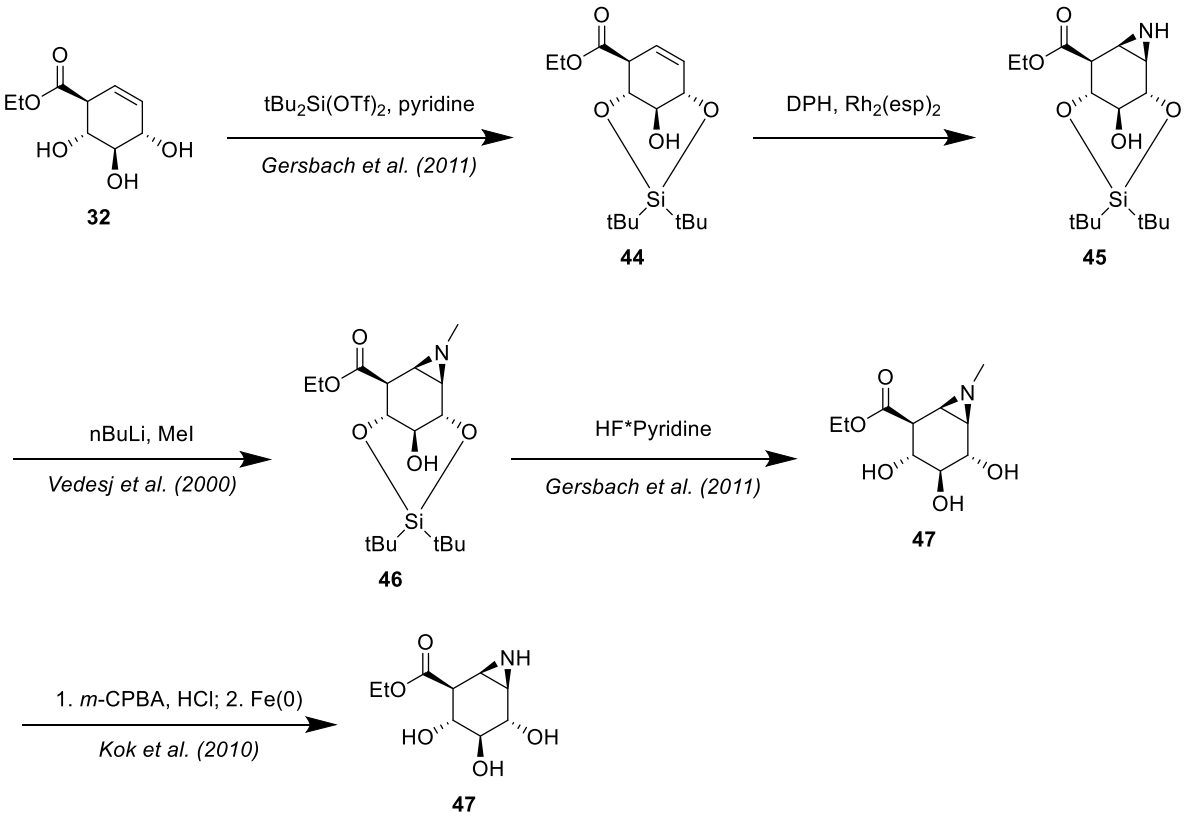

Figure 38. Proposed, hypothetical synthesis pathway for the synthesis of the β-cyclophellitol aziridine derivative **47**.

5.4. Aziridine-compatible de-esterification reaction.

Any proposed route towards a β-cyclophellitol aziridine derivative described in this project (such as the one seen in figure 38) leads to a structure with an ester

functionality, which would require conversion into a carboxylate. As mentioned previously, this could potentially occur *in vivo*[129], though an alternative mild de-esterification may be desired in cases where this is not possible, i.e. when working *in vitro*.

Whilst current literature offers a wide array of de-esterification methods (such as using hydrogen with palladium or platinum on carbon)[168], these methods often lead to the opening of the aziridine ring. Nevertheless, the usage of either methanolic- or ethanolic alkali hydroxide solutions has been reported to be effective at facilitating the desired de-esterification without ring opening, and, though neutralisation with an acid such as hydrogen chloride would lead to undesired side reactions, the usage of an acidic Dower ion exchange resin such as Dowex 50W-X2 is described to be compatible with the aziridine functionality.[169,170]

5.5. Improving the selectivity of the irreversible inhibitor.

As described previously within the scope of this thesis, the cyclophellitol aziridine derivative with carboxylate functionality proves to be significantly more specific than its predecessors. However, it is still not perfect, with the probe also binding to glucocerebrosidase and β-galactosidase, as well as ProHSPE, a proenzyme of *endo*-acting heparanase.[123,126]

As *Wu et al. (2015)* have shown, *endo*-acting heparanase interacts not only with the cyclophellitol scaffold, but also the heparan sulfate moiety (as shown in figure 15).[94] This would suggest that adding an additional sulfonated monosaccharide may yield improvements in binding to *endo*-acting heparanase.

Naggi et al. (2005) have previously researched the usage of sulfonated polysaccharides for the modulation of heparanase activity, and this data could potentially be used as a foundation for designing a more selective irreversible inhibitor based on the cyclophellitol aziridine derivative with carboxylate functionality.[106]

6. Experimental section

6.1. General information

Air- and moisture-sensitive reactions were carried out under a nitrogen atmosphere. Moisture- and air-sensitive reagents were transferred into disposable syringes and cannulas previously rinsed with nitrogen. The chemicals used were purchased from the companies ACROS, ALFA AESAR, APPLICHEM, CARBOLUTION CHEMICALS, FLUKA, MERCK, ROTH, SIGMA-ALDRICH and VWR CHEMICALS and used directly.

6.2. Solvents

The solvents used for the reactions were of "for synthesis" or "for analysis" quality and were used without further purification. All dry solvents were stored under a nitrogen atmosphere and on molecular sieve.

6.3. NMR

All NMR spectra were measured on an AGILENT 400-MR DD2 equipped with a OneNMR probe or a BRUKER 600 MHz with a BBI probe. In the ^{1}H and ^{13}C experiments, the shifts were related to the residual proton content of the solvent and to the carbon atoms of the solvent:

	^{1}H-NMR	^{13}C-NMR
d_1-Chloroform	7.26 ppm	77.0 ppm
d_6-DMSO	2.50 ppm	39.5 ppm
d_4-Methanol	3.31 ppm	49.0 ppm
D_2O	4.79 ppm	-

All chemical shifts δ are in ppm and all coupling constants J in Hz. The following abbreviations were used to describe the spectra: s (singlet), d (doublet), t (triplet), and m (multiplet). It should be noted that the integrations reported may be higher than expected for the target compounds due to impurities that were not removed from the sample, as they were deemed unproblematic for further reactions.

6.4. Experiments

6.4.1. (2R,3R,4R)-2-(hydroxymethyl)-5-methoxytetrahydrofuran-3,4-diol (**16**).

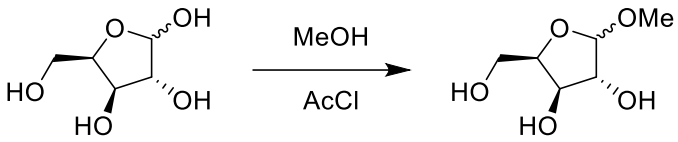

15 **16**

480 mL dry methanol was cooled with an ice bath, and acetyl chloride (7.6 mL, 107 mmol, 0.8 eq.) was added dropwise. After 10 minutes of stirring, D-Xylose (20 g, 133 mmol, 1 eq.) was added. The reaction mixture was stirred for 6 hours. The reaction was quenched by adding powdered $NaHCO_3$ until a pH of 7. Consequently, the mixture was reduced to a volume of approximately 100 mL, after which it was diluted to a volume of 500 mL with DCM. The mixture was filtered through a celite pad, and the solvent was removed *in vacuo* to yield **16** as a crude product. (25.6 g) as a sticky, white solid.

The sample was not further purified at this stage, which led to a yield with a mass that exceeds 100% of the theoretical yield (117%). α and β were not separated.

^{1}H NMR (400 MHz, D_2O) δ 4.87 (d, 1H), 4.77 (s, 1H), 4.26 – 4.06 (m, 5H), 3.74 – 3.57 (m, 5H), 3.31 (s, 3H), 3.26 (s, 3H).

^{13}C NMR (101 MHz, D_2O) δ 108.51, 101.94, 82.47, 79.75, 78.17, 76.56, 74.82, 60.96, 60.33, 55.50, 55.08.

6.4.2. (3R,4R,5R)-2-methoxy-5-((trityloxy)methyl)tetrahydrofuran-3,4-diol (**17**).

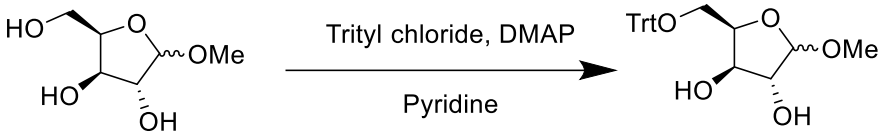

16 **17**

16 (25.6 g, 156 mmol, 1 eq.) was dissolved in 500 mL dry pyridine. Trityl chloride (44.56 g, 160 mmol, 1.05 eq.) and DMAP (1.63 g, 13 mmol, 10 mol%) were added, and the reaction was stirred at 70 °C for 5 hours. The reaction was left to reach room temperature and quenched with ice. The mixture was extracted with chloroform, and the combined organic phases were washed with saturated ammonium chloride solution, followed by water. The organic phase was dried over $MgSO_4$ and the solvent was removed *in vacuo*.

The crude product was purified via column chromatography ($CHCl_3$/MeOH 9:1) to yield **17** (46.07 g, 113.3 mmol, 85%) as a yellow-orange oil. α and β were not separated.

^{1}H NMR (400 MHz, CD_3OD) δ 7.46 (td, 15H), 7.30 – 7.24 (m, 15H), 4.91 (d, 1H), 4.41 (dt, 1H), 4.27 (td, 1H), 4.10 (t, 1H), 3.99 – 3.96 (m, 1H), 3.47 (s, 3H), 3.33 (s, 2H).

^{13}C NMR (101 MHz, CD_3OD) δ 148.64, 144.10, 128.54, 127.31, 126.60, 109.40, 102.35, 86.58, 81.99, 80.36, 77.80, 75.93, 75.75, 63.78, 63.04, 54.55, 54.28.

6.4.3. (3R,4S,5R)-3,4-bis(benzyloxy)-2-methoxy-5-((trityloxy)methyl)tetrahydrofuran (**18**).

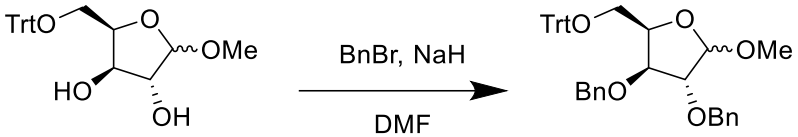

17 **18**

17 (46.07 g, 113 mmol, 1 eq.) was dissolved in 500 mL DMF and cooled with an ice bath. Sodium hydride (22.6 g, 565 mmol, 5 eq.) and benzyl bromide (68 mL, 565 mmol, 5 eq.) were added. The mixture was stirred at 0 °C for one hour, after which it was allowed to reach room temperature and was stirred for another 20 hours. Then, the reaction was quenched with water at 0 °C, and the aqueous phase was extracted with MTBE. The organic phases were combined, washed with brine, and dried over $MgSO_4$. The solvent was removed *in vacuo*.

The crude product was purified via column chromatography (Petroleum ether/Ethyl acetate 9:1 → 3:1) to yield **18** (59.26 g, 101.0 mmol, 89%) as an orange oil.

It should be noted that residual side products could not be separated from the sample. After the column, no further attempts at purifying the sample were made.

^{1}H NMR (400 MHz, MeOD) δ 7.37 – 7.22 (m, 25H), 4.86 (s, 1H), 4.75 – 4.36 (m, 4H), 4.36 – 3.99 (m, 2H), 3.82 – 3.60 (m, 2H), 3.35 (d, 3H), 3.33 (s, 1H).

^{13}C NMR (101 MHz, MeOD) δ 138.12, 137.80, 128.00, 127.97, 127.94, 127.65, 127.55, 127.52, 127.44, 127.36, 127.32, 109.90, 100.41, 83.97, 83.54, 81.31, 72.14, 71.76, 60.91, 53.97.

6.4.4. ((2R,3S,4R)-3,4-bis(benzyloxy)-5-methoxytetrahydrofuran-2-yl)methanol (**19**).

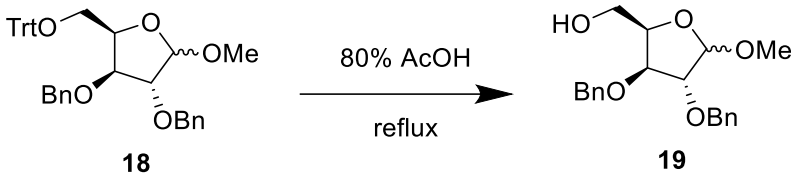

18 **19**

18 (59.26 g, 101 mmol, 1 eq.) was dissolved in 500 mL 80% AcOH and refluxed for 24 hours. The mixture was left to reach room temperature and quenched with brine. The product was then extracted with diethyl ether, and after cooling the organic phase in an ice bath, it was washed with cold saturated $NaHCO_3$ to remove any residual acid. The organic phase was dried over $MgSO_4$ and the solvent was removed *in vacuo*.

The crude product was purified via column chromatography (Petroleum ether/Ethyl acetate 3:1 → 0:1) to yield **19** (34.37 g, 99.8 mmol, 97%) as an orange oil.

It should be noted that residual side products could not be separated from the sample. After the column, no further attempts at purifying the sample were made.

^{1}H NMR (400 MHz, MeOD) δ 7.39 – 7.17 (m, 10H), 4.88 – 4.83 (m, 4H), 4.63 – 4.27 (m, 2H), 4.27 – 3.95 (m, 4H), 3.34 (s, 3H), 3.30 (s, 1H).

^{13}C NMR (101 MHz, MeOD) δ 137.75, 137.63, 128.07, 128.06, 127.69, 127.57, 127.49, 127.39, 107.99, 86.13, 83.42, 72.13, 71.90, 63.25, 54.27.

6.4.5. <u>(2S,3R,4R)-3,4-bis(benzyloxy)-2-(iodomethyl)-5-methoxytetrahydrofuran (**20**).</u>

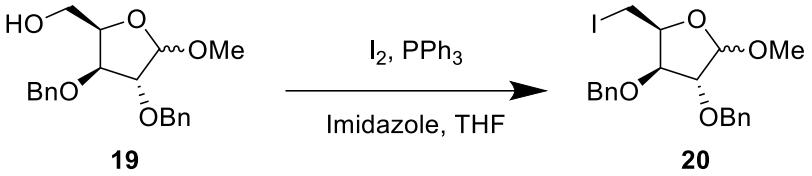

19 **20**

19 (34.37 g, 100 mmol, 1 eq.) was dissolved in 300 mL dry THF. Triphenylphosphine (39.27 g, 150 mmol, 1.5 eq.) and imidazole (13.59 g, 200 mmol, 2 eq.) were added to the solution. Iodine (37.99 g, 150 mmol, 1.5 eq.) was added dropwise as a solution in 100 mL dry THF, and the mixture was brought to reflux for 4 hours. The mixture was then left to reach room temperature, and was filtered through a celite pad. The solvent was removed *in vacuo*, and the crude product was dissolved in ethyl acetate, which was then washed with a saturated sodium thiosulfate solution. The organic phase was dried over $MgSO_4$ and the solvent was removed *in vacuo*.

The crude product was purified via column chromatography (Petroleum ether/Ethyl acetate 8:1) to yield **20** (30.09 g, 66.2 mmol, 67%) as a clear oil. Additionally, 8.22 g of **19** could be recovered.

The purified product still contained triphenylphosphine oxide (TPPO) as a side product, as confirmed via ^{31}P-NMR.

^{1}H NMR (400 MHz, $CDCl_3$) δ 7.34 – 7.25 (m, 10H), 4.92 (d, 2H), 4.64 – 4.36 (m, 4H), 4.00 (d, 2H), 3.39 (d, 4H), 3.17 (dd, 1H).

^{13}C NMR (101 MHz, $CDCl_3$) δ 132.75, 129.17, 129.05, 128.48, 128.43, 128.38, 128.21, 128.01, 127.82, 127.75, 108.27, 100.91, 86.49, 82.00, 81.83, 81.66, 77.70, 72.69, 72.12, 56.03, 55.54, 4.28, 2.78.

^{31}P NMR (162 MHz, $CDCl_3$) δ 44.23 (TPPO).

6.4.6. (2R,3R)-2,3-bis(benzyloxy)pent-4-enal (**21**).

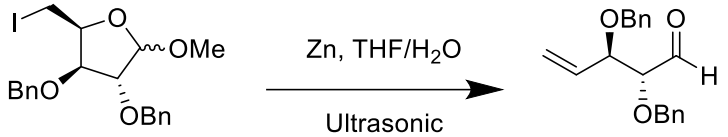

20 **21**

Zinc (21.00 g, 308 mmol, 10 eq.) was added to 70 mL 1M HCl and stirred for 15 minutes. The zinc was washed with water and diethyl ether and then dried *in vacuo* while heating with a heat gun.

20 (14.00 g, 31 mmol, 1 eq.) was dissolved in a 500 mL 9:1 solution of dry THF and degassed water. The activated zinc was added, and the mixture was sonicated at 40 °C for three hours. Upon completion, the reaction mixture was filtered through a celite pad, which was washed with diethyl ether. The organic phase was washed with H_2O, dried over $MgSO_4$ and the solvent was removed *in vacuo*.

The crude product was purified via column chromatography (Petroleum ether/Ethyl acetate 8:1) to yield **21** (4.48 g, 15.1 mmol, 49%) as a clear oil.

The resulting aldehyde was unstable, and required storing under an inert atmosphere in the freezer during the project to prevent decomposition.[171]

^{1}H NMR (400 MHz, $CDCl_3$) δ 9.67 (d, 1H), 7.35 – 7.21 (m, 11H), 5.92 (ddd, 1H), 5.37 – 5.28 (m, 2H), 4.74 (d, 2H), 4.43 – 4.31 (m, 2H), 3.93 – 3.77 (m, 1H).

^{13}C NMR (101 MHz, $CDCl_3$) δ 202.48, 133.78, 129.78, 128.46, 128.34, 128.13, 128.09, 127.90, 127.74, 126.79, 119.84, 85.12, 79.91, 73.43, 70.64.

6.4.7. Ethyl (2S,3S,4S,5R)-4,5-bis(benzyloxy)-3-hydroxy-2-vinylhept-6-enoate (**23**).

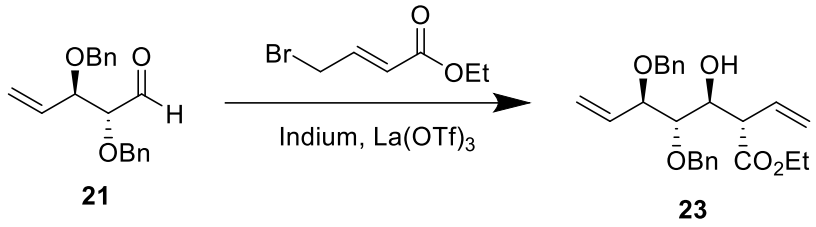

21 **23**

21 (4.48 g, 15.2 mmol, 1 eq.), a 75% solution of ethyl 4-bromocrotonate (9.05 ml, 49.25 mmol, 3.24 eq.), indium powder (4.07 g, 35.42 mmol, 2.33 eq.) and $La(OTf)_3$ (18.71 g, 31.92 mmol, 2.1 eq.) were added to 100 ml water and stirred at room temperature in the dark for two days. The mixture was then filtered through a celite pad, which was rinsed with MTBE. The filtrate was extracted with 3 x 100 mL MTBE, and the organic phase was dried over $MgSO_4$. The solvent was removed *in vacuo*.

The crude product was purified via column chromatography (Petroleum ether/Ethyl acetate 9:1) to yield **23** (3.28 g, 8.0 mmol, 53%) as a clear oil.

^{1}H NMR (400 MHz, $CDCl_3$) δ 7.37 – 7.23 (m, 10H), 6.00 – 5.65 (m, 1H), 5.45 – 5.33 (m, 2H), 5.22 – 5.10 (m, 2H), 5.04 – 4.89 (m, 1H), 4.73 – 4.44 (m, 1H), 4.44 – 4.32 (m, 1H), 4.25 – 4.12 (m, 1H), 4.11 (s, 2H), 4.08 – 3.93 (m, 1H), 3.54 (dd, 1H), 3.50 – 3.22 (m, 1H), 2.71 (d, 1H), 1.22 (td, 3H).

^{13}C NMR (101 MHz, $CDCl_3$) δ 172.46, 138.41, 138.31, 134.90, 132.88, 128.36, 128.34, 128.13, 127.96, 127.95, 127.80, 127.72, 127.53, 119.93, 119.88, 82.87, 79.37, 74.51, 72.09, 70.76, 60.81, 55.12, 53.91, 14.08.

6.4.8. Ethyl (1S,4S,5S,6R)-4,5-bis(benzyloxy)-6-hydroxycyclohex-2-ene-1-carboxylate (**24**).

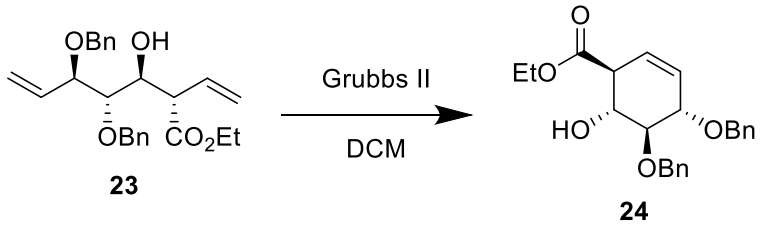

23 **24**

Grubb's II catalyst (849 mg, 1 mmol, 5 mol%) was added to a solution of 23 (3.28 g, 8 mmol, 1 eq.) in 150 ml dry, degassed 1:1 mixture of DCM and toluene. The reaction mixture was stirred at room temperature for 48 hours in the dark. Consequently, 2 mL DMSO was added, and the reaction was stirred overnight. The solvent was then removed *in vacuo*.

The crude product was purified via column chromatography (Petroleum ether/Ethyl acetate 6:1) to yield **24** (2.53 g, 6.6 mmol, 83%) as a clear oil.

^{1}H NMR (400 MHz, $CDCl_3$) δ 7.38 – 7.23 (m, 11H), 5.79 (dt, 1H), 5.66 (dt, 1H), 4.95 (d, 1H), 4.79 (dd, 2H), 4.69 (d, 1H), 4.26 – 4.05 (m, 4H), 3.65 (ddd, 1H), 3.00 – 2.96 (m, 1H), 1.26 (dq, 3H).

^{13}C NMR (101 MHz, $CDCl_3$) δ 171.96, 138.46, 138.03, 128.53, 128.51, 128.26, 127.92, 127.85, 127.83, 124.08, 82.53, 79.25, 77.31, 77.10, 76.88, 74.89, 71.93, 70.42, 61.31, 50.12, 14.23.

6.4.9. Ethyl (1S,4S,5R,6R)-4,5,6-trihydroxycyclohex-2-ene-1-carboxylate (**32**).

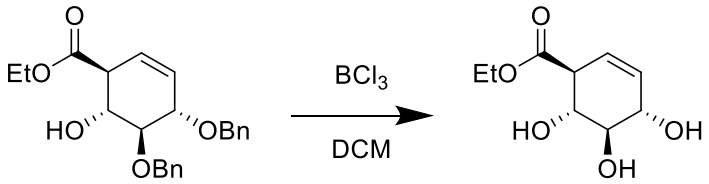

24 **32**

24 (100 mg, 0.26 mmol, 1 eq.) was dissolved in 5 mL dry DCM. After cooling the mixture to -78 °C with an acetone/dry ice bath, 2.6 mL of a 1 M BCl_3 solution in DCM was added, and the reaction mixture was stirred for three hours. Then, the reaction was quenched by adding 15 mL of a 1:1 mixture of MeOH/DCM, and the reaction mixture was slowly brought to room temperature. The solvent, as well as by-products formed during the quenching, were removed *in vacuo.*

The crude product was purified via column chromatography (DCM/Methanol 10:1) to yield **32** (39 mg, 0.2 mmol, 74%) as a clear oil.

MS (ESI, MeOH) positive: *m/z* = 225.08 $[M+Na]^+$, 241.07 $[M+K]^+$

^{1}H NMR (400 MHz MeOD) δ 5.78 – 5.59 (m, 1H), 5.50 (dt, 1H), 4.17 (q, 2H), 4.10 – 3.91 (m, 1H), 3.86 (dd, 1H), 3.56 – 3.34 (m, 1H), 3.14 (dp, 1H), 1.30 – 1.21 (m, 3H).

^{13}C NMR (101 MHz, MeOD) δ 172.61, 131.36, 122.78, 122.69, 122.52, 76.65, 71.83, 70.79, 60.77, 51.15, 13.03.

6.4.10. (1R,2R,3S,6S)-6-(ethoxycarbonyl)cyclohex-4-ene-1,2,3-triyl triacetate (**33**).

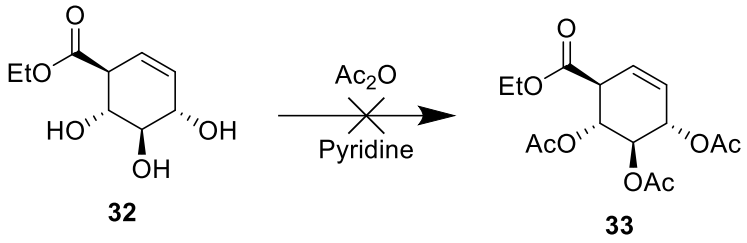

32 **33**

32 (30 mg, 0.15 mmol, 1 eq.) was dissolved in 9 mL of a 2:1 pyridine/Ac_2O solution and stirred at room temperature until the starting material was completely consumed, as indicated by TLC. The reaction mixture was concentrated *in vacuo*, and the compounds were separated via column chromatography (Petroleum ether/Ethyl acetate 6:1). **33** could not be isolated.

7. References

1. Moss, G. P., Smith, P. A. S. & Tavernier, D. Glossary of class names of organic compounds and reactivity intermediates based on structure (IUPAC Recommendations 1995). *Pure Appl. Chem.* **67**, 1307–1375 (1995).

2. Seeberger, P., Finney, N. & Rabuka, D. Chemical and Enzymatic Synthesis of Glycans and Glycoconjugates. in *Essentials of Glycobiology* (Cold Spring Harbor Laboratory Press, 2019).

3. Dwek, R. A. Glycobiology: Toward Understanding the Function of Sugars. *Chem. Rev.* **96**, 683–720 (1996).

4. Imperiali, B. & O'Connor, S. E. Effect of N-linked glycosylation on glycopeptide and glycoprotein structure. *Curr. Opin. Chem. Biol.* **3**, 643–649 (1999).

5. Hounsell, E. F., Davies, M. J. & Renouf, D. V. O-linked protein glycosylation structure and function. *Glycoconj. J.* **13**, 19–26 (1996).

6. Patterson, M. C. Metabolic mimics: the disorders of N-linked glycosylation. in *Seminars in pediatric neurology* vol. 12 144–151 (Elsevier, 2005).

7. Wang, X. Structure, mechanism and engineering of plant natural product glycosyltransferases. *FEBS Lett.* **583**, 3303–3309 (2009).

8. Méndez, C. & Salas, J. A. Altering the glycosylation pattern of bioactive compounds. *Trends Biotechnol.* **19**, 449–456 (2001).

9. Steen, P. Van den, Rudd, P. M., Dwek, R. A. & Opdenakker, G. Concepts and Principles of O-Linked Glycosylation. *Crit. Rev. Biochem. Mol. Biol.* **33**, 151–208 (1998).

10. Taylor, M. E. & Drickamer, K. *Introduction to glycobiology*. (Oxford university press, 2011).

11. Varki, A. *et al.* Essentials of Glycobiology. (2015).

12. Mohanty, S., Chaudhary, B. P. & Zoetewey, D. Structural Insight into the Mechanism of N-Linked Glycosylation by Oligosaccharyltransferase. *Biomolecules* **10**, 624 (2020).

13. Nakagawa, H. *et al.* Detection of altered N-glycan profiles in whole serum from

rheumatoid arthritis patients. *J. Chromatogr. B* **853**, 133–137 (2007).

14. Kodar, K., Stadlmann, J., Klaamas, K., Sergeyev, B. & Kurtenkov, O. Immunoglobulin G Fc N-glycan profiling in patients with gastric cancer by LC-ESI-MS: relation to tumor progression and survival. *Glycoconj. J.* **29**, 57–66 (2012).

15. Brown, R. B., Hollingsworth, M. A. & Schaffer, J. E. Protein Modifications | Mucin Family of Glycoproteins☆. in (ed. Jez, J. B. T.-E. of B. C. I. I. I. (Third E.) 167–172 (Elsevier, 2021). doi:https://doi.org/10.1016/B978-0-12-819460-7.00210-3.

16. Oman, T. J., Boettcher, J. M., Wang, H., Okalibe, X. N. & van der Donk, W. A. Sublancin is not a lantibiotic but an S-linked glycopeptide. *Nat. Chem. Biol.* **7**, 78–80 (2011).

17. Stepper, J. *et al.* Cysteine S-glycosylation, a new post-translational modification found in glycopeptide bacteriocins. *FEBS Lett.* **585**, 645–650 (2011).

18. Wan, L. Q. *et al.* Nonenzymatic Stereoselective S-Glycosylation of Polypeptides and Proteins. *J. Am. Chem. Soc.* **143**, 11919–11926 (2021).

19. Compañón, I. *et al.* Structure-based design of potent tumor-associated antigens: modulation of peptide presentation by single-atom O/S or O/Se substitutions at the glycosidic linkage. *J. Am. Chem. Soc.* **141**, 4063–4072 (2019).

20. De Leon, C. A., Levine, P. M., Craven, T. W. & Pratt, M. R. The sulfur-linked analogue of O-GlcNAc (S-GlcNAc) is an enzymatically stable and reasonable structural surrogate for O-GlcNAc at the peptide and protein levels. *Biochemistry* **56**, 3507–3517 (2017).

21. Ihara, Y. *et al.* C-mannosylation: modification on tryptophan in cellular proteins. in *Glycoscience: biology and medicine* 1091–1100 (Springer Japan, 2015).

22. Lee, J. *et al.* Novel C-aryl glucoside SGLT2 inhibitors as potential antidiabetic agents: 1, 3, 4-Thiadiazolylmethylphenyl glucoside congeners. *Bioorg. Med. Chem.* **18**, 2178–2194 (2010).

23. Gutmann, A. & Nidetzky, B. Enzymatic C-glycosylation: Insights from the study of a complementary pair of plant O- and C-glucosyltransferases. *Pure Appl. Chem.* **85**, 1865–1877 (2013).

24. Xu, C. & Ng, D. T. W. Glycosylation-directed quality control of protein folding. *Nat. Rev. Mol. Cell Biol.* **16**, 742–752 (2015).

25. Molinari, M. N-glycan structure dictates extension of protein folding or onset of disposal. *Nat. Chem. Biol.* **3**, 313–320 (2007).

26. Wormald, M. R. & Dwek, R. A. Glycoproteins: Glycan presentation and protein-fold stability. *Structure* **7**, 155–160 (1999).

27. Kleene, R. & Schachner, M. Glycans and neural cell interactions. *Nat. Rev. Neurosci.* **5**, 195–208 (2004).

28. Sperandio, M., Gleissner, C. A. & Ley, K. Glycosylation in immune cell trafficking. *Immunol. Rev.* **230**, 97–113 (2009).

29. Taylor, M. E., Drickamer, K., Schnaar, R. L., Etzler, M. E. & Varki, A. Discovery and Classification of Glycan-Binding Proteins. *Essentials Glycobiol.* 1–14 (2015).

30. Strasser, R. Biological significance of complex N-glycans in plants and their impact on plant physiology. *Front. Plant Sci.* **5**, (2014).

31. Stone, J. A., Nicola, A. V., Baum, L. G. & Aguilar, H. C. Multiple Novel Functions of Henipavirus O-glycans: The First O-glycan Functions Identified in the Paramyxovirus Family. *PLoS Pathog.* **12**, 1–20 (2016).

32. Miller, N. L., Clark, T., Raman, R. & Sasisekharan, R. Glycans in Virus-Host Interactions: A Structural Perspective. *Front. Mol. Biosci.* **8**, (2021).

33. Zhao, X., Chen, H. & Wang, H. Glycans of SARS-CoV-2 Spike Protein in Virus Infection and Antibody Production. *Front. Mol. Biosci.* **8**, (2021).

34. Hu, B., Guo, H., Zhou, P. & Shi, Z.-L. Characteristics of SARS-CoV-2 and COVID-19. *Nat. Rev. Microbiol.* **19**, 141–154 (2021).

35. Cui, J., Li, F. & Shi, Z. L. Origin and evolution of pathogenic coronaviruses. *Nat. Rev. Microbiol.* **17**, 181–192 (2019).

36. Falkowska, E. *et al.* Broadly neutralizing HIV antibodies define a glycan-dependent epitope on the prefusion conformation of gp41 on cleaved envelope trimers. *Immunity* **40**, 657–668 (2014).

37. Walls, A. C. *et al.* Structure, function, and antigenicity of the SARS-CoV-2 spike glycoprotein. *Cell* **181**, 281–292 (2020).

38. Bagdonaite, I. & Wandall, H. H. Global aspects of viral glycosylation. *Glycobiology* **28**, 443–467 (2018).

39. Vollmer, W., Massidda, O. & Tomasz, A. The cell wall of Streptococcus pneumoniae. *Microbiol. Spectr.* **7**, 3–7 (2019).

40. Theodoratou, E. *et al.* The role of glycosylation in IBD. *Nat. Rev. Gastroenterol. Hepatol.* **11**, 588–600 (2014).

41. Walther, T. *et al.* Glycomic Analysis of Human Respiratory Tract Tissues and Correlation with Influenza Virus Infection. *PLOS Pathog.* **9**, e1003223 (2013).

42. Tiralongo, J. *et al.* YesU from Bacillus subtilis preferentially binds fucosylated glycans. *Sci. Rep.* **8**, 1–10 (2018).

43. Mattox, D. E. & Bailey-Kellogg, C. Comprehensive analysis of lectin-glycan interactions reveals determinants of lectin specificity. *PLOS Comput. Biol.* **17**, e1009470 (2021).

44. Xie, Y. *et al.* Determination of the glycoprotein specificity of lectins on cell membranes through oxidative proteomics. *Chem. Sci.* **11**, 9501–9512 (2020).

45. Lekholm, E., Ceder, M. M., Forsberg, E. C., Schiöth, H. B. & Fredriksson, R. Differentiation of two human neuroblastoma cell lines alters SV2 expression patterns. *Cell. Mol. Biol. Lett.* **26**, 5 (2021).

46. Yao, G. *et al.* N-linked glycosylation of SV2 is required for binding and uptake of botulinum neurotoxin A. *Nat. Struct. Mol. Biol.* **23**, 656–662 (2016).

47. Lavín de Juan, L. *et al.* Pharmaceutical applications of lectins. *J. Drug Deliv. Sci. Technol.* **42**, 126–133 (2017).

48. Lima, M. & Baynes, J. W. Glycation. *Encycl. Biol. Chem. Second Ed.* **2**, 405–411 (2013).

49. Walsh, C. *Posttranslational modification of proteins: expanding nature's inventory*. (Roberts and Company Publishers, 2006).

50. Jung, S. T., Kang, T. H., Kelton, W. & Georgiou, G. Bypassing glycosylation: engineering aglycosylated full-length IgG antibodies for human therapy. *Curr. Opin. Biotechnol.* **22**, 858–867 (2011).

51. Samuel, G. & Reeves, P. Biosynthesis of O-antigens: genes and pathways involved in nucleotide sugar precursor synthesis and O-antigen assembly. *Carbohydr. Res.* **338**, 2503–2519 (2003).

52. Gerin, I. *et al.* ISPD produces CDP-ribitol used by FKTN and FKRP to transfer ribitol phosphate onto α-dystroglycan. *Nat. Commun.* **7**, 1–15 (2016).

53. Mikkola, S. Nucleotide Sugars in Chemistry and Biology. *Molecules* **25**, 5755 (2020).

54. Reily, C., Stewart, T. J., Renfrow, M. B. & Novak, J. Glycosylation in health and disease. *Nat. Rev. Nephrol.* **15**, 346–366 (2019).

55. Brockhausen, I. Mucin-type O-glycans in human colon and breast cancer: Glycodynamics and functions. *EMBO Rep.* **7**, 599–604 (2006).

56. Hassinen, A. & Kellokumpu, S. Organizational Interplay of Golgi N-Glycosyltransferases Involves Organelle Microenvironment-Dependent Transitions between Enzyme Homo- and Heteromers*. *J. Biol. Chem.* **289**, 26937–26948 (2014).

57. Moremen, K. W. & Haltiwanger, R. S. Emerging structural insights into glycosyltransferase-mediated synthesis of glycans. *Nat. Chem. Biol.* **15**, 853–864 (2019).

58. Breton, C., Šnajdrová, L., Jeanneau, C., Koča, J. & Imberty, A. Structures and mechanisms of glycosyltransferases. *Glycobiology* **16**, 29R-37R (2006).

59. Schuman, B., Evans, S. & Fyles, T. Geometric Attributes of Retaining Glycosyltransferase Enzymes Favor an Orthogonal Mechanism. *PLoS One* **8**, e71077 (2013).

60. Gastinel, L. N. *et al.* Bovine α1,3-galactosyltransferase catalytic domain

structure and its relationship with ABO histo-blood group and glycosphingolipid glycosyltransferases. *EMBO J.* **20**, 638–649 (2001).

61. Nagano, N., Noguchi, T. & Akiyama, Y. Systematic comparison of catalytic mechanisms of hydrolysis and transfer reactions classified in the EzCatDB database. *Proteins Struct. Funct. Bioinforma.* **66**, 147–159 (2007).

62. Davies, G. J. Sweet secrets of synthesis. *Nat. Struct. Biol.* **8**, 98–100 (2001).

63. Persson, K. *et al.* Crystal structure of the retaining galactosyltransferase LgtC from Neisseria meningitidis in complex with donor and acceptor sugar analogs. *Nat. Struct. Biol.* **8**, 166–175 (2001).

64. Gibson, R. P., Turkenburg, J. P., Charnock, S. J., Lloyd, R. & Davies, G. J. Insights into trehalose synthesis provided by the structure of the retaining glucosyltransferase OtsA. *Chem. Biol.* **9**, 1337–1346 (2002).

65. Flint, J. *et al.* Structural dissection and high-throughput screening of mannosylglycerate synthase. *Nat. Struct. Mol. Biol.* **12**, 608–614 (2005).

66. Soya, N., Fang, Y., Palcic, M. M. & Klassen, J. S. Trapping and characterization of covalent intermediates of mutant retaining glycosyltransferases. *Glycobiology* **21**, 547–552 (2011).

67. Lairson, L. L., Henrissat, B., Davies, G. J. & Withers, S. G. Glycosyltransferases: structures, functions, and mechanisms. *Annu. Rev. Biochem.* **77**, 521–555 (2008).

68. Goedl, C. & Nidetzky, B. Sucrose phosphorylase harbouring a redesigned, glycosyltransferase-like active site exhibits retaining glucosyl transfer in the absence of a Covalent intermediate. *ChemBioChem* **10**, 2333–2337 (2009).

69. Rose, D. R. Structure, mechanism and inhibition of Golgi α-mannosidase II. *Curr. Opin. Struct. Biol.* **22**, 558–562 (2012).

70. A Perez-Garcia, L., Martinez-Duncker, I. & M Mora Montes, H. The endoplasmic reticulum alpha-Glycosidases as potential targets for virus control. *Curr. Protein Pept. Sci.* **18**, 1090–1097 (2017).

71. Stradwick, L., Inglis, D., Kelly, J. & Pickering, G. Development and application

of assay for determining β-glucosidase activity in human saliva. *Flavour* **6**, 1–8 (2017).

72. Kaoutari, A. El, Armougom, F., Gordon, J. I., Raoult, D. & Henrissat, B. The abundance and variety of carbohydrate-active enzymes in the human gut microbiota. *Nat. Rev. Microbiol.* **11**, 497–504 (2013).

73. Hassan, M. I. *et al.* High resolution crystal structure of human β-glucuronidase reveals structural basis of lysosome targeting. *PLoS One* **8**, e79687 (2013).

74. Withers, S. & Williams, S. Glycoside hydrolases. *CAZypedia, available URL https//www. cazypedia. org/index. php/Glycoside_hydrolases, accessed 10 June 2016* (2013).

75. Bruni, C. B., Sica, V., Auricchio, F. & Covelli, I. Further kinetic and structural characterization of the lysosomal α-D-glucoside glucohydrolase from cattle liver. *Biochim. Biophys. Acta (BBA)-Enzymology* **212**, 470–477 (1970).

76. Chiba, S. Molecular mechanism in α-glucosidase and glucoamylase. *Biosci. Biotechnol. Biochem.* **61**, 1233–1239 (1997).

77. Gloster, T. M., Turkenburg, J. P., Potts, J. R., Henrissat, B. & Davies, G. J. Divergence of catalytic mechanism within a glycosidase family provides insight into evolution of carbohydrate metabolism by human gut flora. *Chem. Biol.* **15**, 1058–1067 (2008).

78. Koshland Jr, D. E. Stereochemistry and the mechanism of enzymatic reactions. *Biol. Rev.* **28**, 416–436 (1953).

79. Davies, G. & Henrissat, B. Structures and mechanisms of glycosyl hydrolases. *Structure* **3**, 853–859 (1995).

80. Kuroki, R., Weaver, L. H. & Matthews, B. W. Structure-based design of a lysozyme with altered catalytic activity. *Nat. Struct. Biol.* **2**, 1007–1011 (1995).

81. Brockerman, J. A., Okon, M., Withers, S. G. & McIntosh, L. P. The pK a values of the catalytic residues in the retaining glycoside hydrolase T26H mutant of T4 lysozyme. *Protein Sci.* **28**, 620–632 (2019).

82. Trincone, A. Uncommon Glycosidases for the Enzymatic Preparation of

Glycosides. *Biomolecules* **5**, 2160–2183 (2015).

83. CAZy. Glycoside Hydrolase family classification. http://www.cazy.org/Glycoside-Hydrolases.html (2022).

84. McCarter, J. D. & Withers, G. S. Mechanisms of enzymatic glycoside hydrolysis. *Curr. Opin. Struct. Biol.* **4**, 885–892 (1994).

85. Naz, H. *et al.* Human β-glucuronidase: structure, function, and application in enzyme replacement therapy. *Rejuvenation Res.* **16**, 352–363 (2013).

86. Pollet, R. M. *et al.* An Atlas of β-Glucuronidases in the Human Intestinal Microbiome. *Structure* **25**, 967-977.e5 (2017).

87. Walsh, J. *et al.* Impact of host and environmental factors on β-glucuronidase enzymatic activity: Implications for gastrointestinal serotonin. *Am. J. Physiol. - Gastrointest. Liver Physiol.* **318**, G816–G826 (2020).

88. van den Broek, B. T. A., Smit, A. L., Boelens, J. J. & van Hasselt, P. M. Hearing loss in patients with mucopolysaccharidoses-1 and-6 after hematopoietic cell transplantation: a longitudinal analysis. *J. Inherit. Metab. Dis.* **43**, 1279–1287 (2020).

89. Breyer, S. R. *et al.* Hip pathologies in mucopolysaccharidosis type III. *J. Orthop. Surg. Res.* **16**, 1–8 (2021).

90. Lee, C.-L. *et al.* Otorhinolaryngological management in Taiwanese patients with mucopolysaccharidoses. *Int. J. Med. Sci.* **18**, 3373 (2021).

91. Wolfe, J. H. *et al.* Reversal of pathology in murine mucopolysaccharidosis type VII by somatic cell gene transfer. *Nature* **360**, 749–753 (1992).

92. Vogler, C. *et al.* Enzyme replacement in murine mucopolysaccharidosis type VII: neuronal and glial response to β-glucuronidase requires early initiation of enzyme replacement therapy. *Pediatr. Res.* **45**, 838–844 (1999).

93. Rivara, S., Milazzo, F. M. & Giannini, G. Heparanase: A rainbow pharmacological target associated to multiple pathologies including rare diseases. *Future Med. Chem.* **8**, 647–680 (2016).

94. Wu, L., Viola, C. M., Brzozowski, A. M. & Davies, G. J. Structural

characterization of human heparanase reveals insights into substrate recognition. *Nat. Struct. Mol. Biol.* **22**, 1016–1022 (2015).

95. Nasser, N. J. Heparanase involvement in physiology and disease. *Cell. Mol. Life Sci.* **65**, 1706–1715 (2008).

96. Tímár, J. *et al.* Proteoglycans and tumor progression: Janus-faced molecules with contradictory functions in cancer. in *Seminars in cancer biology* vol. 12 173–186 (Elsevier, 2002).

97. Belting, M. Heparan sulfate proteoglycan as a plasma membrane carrier. *Trends Biochem. Sci.* **28**, 145–151 (2003).

98. Iozzo, R. V. Matrix proteoglycans: from molecular design to cellular function. *Annu. Rev. Biochem.* **67**, 609–652 (1998).

99. Bishop, J. R., Schuksz, M. & Esko, J. D. Heparan sulphate proteoglycans fine-tune mammalian physiology. *Nature* **446**, 1030–1037 (2007).

100. Iozzo, R. V & Sanderson, R. D. Proteoglycans in cancer biology, tumour microenvironment and angiogenesis. *J. Cell. Mol. Med.* **15**, 1013–1031 (2011).

101. Lindahl, U. & Kjellén, L. Pathophysiology of heparan sulphate: many diseases, few drugs. *J. Intern. Med.* **273**, 555–571 (2013).

102. Waterman, M. *et al.* Heparanase upregulation by colonic epithelium in inflammatory bowel disease. *Mod. Pathol.* **20**, 8–14 (2007).

103. Li, R. W. *et al.* Dramatic regulation of heparanase activity and angiogenesis gene expression in synovium from patients with rheumatoid arthritis. *Arthritis Rheum. Off. J. Am. Coll. Rheumatol.* **58**, 1590–1600 (2008).

104. Bornstein, J., Cohen, Y., Zarfati, D., Sela, S. & Ophir, E. Involvement of heparanase in the pathogenesis of localized vulvodynia. *Int. J. Gynecol. Pathol.* **27**, 136–141 (2008).

105. Wang, B. *et al.* Accelerated resolution of AA amyloid in heparanase knockout mice is associated with matrix metalloproteases. *PLoS One* **7**, e39899 (2012).

106. Naggi, A. *et al.* Modulation of the heparanase-inhibiting activity of heparin through selective desulfation, graded N-acetylation, and glycol splitting. *J. Biol.*

Chem. **280**, 12103–12113 (2005).

107. Freeman, C. *et al.* Use of sulfated linked cyclitols as heparan sulfate mimetics to probe the heparin/heparan sulfate binding specificity of proteins. *J. Biol. Chem.* **280**, 8842–8849 (2005).

108. Weissmann, M. *et al.* Heparanase-neutralizing antibodies attenuate lymphoma tumor growth and metastasis. *Proc. Natl. Acad. Sci.* **113**, 704–709 (2016).

109. Miao, H. *et al.* Inhibition of heparanase activity and tumor metastasis by laminarin sulfate and synthetic phosphorothioate oligodeoxynucleotides. *Int. J. Cancer* **83**, 424–431 (1999).

110. Dinos, G. P. Kinetic study of irreversible inhibition of an enzyme consumed in the reaction it catalyses. Application to the inhibition of the puromycin reaction by spiramycin and hydroxylamine. *J. Enzyme Inhib.* **12**, 79–99 (1997).

111. Patrick, G. 'Enzymes as Drug Targets'. in *An Introduction to Medicinal Chemistry* 95 (2017).

112. Lundblad, R. L. *Chemical reagents for protein modification*. (CRC press, 2004).

113. Hiratake, J. Enzyme inhibitors as chemical tools to study enzyme catalysis: rational design, synthesis, and applications. *Chem. Rec.* **5**, 209–228 (2005).

114. Pereira, D. M., Andrade, C., Valentão, P. & Andrade, P. B. Natural products as enzyme inhibitors. *Nat. Prod. Target. Clin. Relev. Enzym.* **1**, (2017).

115. Fiesco-Roa, M. O., Giri, N., McReynolds, L. J., Best, A. F. & Alter, B. P. Genotype-phenotype associations in Fanconi anemia: A literature review. *Blood Rev.* **37**, 100589 (2019).

116. Buynak, J. D. Cutting and stitching: the cross-linking of peptidoglycan in the assembly of the bacterial cell wall. *ACS Chem. Biol.* **2**, 602–605 (2007).

117. Katz, A. H. & Caufield, C. E. Structure-based design approaches to cell wall biosynthesis inhibitors. *Curr. Pharm. Des.* **9**, 857–866 (2003).

118. Kuhr, R. J. & Dorough, H. W. *Carbamate insecticides: chemistry, biochemistry, and toxicology.* (CRC Press, Inc., 1976).

119. Tan, S., Evans, R. & Singh, B. Herbicidal inhibitors of amino acid biosynthesis

and herbicide-tolerant crops. *Amino Acids* **30**, 195–204 (2006).

120. Atsumi, S. *et al.* Production, isolation and structure determination of a novel β-glucosidase inhibitor, cyclophellitol, from Phellinus sp. *J. Antibiot. (Tokyo).* **43**, 49–53 (1990).

121. Gloster, T. M., Madsen, R. & Davies, G. J. Structural basis for cyclophellitol inhibition of a β-glucosidase. *Org. Biomol. Chem.* **5**, 444–446 (2007).

122. Tatsuta, K., Niwata, Y., Umezawa, K., Toshima, K. & Nakata, M. Syntheses and enzyme inhibiting activities of cyclophellitol analogs. *J. Antibiot. (Tokyo).* **44**, 912–914 (1991).

123. Kallemeijn, W. W. *et al.* Novel activity-based probes for broad-spectrum profiling of retaining β-exoglucosidases in situ and in vivo. *Angew. Chemie - Int. Ed.* **51**, 12529–12533 (2012).

124. Ben Bdira, F. *et al.* Hydrophobic Interactions Contribute to Conformational Stabilization of Endoglycoceramidase II by Mechanism-Based Probes. *Biochemistry* **55**, 4823–4835 (2016).

125. Erhardt, P. *et al.* Glossary and tutorial of xenobiotic metabolism terms used during small molecule drug discovery and development (IUPAC Technical Report). *Pure Appl. Chem.* **93**, 273–403 (2021).

126. Wu, L. *et al.* Activity-based probes for functional interrogation of retaining β-glucuronidases. *Nat. Chem. Biol.* **13**, 867–873 (2017).

127. Li, K. Y. *et al.* Synthesis of cyclophellitol, cyclophellitol aziridine, and their tagged derivatives. *European J. Org. Chem.* **2014**, 6030–6043 (2014).

128. Jat, J. L. *et al.* Direct stereospecific synthesis of unprotected N-H and N-Me aziridines from olefins. *Science (80-.).* **343**, 61–65 (2014).

129. Tsai, C. S. *et al.* Cell-permeable probe for identification and imaging of sialidases. *Proc. Natl. Acad. Sci. U. S. A.* **110**, 2466–2471 (2013).

130. Ness, R. K. & Fletcher, H. G. The Anomeric 2,3,5-Tri-O-benzoyl-D-arabinosyl Bromides and Other D-Arabinofuranose Derivatives. *J. Am. Chem. Soc.* **80**, 2007–2010 (1958).

131. Alcaide, A., Trapero, A., Pérez, Y. & Llebaria, A. Galacto configured N-aminoaziridines: a new type of irreversible inhibitor of β-galactosidases. *Org. Biomol. Chem.* **13**, 5690–5697 (2015).

132. Skaanderup, P. R., Poulsen, C. S., Hyldtoft, L., Jørgensen, M. R. & Madsen, R. Regioselective conversion of primary alcohols into iodides in unprotected methyl furanosides and pyranosides. *Synthesis (Stuttg).* 1721–1727 (2002) doi:10.1055/s-2002-33641.

133. Jeffrey, R. *et al.* Synthesis of 2,3-O-benzyl-ribose and xylose and their equilibration. *Tetrahedron Asymmetry* **25**, 1424–1429 (2014).

134. DeWall, G. Sodium hydride and DMF. *Chem. Informationsd.* **14**, no-no (1983).

135. Yang, Q. *et al.* Explosion Hazards of Sodium Hydride in Dimethyl Sulfoxide, N, N-Dimethylformamide, and N, N-Dimethylacetamide. *Org. Process Res. Dev.* **23**, 2210–2217 (2019).

136. France, R. R. *et al.* Selective electrochemical glycosylation by reactivity tuning. *Org. Biomol. Chem.* **2**, 2195–2202 (2004).

137. Mustafa, N. R., Spelbos, V. S., Witkamp, G.-J., Verpoorte, R. & Choi, Y. H. Solubility and Stability of Some Pharmaceuticals in Natural Deep Eutectic Solvents-Based Formulations. *Molecules* **26**, (2021).

138. Limousin, C. *et al.* Halogenation of carbohydrates by triphenylphosphine complex reagents in highly concentrated solution under microwave activation or conventional heating. *Carbohydr. Res.* **312**, 23–31 (1998).

139. Cotton, F. A. & Kibala, P. A. Reactions of iodine with triphenylphosphine and triphenylarsine. *J. Am. Chem. Soc.* **109**, 3308–3312 (1987).

140. Garegg, P. J., Regberg, T., Stawinski, J. & Strömberg, R. A Phosphorus Nuclear Magnetic Resonance Spectroscopic Study of the. 9–12 (1987).

141. Bernet, B. & Vasella, A. Carbocyclische Verbindungen aus Monosacchariden. II. Umsetzungen in der Mannosereihe. *Helv. Chim. Acta* **62**, 2400–2410 (1979).

142. Cintas, P. *Activated metals in organic synthesis*. (1993).

143. Win-Mason, A. L., Dangerfield, E. M., Tyler, P. C., Stocker, B. L. & Timmer, M.

S. M. Stereoselective Strecker and carbamate annulation methodology for the synthesis of 1-amino-1,2,5-trideoxy-2,5-imino-L-iditol. *European J. Org. Chem.* 4008–4014 (2011) doi:10.1002/ejoc.201100523.

144. Augé, J., Lubin-Germain, N., Marque, S. & Seghrouchni, L. Indium-catalyzed Barbier allylation reaction. *J. Organomet. Chem.* **679**, 79–83 (2003).

145. Diana, S.-C., Sim, K.-Y. & Loh, T.-P. Lathanum Trifluoromethanesulfonate [La (OTf) 3] Promoted Indium-Mediated Coupling of Ethyl 4-Bromocrotonate with Carbonyl Compounds in Water. (1996).

146. Wang, R. *et al.* Ytterbium trifluoromethanesulfonate [Yb (OTf) 3] promoted indium mediated allylation reactions of carbonyl compounds in aqueous media. *Tetrahedron: Asymmetry* **6**, 1825–1828 (1995).

147. Loh, T.-P., Cao, G.-Q. & Pei, J. Studies towards total synthesis of antillatoxin: Investigation of the indium-mediated allylation reactions of carbonyl compounds with β-bromocrotylbromide in water. *Tetrahedron Lett.* **39**, 1453–1456 (1998).

148. Pump, E. *et al.* Regio, stereo and chemoselectivity of 2nd generation Grubbs ruthenium-catalyzed olefin metathesis. *Catal. Today* (2020).

149. Forman, G. S. & Tooze, R. P. Improved cross-metathesis of acrylate esters catalyzed by 2nd generation ruthenium carbene complexes. *J. Organomet. Chem.* **690**, 5863–5866 (2005).

150. Kobayashi, Y. *et al.* A medium fluorous Grubbs–Hoveyda 2nd generation catalyst for phase transfer catalysis of ring closing metathesis reactions. *Tetrahedron Lett.* **56**, 1363–1366 (2015).

151. Xie, J., Ménand, M. & Valéry, J. M. Regioselective debenzylation of C-glycosyl compounds by boron trichloride. *Carbohydr. Res.* **340**, 481–487 (2005).

152. Achinivu, E. C., Howard, R. M., Li, G., Gracz, H. & Henderson, W. A. Lignin extraction from biomass with protic ionic liquids. *Green Chem.* **16**, 1114–1119 (2014).

153. Lu, P.-H., Yang, C.-S., Devendar, B. & Liao, C.-C. Syntheses of Optically Pure Conduramines via the Strategy of Hetero Diels− Alder Reaction of Masked o-

Benzoquinones with Homochiral Nitroso Dienophiles. *Org. Lett.* **12**, 2642–2645 (2010).

154. Chang, Y.-K., Lo, H.-J. & Yan, T.-H. A Flexible Strategy Based on a C 2-Symmetric Pool of Chiral Substrates: Concise Synthesis of (+)-Valienamine, Key Intermediate of (+)-Pancratistatin, and Conduramines A-1 and E. *Org. Lett.* **11**, 4278–4281 (2009).

155. Rajender, A. & Rao, B. V. Stereoselective synthesis of (−)-conduramine C-1 and (−)-conduramine D-1. *Tetrahedron Lett.* **54**, 2329–2331 (2013).

156. Dou, Q. & Jiang, Z. A Facile Route to Ursodeoxycholic Acid Based on Stereocontrolled Conversion and Aggregation Behavior Research. *Synth.* **48**, 588–594 (2016).

157. Liang, Y.-Y. *et al.* Efficient synthesis of cholic acid derivates through stereoselective C–H functionalization from hyodeoxycholic acid. *Steroids* **157**, 108594 (2020).

158. Zhou, P. *et al.* Design, synthesis, biological evaluation and cocrystal structures with tubulin of chiral β-lactam bridged combretastatin A-4 analogues as potent antitumor agents. *Eur. J. Med. Chem.* **144**, 817–842 (2018).

159. Hribernik, N., Tamburrini, A., Falletta, E. & Bernardi, A. One pot synthesis of thio -glycosides via aziridine opening reactions. *Org. Biomol. Chem.* **19**, 233–247 (2021).

160. Yang, G., Franck, R. W., Bittman, R., Samadder, P. & Arthur, G. Synthesis and growth inhibitory properties of glucosamine-derived glycerolipids. *Org. Lett.* **3**, 197–200 (2001).

161. Martínez-Castro, E., Suárez-Pantiga, S. & Mendoza, A. Scalable Synthesis of Esp and Rhodium (II) Carboxylates from Acetylacetone and RhCl3· x H2O. *Org. Process Res. Dev.* **24**, 1207–1212 (2020).

162. Gersbach, P. *et al.* A ring-closing metathesis (RCM)-based approach to mycolactonesa A/B. *Chem. - A Eur. J.* **17**, 13017–13031 (2011).

163. Ayi, A. I., Remli, M. & Guedj, R. A novel synthesis of 3-fluorophenylalanine and some of its derivatives. *J. Fluor. Chem.* **3**, 675–687 (1981).

164. Alvernhe, G. M., Ennakoua, C. M., Lacombe, S. M. & Laurent, A. J. Ring opening of aziridines by different fluorinating reagents: three synthetic routes to. alpha.,. beta.-fluoro amines with different stereochemical pathways. *J. Org. Chem.* **46**, 4938–4948 (1981).

165. Wade, T. N. Preparation of fluoro amines by the reaction of aziridines with hydrogen fluoride in pyridine solution. *J. Org. Chem.* **45**, 5328–5333 (1980).

166. Vedejs, E., Klapars, A., Naidu, B. N. & Piotrowski, D. W. Enantiocontrolled Synthesis of (1S,2S)-6-Desmethyl-(methylaziridino)mitosene E. 5401–5402 (2000).

167. Kok, G. B., Pye, C. C., Singer, R. D. & Scammells, P. J. Two-step iron(0)-mediated N-demethylation of N -methyl alkaloids. *J. Org. Chem.* **75**, 4806–4811 (2010).

168. Frost, L. *et al.* Synthesis of diacylated γ-glutamyl-cysteamine prodrugs, and in vitro evaluation of their cytotoxicity and intracellular delivery of cysteamine. *Eur. J. Med. Chem.* **109**, 206–215 (2016).

169. Berger, G. *et al.* Synthesis and in vitro characterization of platinum (II) anticancer coordinates using FTIR spectroscopy and NCI COMPARE: a fast method for new compound discovery. *Bioorg. Med. Chem.* **22**, 3527–3536 (2014).

170. Martichonok, V., Plouffe, C., Storer, A. C., Ménard, R. & Jones, J. B. Aziridine Analogs of [[trans-(Epoxysuccinyl)-l-leucyl]amino]-4-guanidinobutane (E-64) as Inhibitors of Cysteine Proteases. *J. Med. Chem.* **38**, 3078–3085 (1995).

171. Hansen, F. G., Bundgaard, E. & Madsen, R. A short synthesis of (+)-cyclophellitol. *J. Org. Chem.* **70**, 10139–10142 (2005).

8. Table of Figures

9. Table of Tables

10. Appendix

10.1. Spectra

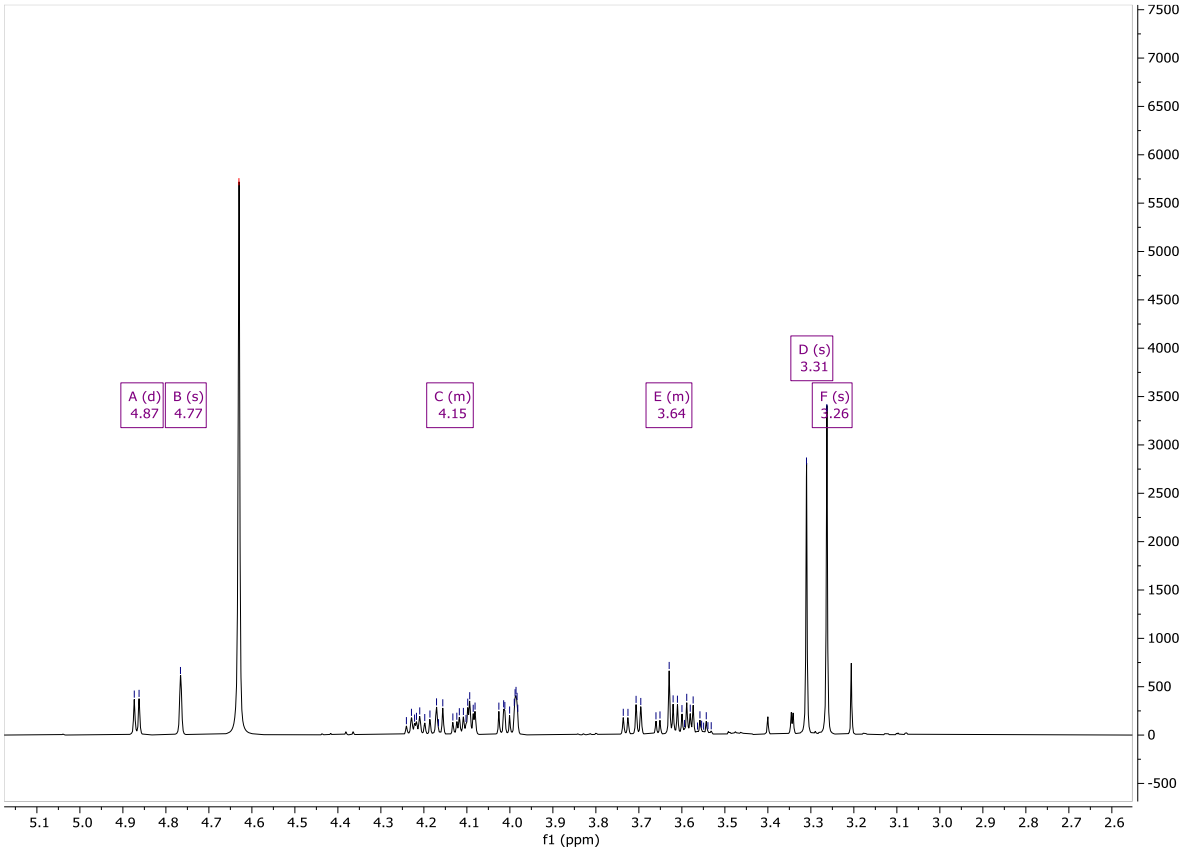

Figure 39. ^{1}H NMR spectrum of **16**.

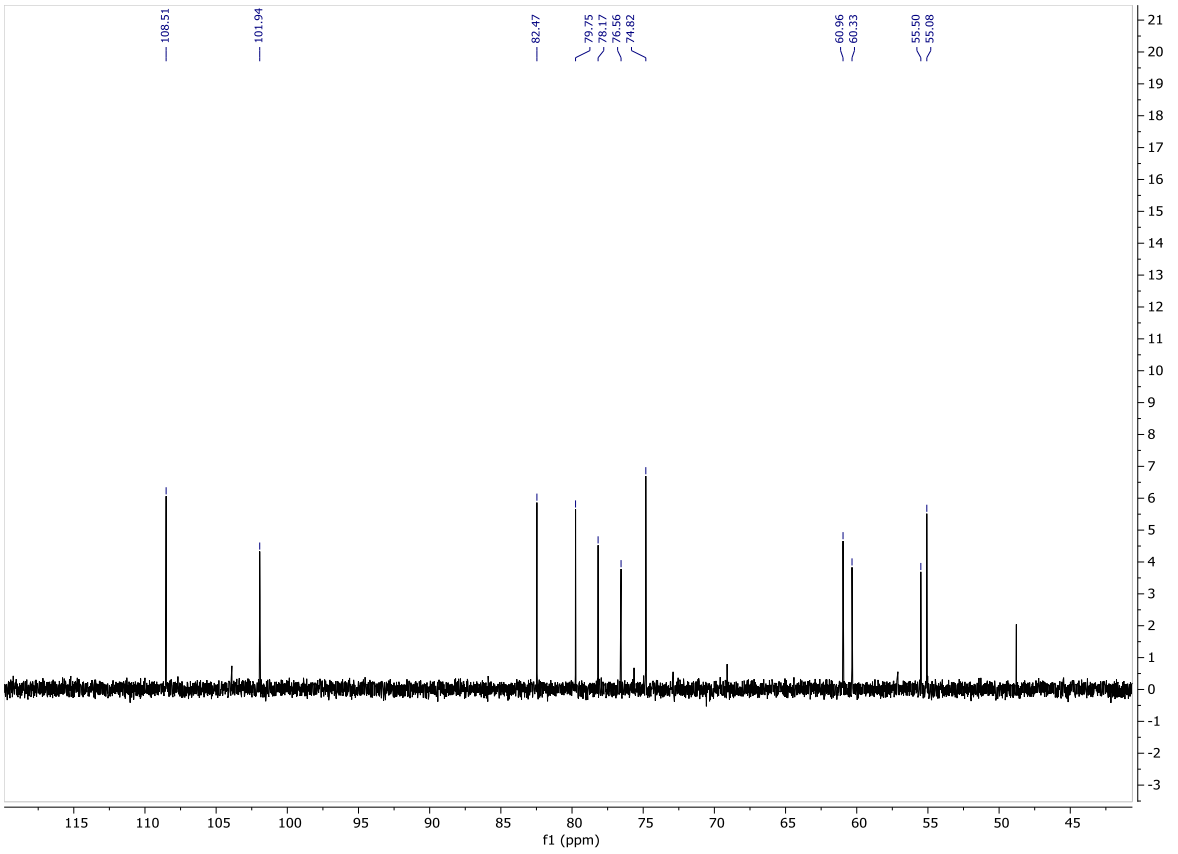

Figure 40. ^{13}C NMR spectrum of **16**.

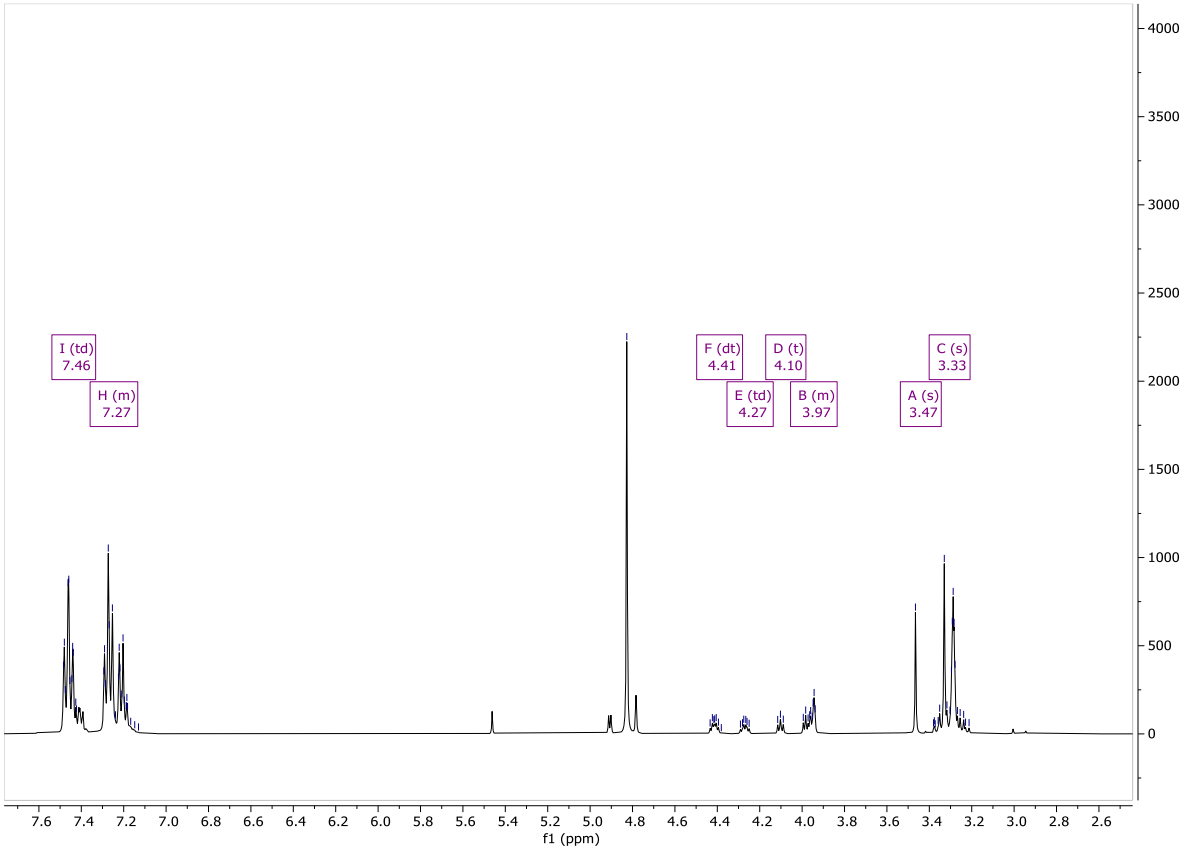

Figure 41. ^{1}H NMR spectrum of **17**.

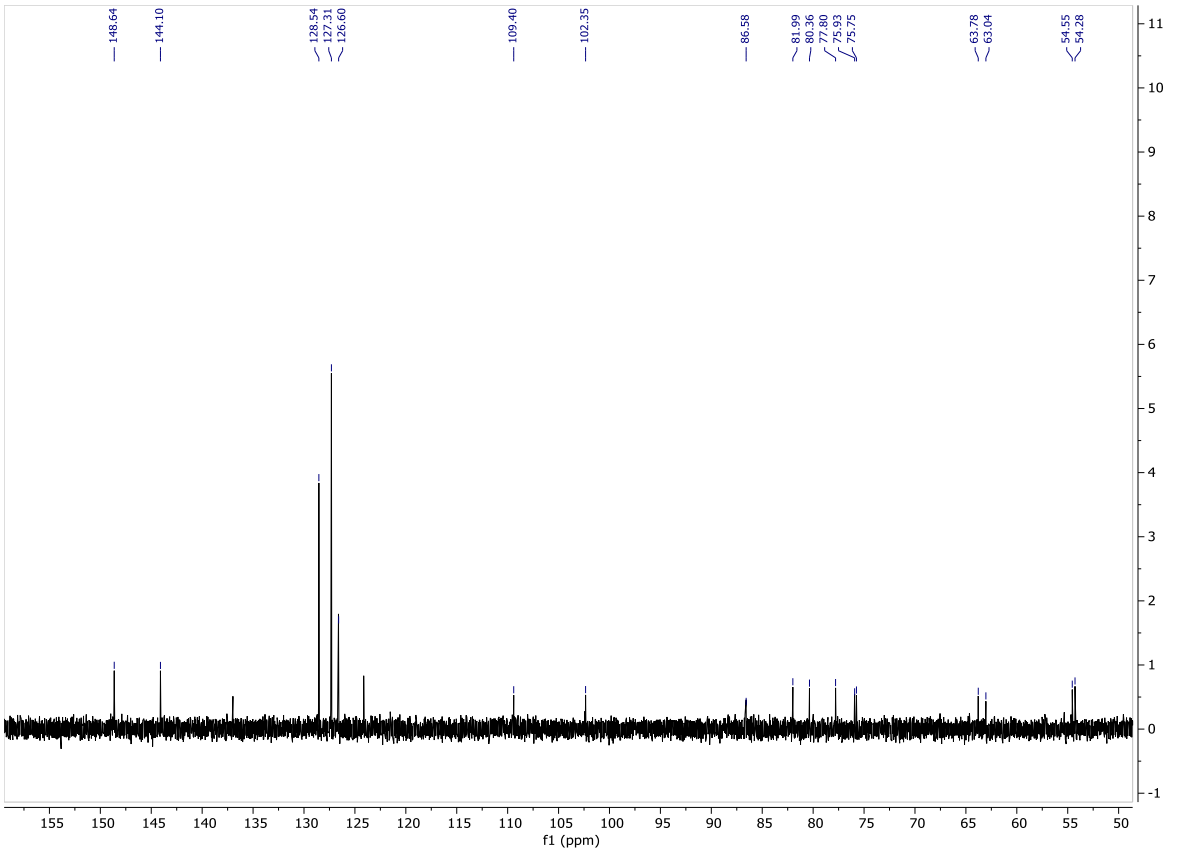

Figure 42. ^{13}C NMR spectrum of **17**.

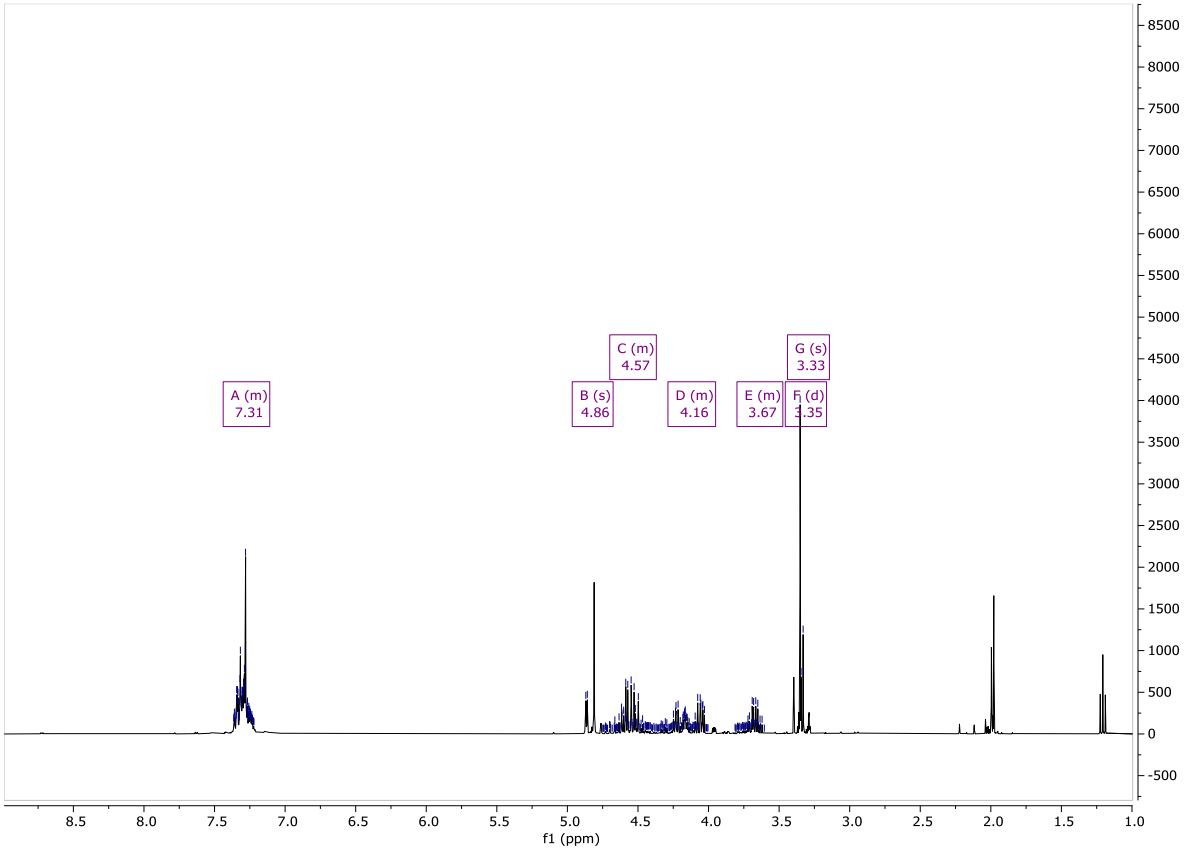

Figure 43.^{1}H NMR spectrum of **18**.

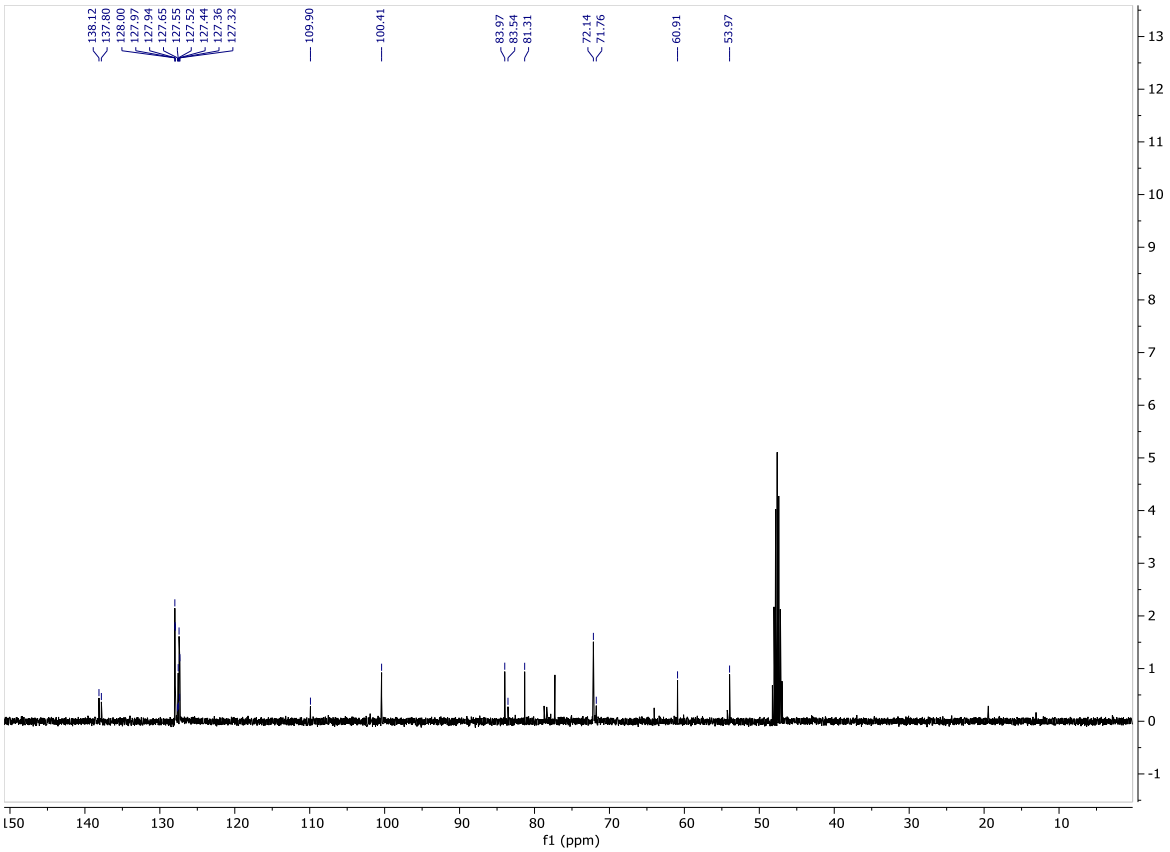

Figure 44. ^{13}C NMR spectrum of **18**.

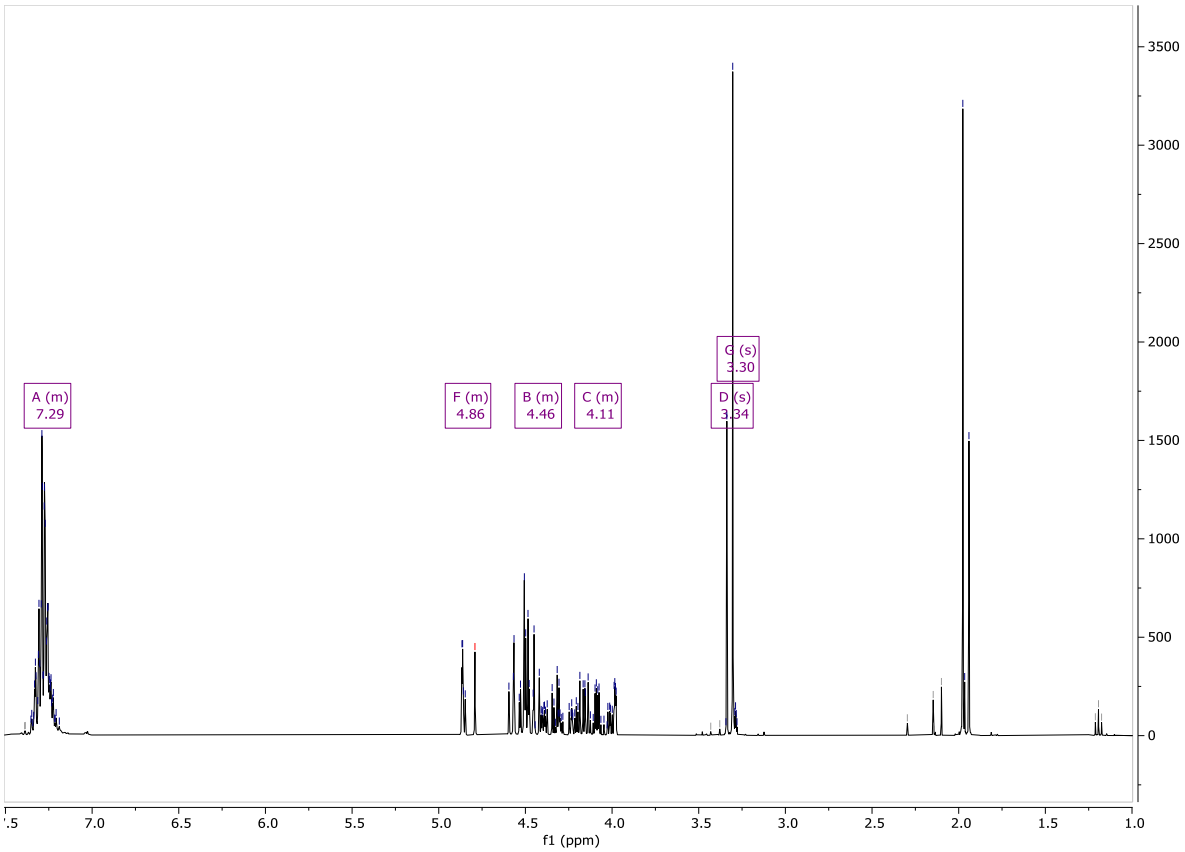

Figure 45. ^{1}H NMR spectrum of **19**.

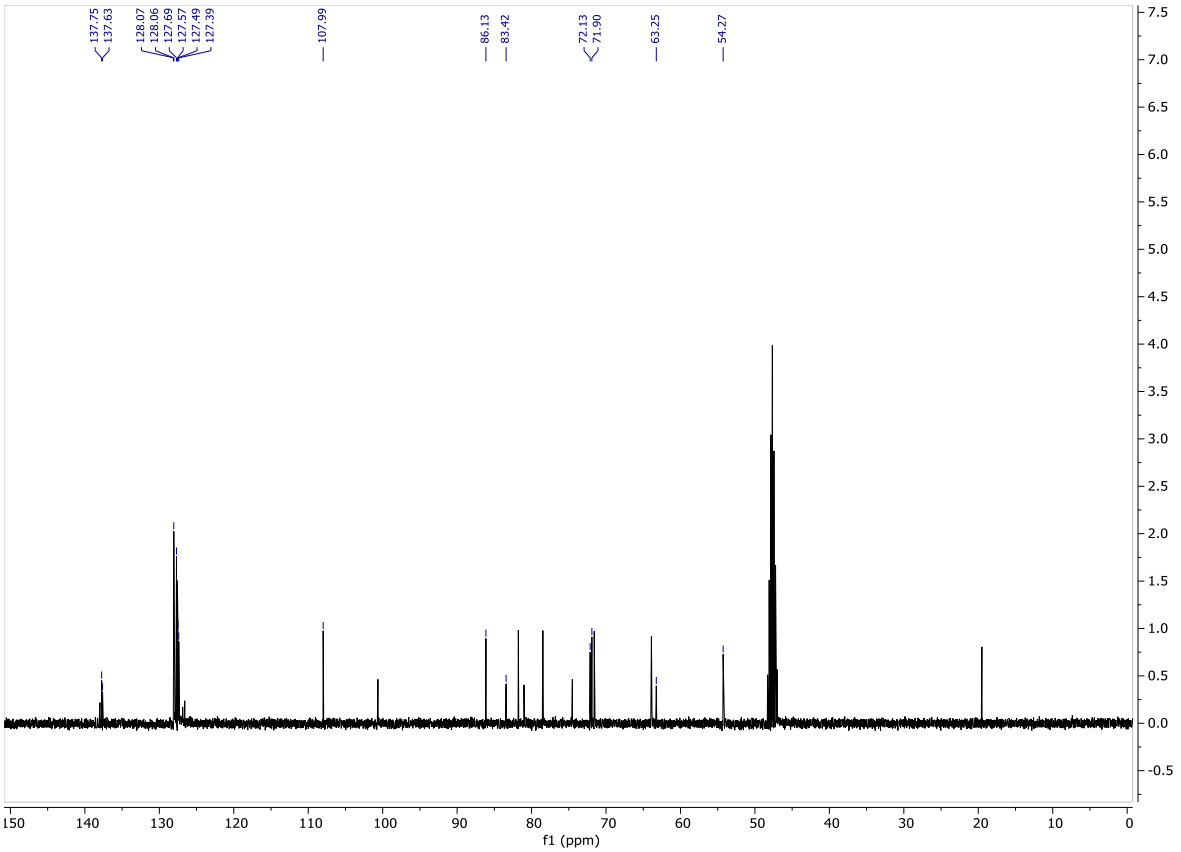

Figure 46. ^{13}C NMR spectrum of **19**.

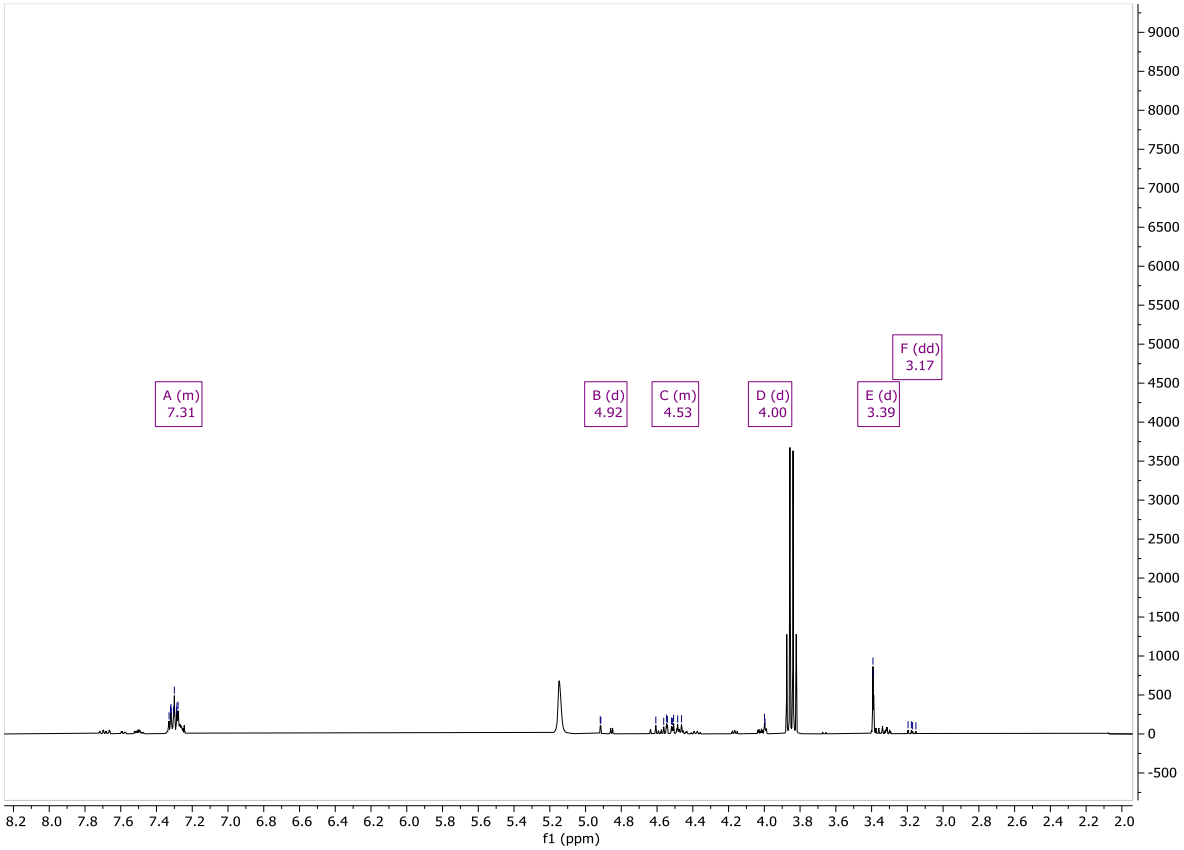

Figure 47. ^{1}H NMR spectrum of **20**.

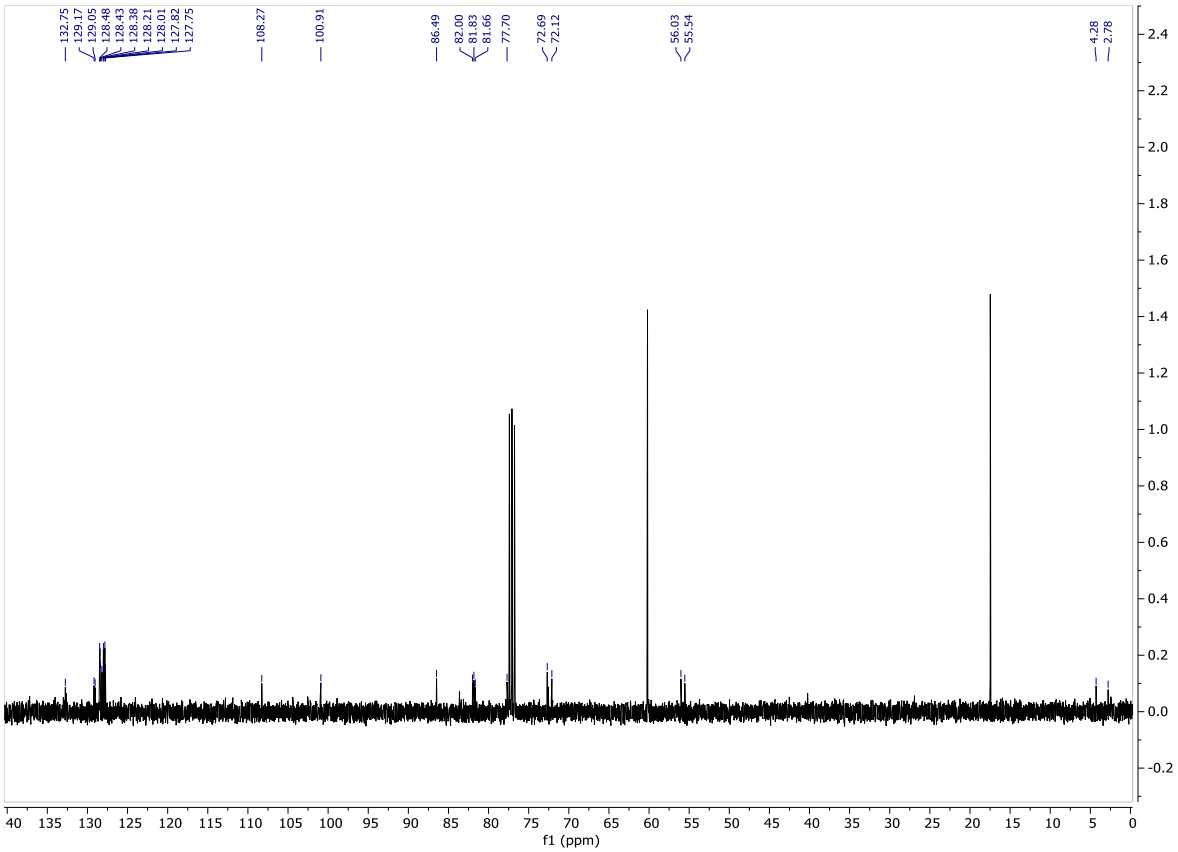

Figure 48. ^{13}C NMR spectrum of **20.**

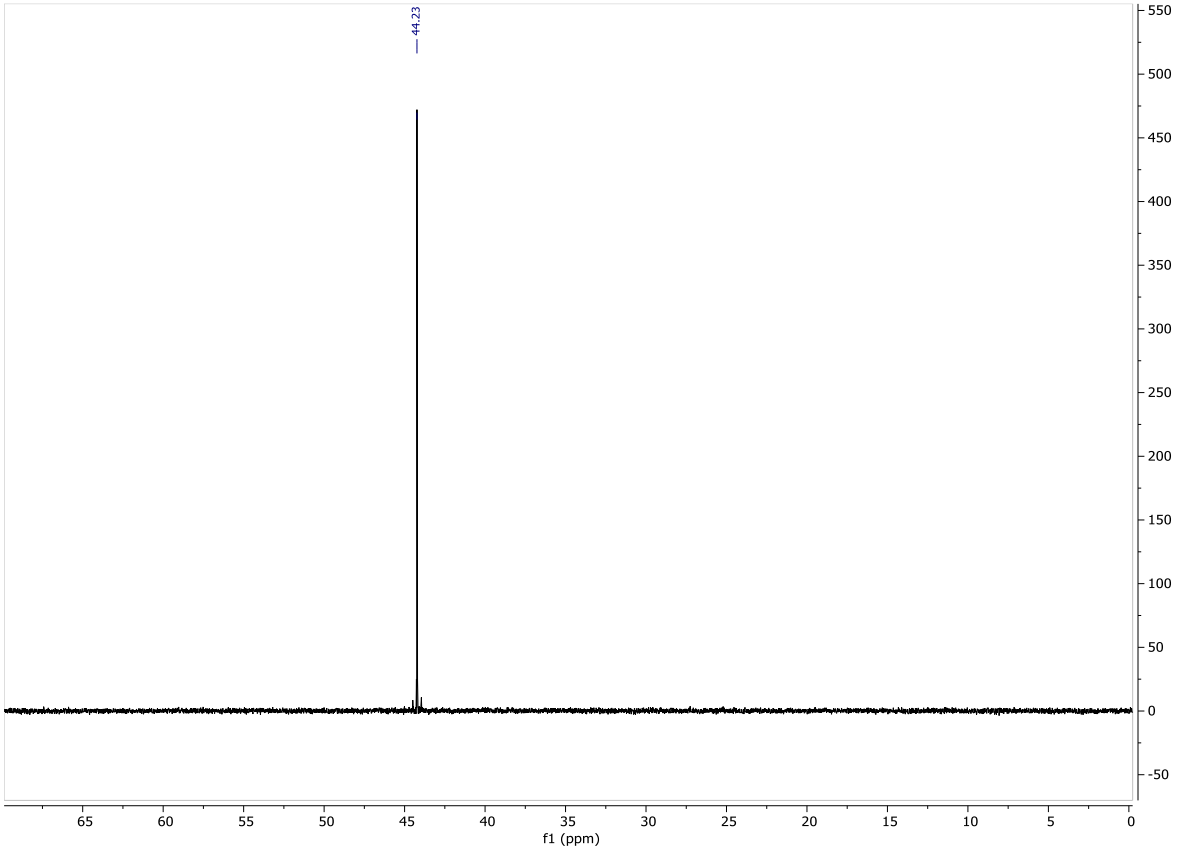

Figure 49. ^{31}P NMR spectrum of **20** (TPPO impurity).

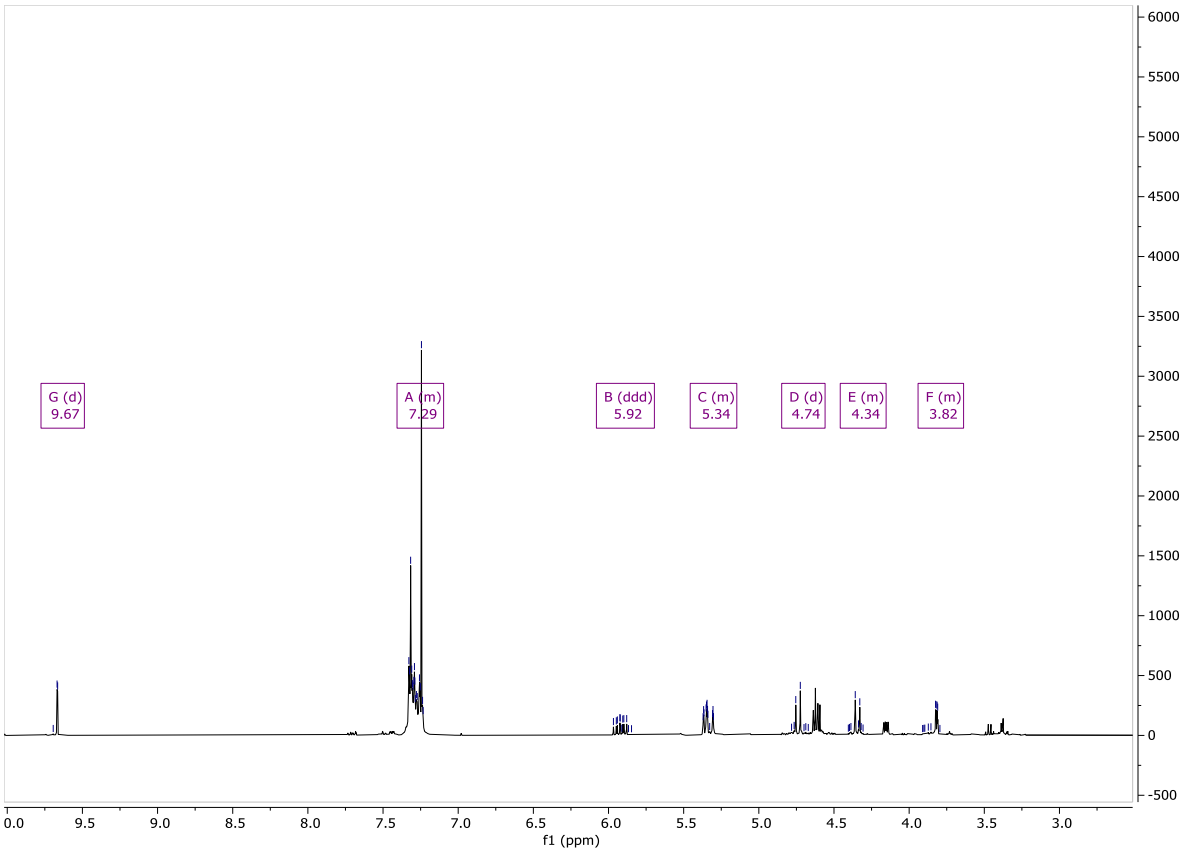

Figure 50. ^{1}H NMR spectrum of **21**.

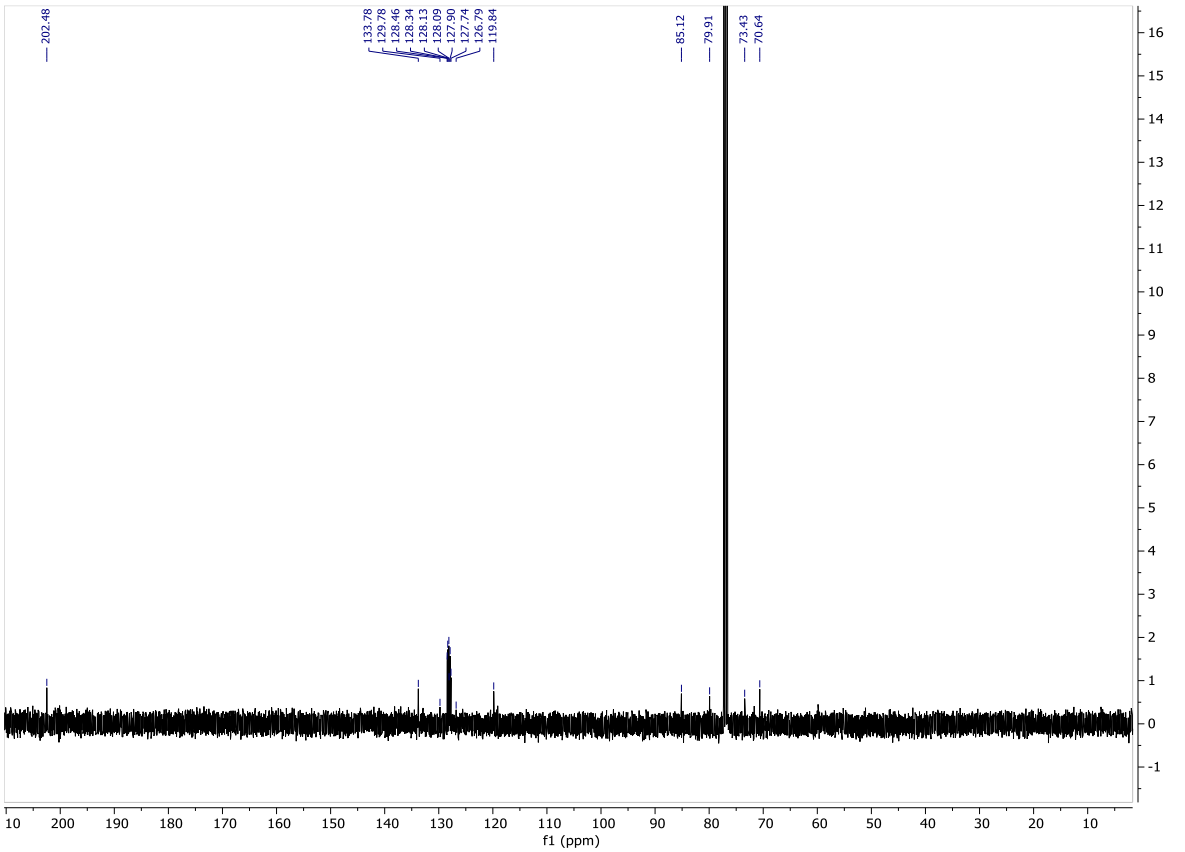

Figure 51. ^{13}C NMR spectrum of **21**.

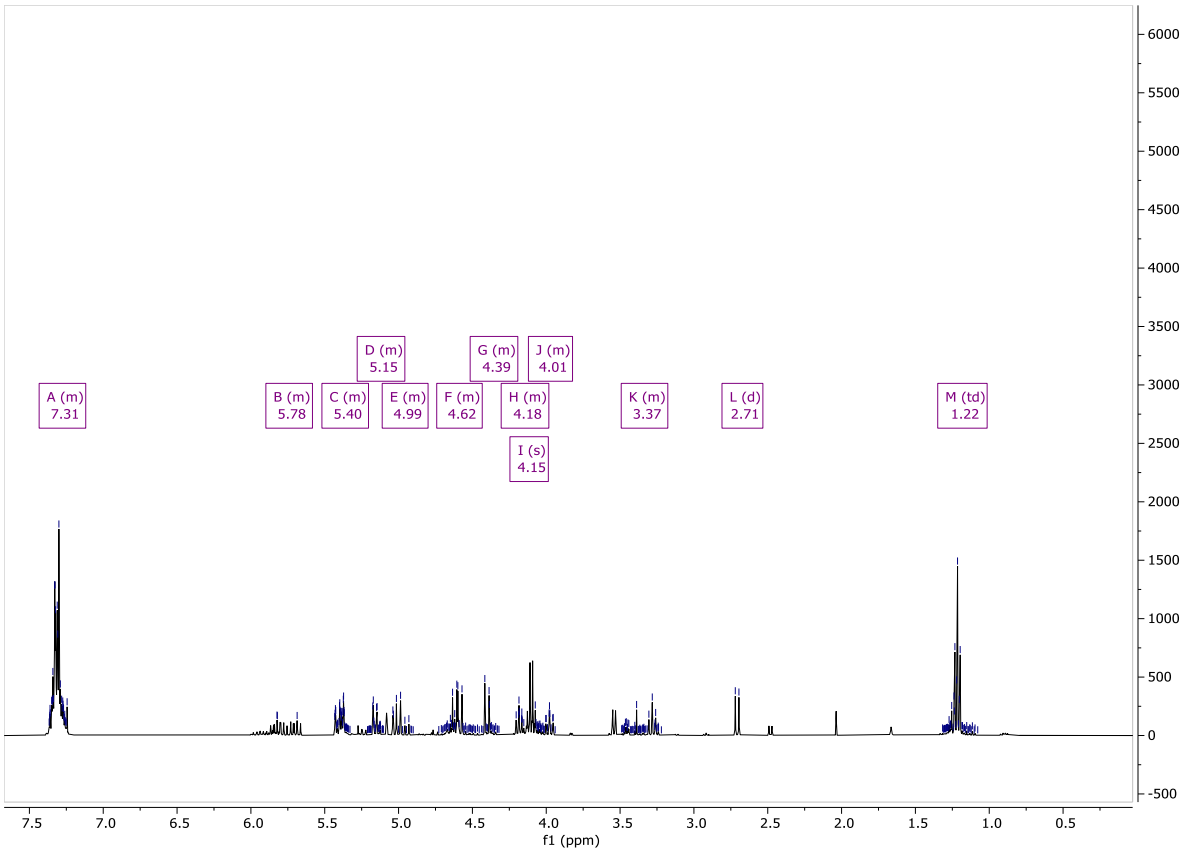

Figure 52. ^{1}H NMR spectrum of **23**.

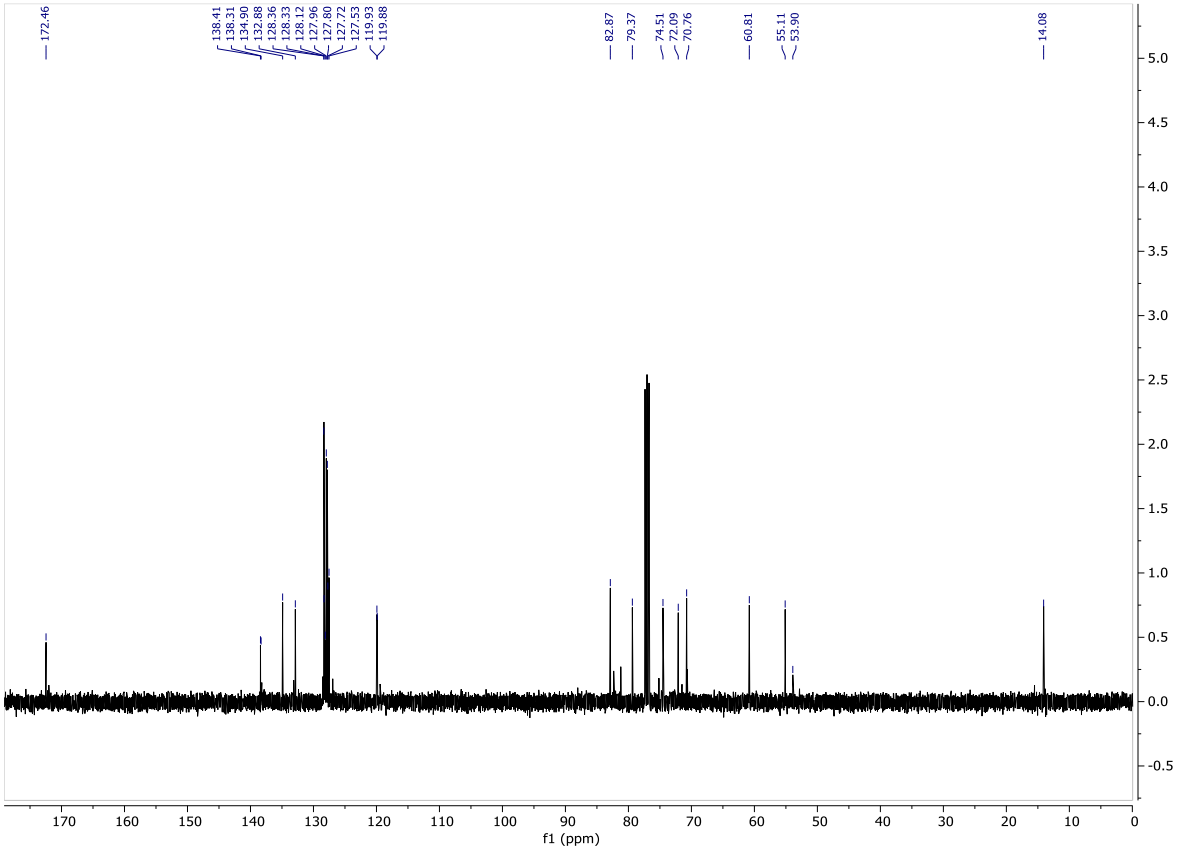

Figure 53. ^{13}C NMR spectrum of **23**.

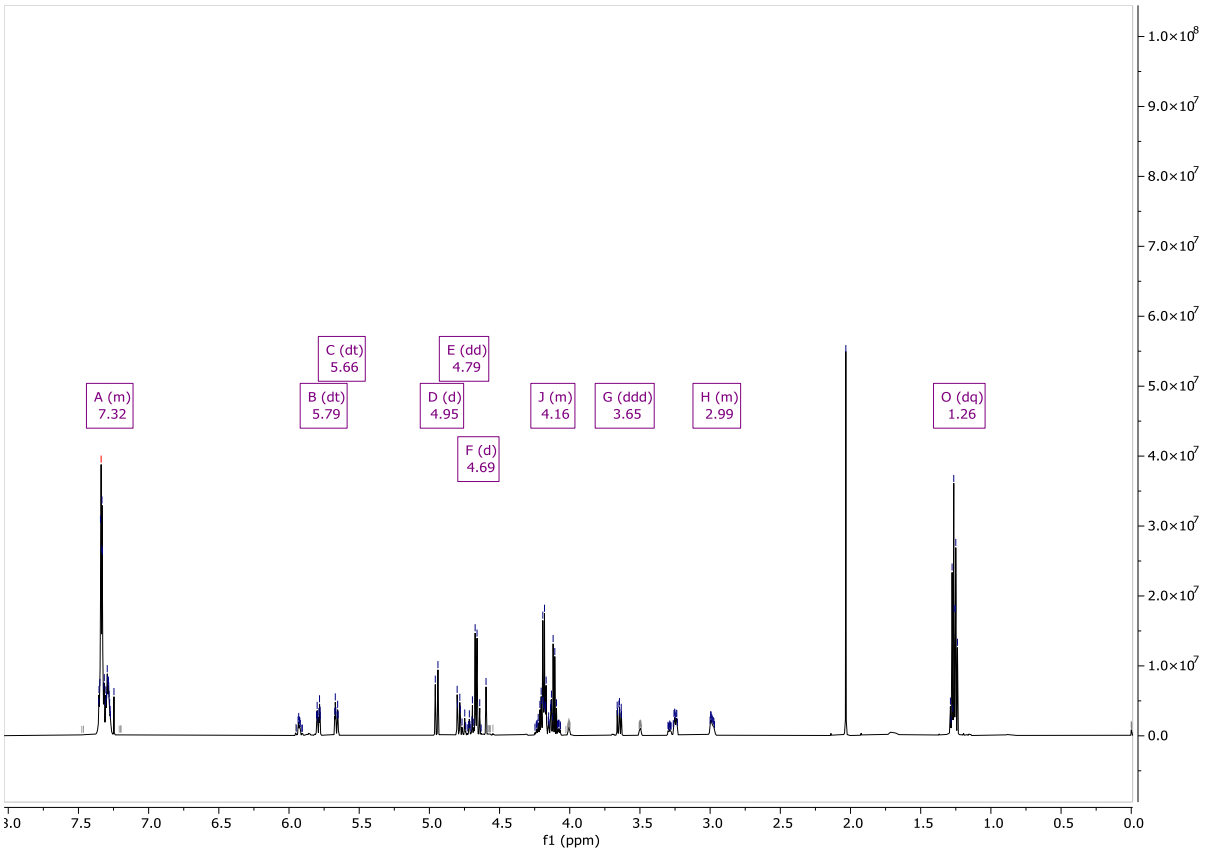

Figure 54. ^{1}H NMR spectrum of **24**.

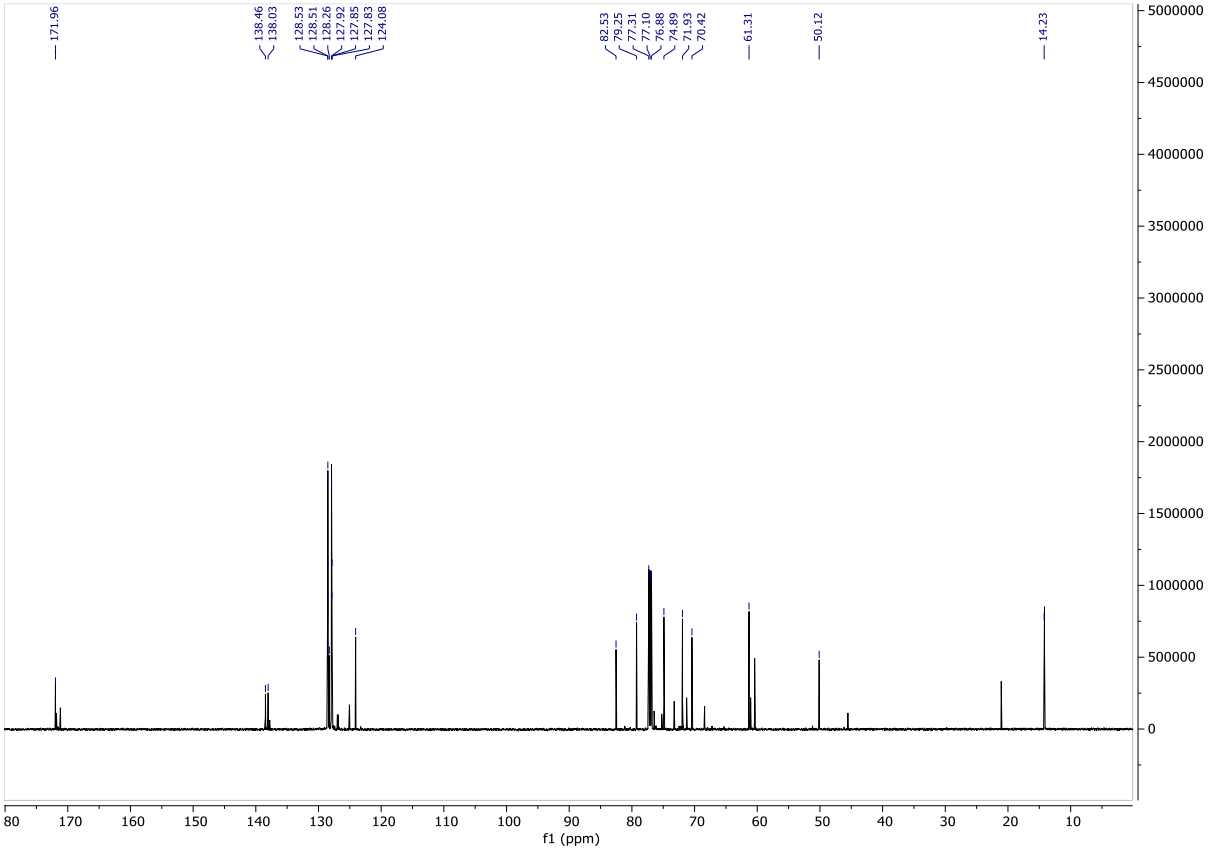

Figure 55. ^{13}C NMR spectrum of **24**.

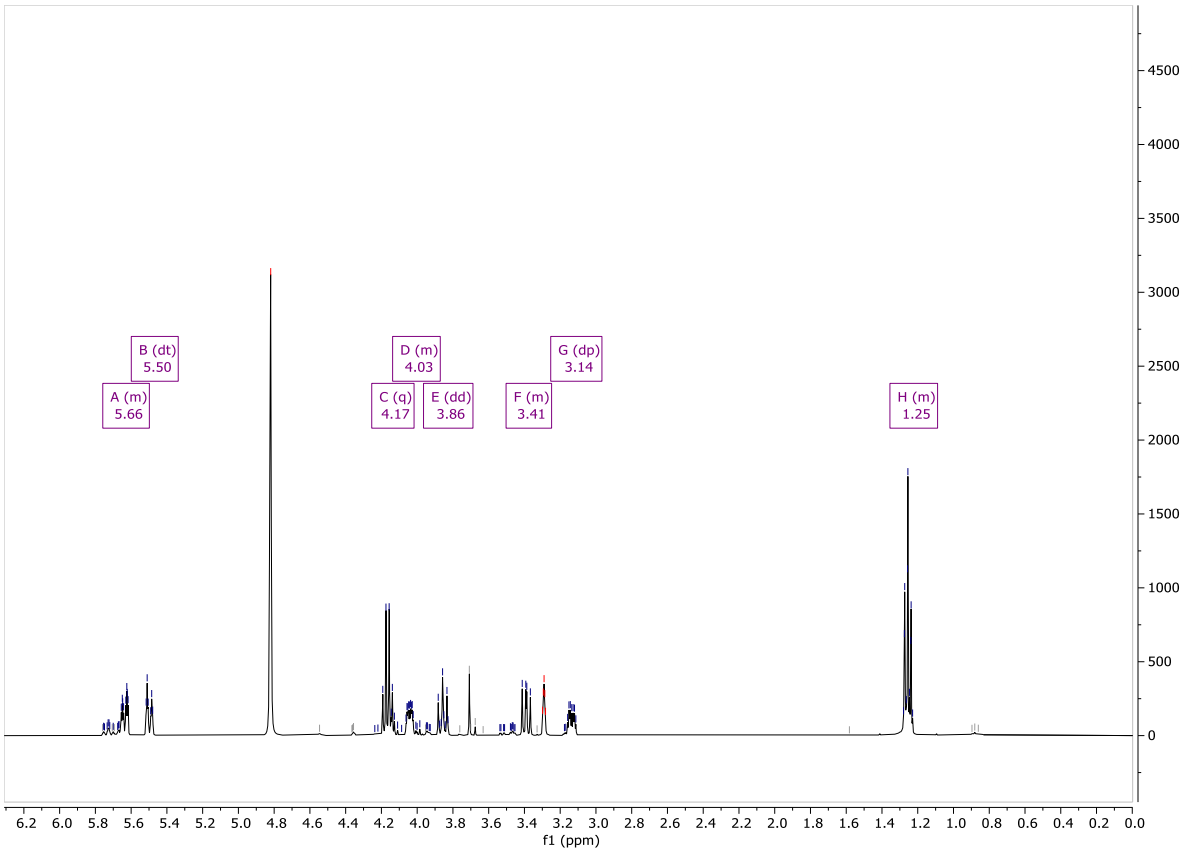

Figure 56. ^{1}H NMR spectrum of **32**.

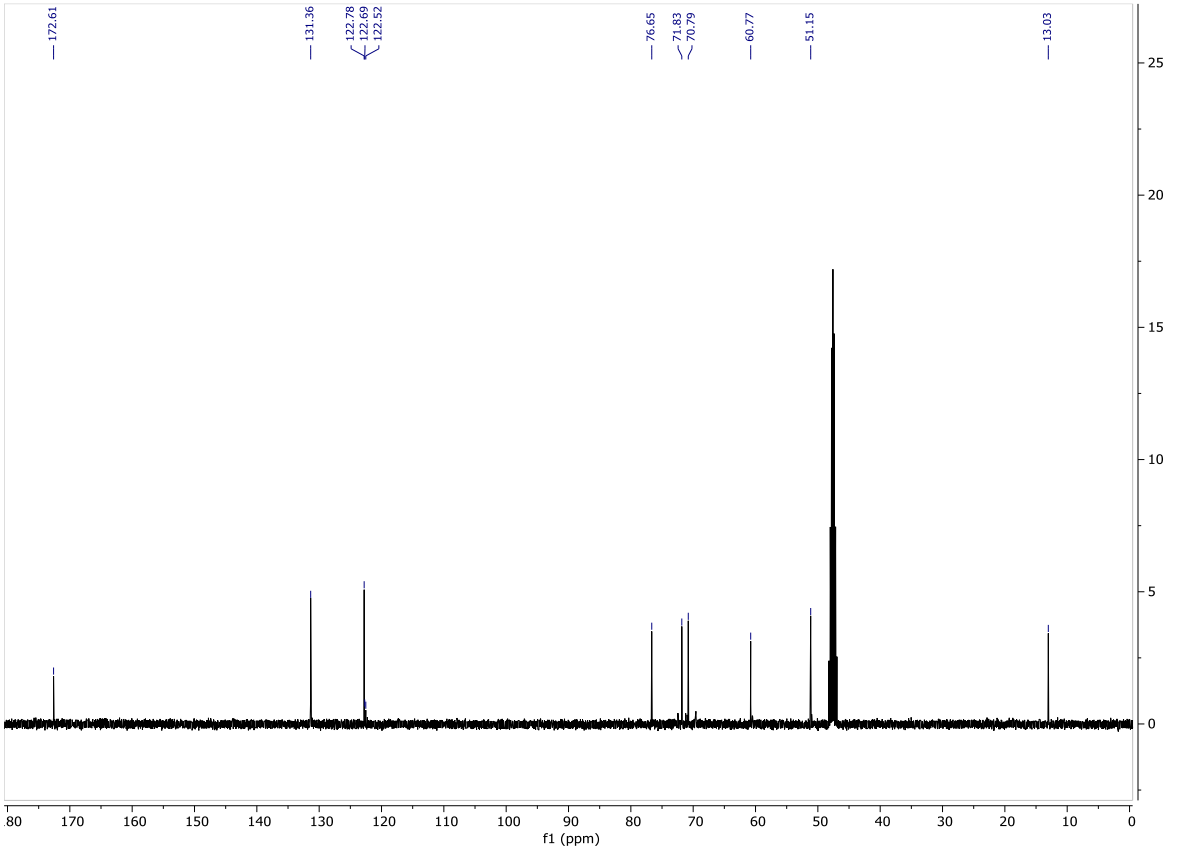

Figure 57. ^{13}C NMR spectrum of **32**.

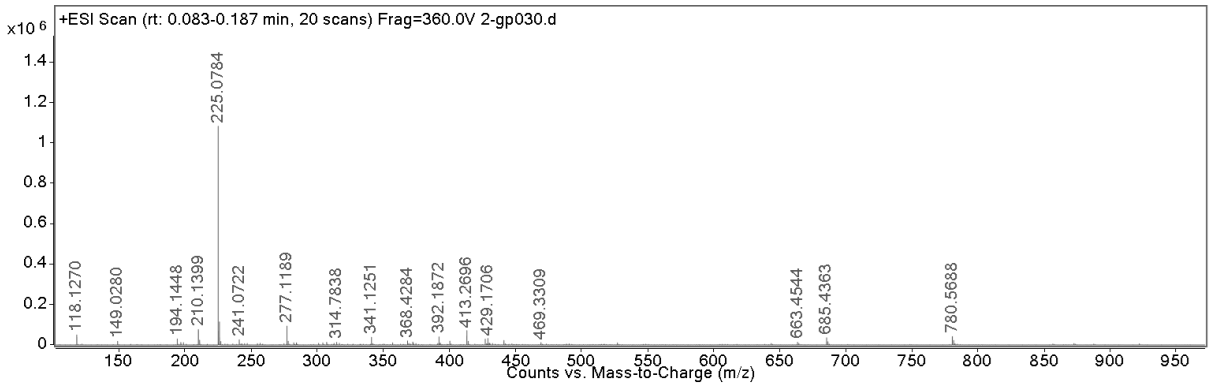

Figure 58. Positive ESI mass spectrum of **32**.

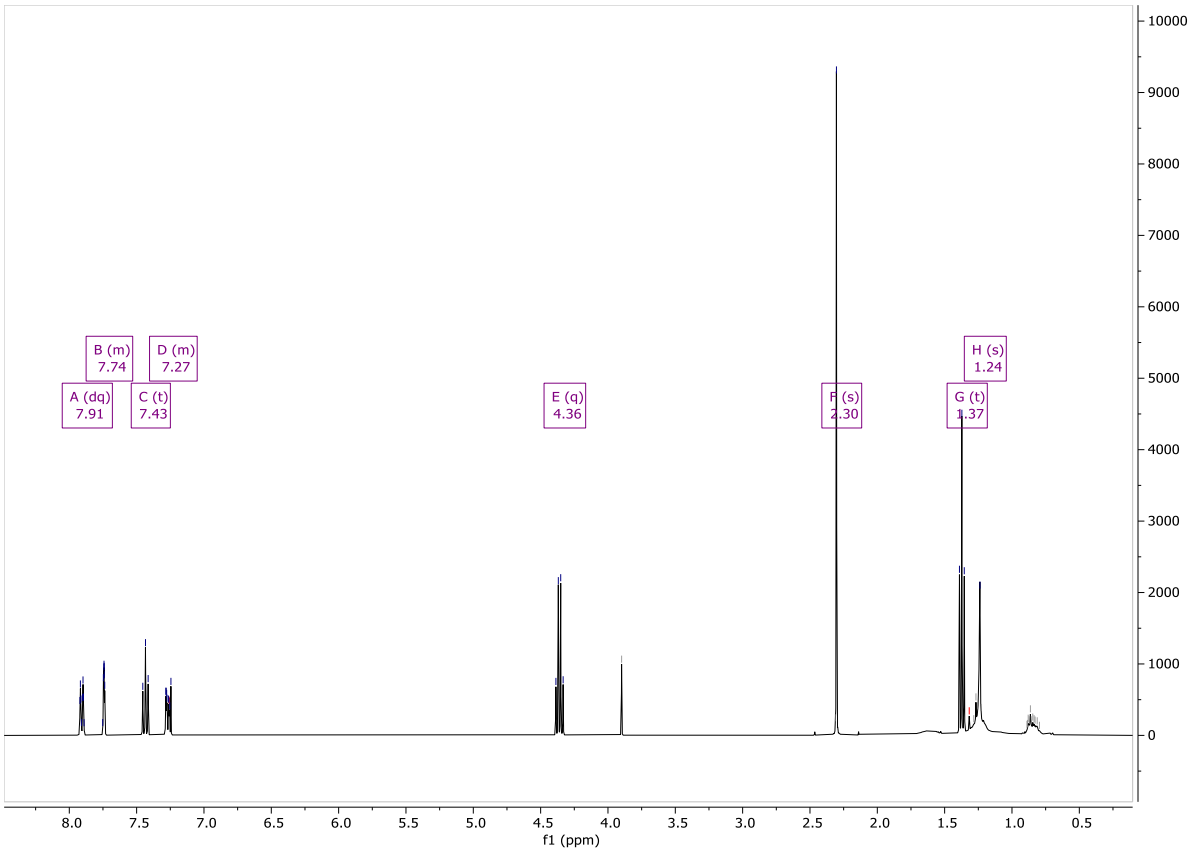

Figure 59. ^{1}H NMR spectrum of unidentified product during acetylation of **32**.

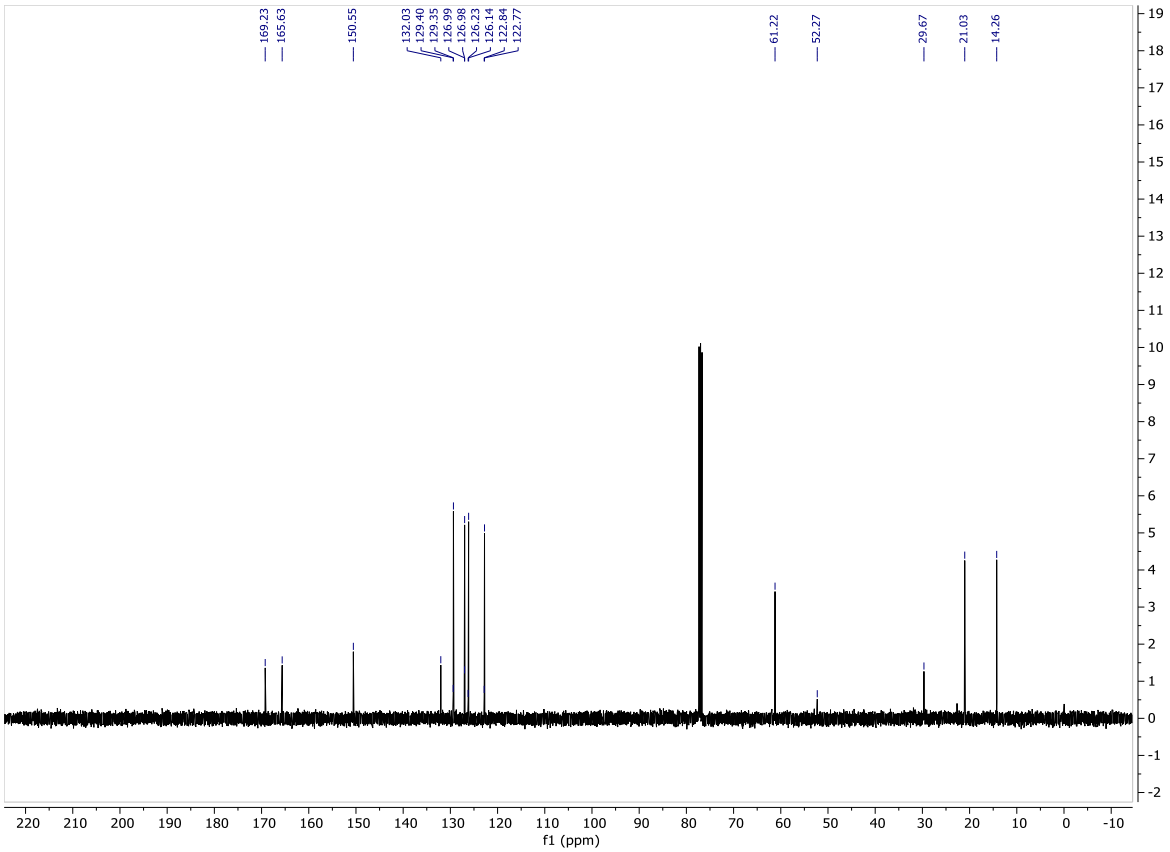

Figure 60. ^{13}C NMR spectrum of unidentified product during acetylation of **32**.